MIT

INCORPORATION OF CHANNEL LOSSES IN THE GEOMORPHOLOGIC IUH

by
Mario A. Diaz-Granados
Rafael L. Bras
and
Juan B. Valdes

RALPH M. PARSONS LABORATORY
HYDROLOGY AND WATER RESOURCE SYSTEMS

Report Number 293

Prepared with the Support of
The Agency for International Development
The United States Department of State

July 1983

DEPARTMENT
OF
CIVIL
ENGINEERING

SCHOOL OF ENGINEERING
MASSACHUSETTS INSTITUTE OF TECHNOLOGY
Cambridge, Massachusetts 02139

R83-10 OSP89965

INCORPORATION OF CHANNEL LOSSES IN THE GEOMORPHOLOGIC IUH

by

Mario A. Diaz-Granados
Rafael L. Bras
and
Juan B. Valdes

RALPH M. PARSONS LABORATORY
Hydrology and Water Resource Systems

Department of Civil Engineering
Massachusetts Institute of Technology

Report Number 293

Prepared with the Support of
The Agency for International Development
The United States Department of State

July 1983

PREFACE

This report is one of a series of publications which describe various studies undertaken under the sponsorship of the Technology Adaptation Program at the Massachusetts Institute of Technology.

The United States Deapartment of State, through the Agency for International Development, awarded the Massachusetts Institute of Technology a contract to provide support at MIT for the development, in conjunction with institutions in selected developing countries, of capabilities useful in the adaptation of technologies and problem-solving techniques to the needs of those countries. This particular study describes research conducted in conjunction with Cairo University, Cairo, Egypt.

In the process of making this TAP supported study some insight has been gained into how appropriate technologies can be identified and adapted to the needs of developing countries per se, and it is expected that the recommendations developed will serve as a guide to other developing countries for the solution of similar problems which may be encountered there.

Fred Moavenzadeh

Program Director

ABSTRACT

The infiltration losses along the streams of a basin are included into the Instantaneous Unit Hydrograph (IUH). The IUH is derived as a function of the basin geomorphologic and physiographic characteristics, and the response of the individual channels to upstream and lateral inflows. This response is obtained by solving the linearized continuity and momentum equations, including infiltration losses terms, for the boundary conditions established by the definition of a linear system reponse to an instantaneous unit input. A methodology is proposed for the estimation of the parameters involved in the channel response. Based on this result, a procedure is suggested to include infiltration losses in the common linear reservoir representation of channel segments. Comparisons indicate that this approximation is adequate.

ACKNOWLEDGEMENTS

This study was sponsored by the MIT Technology Adaptation Program, which is funded through a grant from the Agency for International Development, United States Department of State. The views and opinions in this report, however, are those of the authors and do not necessarily reflect those of the sponsors.

The authors would like to acknowledge the complete staff of the Technology Adaptation Program, which includes personnel at both MIT and Cairo University. Their administrative support over the entire period of this study has been more helpful.

The very helpful suggestions given by Diana Kirshen are gratefully acknowledged. This work also profitted from discussions with Professor Peter Eagleson of MIT and the faculty of Cairo University.

A thankful word goes to Ms. Antoinette DiRenzo for patiently typing this work.

Work was performed at the Ralph M. Parsons Laboratory,, Department of Civil Engineering, MIT.

TABLE OF CONTENTS

LIST OF PRINCIPAL SYMBOLS

A_i	average area of a stream of order i.
c_l	celerity of the wave flood, [L/T]
C	Chezy friction coefficient
d	diffusivity index
f_i^*	infiltration capacity, [L/T]
$f_\bullet(\bullet)$	probability density function of the argument
F_o	reference Froude number
$F_\bullet(\bullet)$	cumulative probability distribution of the argument
g	gravitational acceleration, $[L/T^2]$
h(t)	characteristic reponse of the basin, IUH
i	intensity, [L/T]
i_e	effective intensity
i_r	total rainfall intensity
I	infiltrated flow percentage
$I_1[\bullet]$	first order modified Bessel function of the first kind
$J_1[\bullet]$	first order Bessel function of the first kind
k(l)	saturated effective intrinsic permeability, $[L^2]$
K	infiltration coefficient, $[L^{-1}]$
$K_o[\bullet]$	modified Bessel function
$\bar{L}_i$	average length of a stream of order i, [L]
m_i	mean storm intensity, [L/T]
m_{t_b}	mean time between storms, [T]
m_{t_r}	mean storm duration, [T]

m_v	average annual number of independent storm events
N_i	number of streams of order i
P_{ij}	transition probability from channels of order i to channels of order j
$P[\cdot]$	probability of the given argument
q	discharge per unit of width, $[L^2/T]$
$q_I(x,t)$	infiltration rate, $[L/T]$
q_o	reference discharge, $[L^2/T]$
q_p	peak of the IUH, $[T^{-1}]$
$Q(t)$	streamflow, $[L^3/T]$
Q_p	peak discharge, $[L^3/T]$
R_A	area ratio
R_B	bifurcation ratio
R_L	length ratio
s	Laplace transform variable
S_f	friction channel slope
t	time
t_b	time bewteen storms
t_c	concentration time
t_e	duration of the effective rainfall
t_p	peak time of the IUH
t_r	storm duration
T_B	travel time to the outlet of the basin
$u(t)$	upsteam channel inflow response
$u(\cdot)$	unit step function
v	velocity
v_o	reference velocity

$w(x,t)$	surrogate variable of $q(x,t)$
y	flow depth
y_o	reference depth
Z	penetration depth
β	reciprocal of average storm intensity
σ	reciprocal of average storm duration
$\delta(\cdot)$	delta function
λ	parameter of the linear reservoir assumption
λ_Ω^*	parameter of the modified linear reservoir assumption
θ_i	initial probability in the GIUH
Ω	basin order
$\mathcal{L}(\cdot)$	Laplace Transform

LIST OF TABLES

LIST OF FIGURES

Chapter 1

INTRODUCTION

1.1 Motivation

Recently, methodologies have been proposed to relate river response to basin geomorphology (Rodriguez-Iturbe and Valdes, 1979), which are useful in the estimation of the hydrologic behavior in regions with sparse or no data. The Instantaneous Unit Hydrograph, IUH, is interpreted as the probability density function (PDF) of the travel time spent by a drop to reach the outlet of the basin, which is function of the geomorphology quantified by the Horton numbers, and the response of individual channels, assumed to behave like linear reservoirs. This IUH is called the Geomorphologic IUH.

In its derivation, the Strahler's channel ordering scheme is used, which allows to express the cumulative density function (CDF) of the time that a drop takes to travel to the outlet of the basin. In their study it was assumed that no infiltraiton occured in the channels. Later Kirshen and Bras (1982) studied the importance of the linear reservoir assumption for channel response. They used a general linear solution to the one dimensional equations of motion in wide prismatic channels as given by Harley (1967) to obtain the theoretical linear response function (the IUH) as a function of several physiographic factors (slope and Froude number) and the parameters required for linearization. The comparison of the hydrographs produced using the exponential assumption (Rodriguez-Iturbe et al., 1979) and those using the linearization procedures of Kirshen and Bras (1982) showed significant difference in the shape

of the hydrographs. However, no definite conclusion were obtained from their study. Again the effect of infiltration losses in the channel was not considered.

1.2 Scope of Study

The main topic to be addressed in this work is to include the channel infiltration losses in the equations of motion. The goal is to obtain a physically based response for individual channels, which could be incorporated in the geomorphologic theory. This will allow the verification of the linear reservoir behavior assumption adopted by Rodriguez-Iturbe and Valdes (1979).

Chapter 2 of this report reviews the most important aspects of the theory of the Geomorphologic, IUH. Chapter 3 presents the derivation of two analytical expressions of the approximate linear response of a channel with infiltration losses due to upstream and lateral inflows, respectively. These responses, which describe the movement of the flood wave along the channel, are interpreted in this study as the PDFs of the time a drop spends travelling to reach the outlet of the channel. Three PDF's are then used in Chapter 4 to obtain the IUH and discharge hydrographs of three basins: Morovis and Unibon in Puerto Rico and Wadi Umm Salam in Egypt. The results are compared to equivalent GIUH using the exponential assumption but also accounting for infiltration losses. Chapter 5 presents the summary and conclusions.

Chapter 2

THE GEOMORPHOLOGIC IUH

2.1 Introduction

The so-called Geomorphologic Unit Hydrograph, (GIUH), developed recently by Rodriguez-Iturbe and Valdes (1979), and further studied by Gupta et al., (1980), gives an analytical expression for the response of a basin in terms of its macro-catchment characteristics, or catchment geomorphology. The GIUH uses the exponential distribution to represent the travel time in individual channels. The Instantaneous Unit Hydrograph (IUH) is interpreted as the probability density function (PDF) of the travel time of a drop of water landing anywhere in the basin. The geomorphology is quantified by the Horton's numbers, which involve parameters that affect the basin response, such as areas, stream densities and lengths of the channels.

This chapter summarizes the derivation of the geomorphologic unit hydrograph. For further details, the reader is referred to the original papers or to Kirshen and Bras (1982). The original GIUH will later be compared to a result that uses an analytical channel response based on the equations of motion for unsteady flow including the infiltration losses in the channels.

2.2 The IUH and its Probabilistic Interpretation

In linear system theory, the response of a continuous system to an arbitrary input is defined by the convolution equation:

$$Q(t) = \int_0^t i(\tau)h(t-\tau)d\tau$$

In hydrology, Q(t) is the discharge at time t and i(t) is the intensity of the effective precipitation as a function of time. The function h(t) is the characteristic response of the basin and is usually called the Instantaneous Unit Hydrograph, since it is the response to an instantaneous impulse of unit volume applied uniformly over the basin. In other words, this is the distribution of the unit volume at the outlet of the basin. The IUH has units of inverse time; its possible values are non-negative, by definition its area is equal to 1. The above properties are similar to those of probability density functions. Indeed, Gupta et al., (1980) prove the common hypothesis that the IUH is the probability density function of the time that an individual drop of water, falling at a random point in the basin requires to travel to the outlet of the basin.

2.3 Structure of the Drainage Network

Throughout many years, the effect of climate and geology on catchment topography produces an erosional pattern which is characterized by a network of channels. Horton (1945) proposed a method for classifying streams by an ordering scheme and postulated two empirical laws: the law of stream lengths and the law of stream numbers. Strahler (1957) proposed a similar ordering scheme, that has one to one correspondence with Horton's scheme. It is illustrated in Figure 2.1, and the procedure is as follows:

1. Channels that originate at a source are defined to be first order streams.
2. When two streams of order i join, a stream of order i+1 is created.

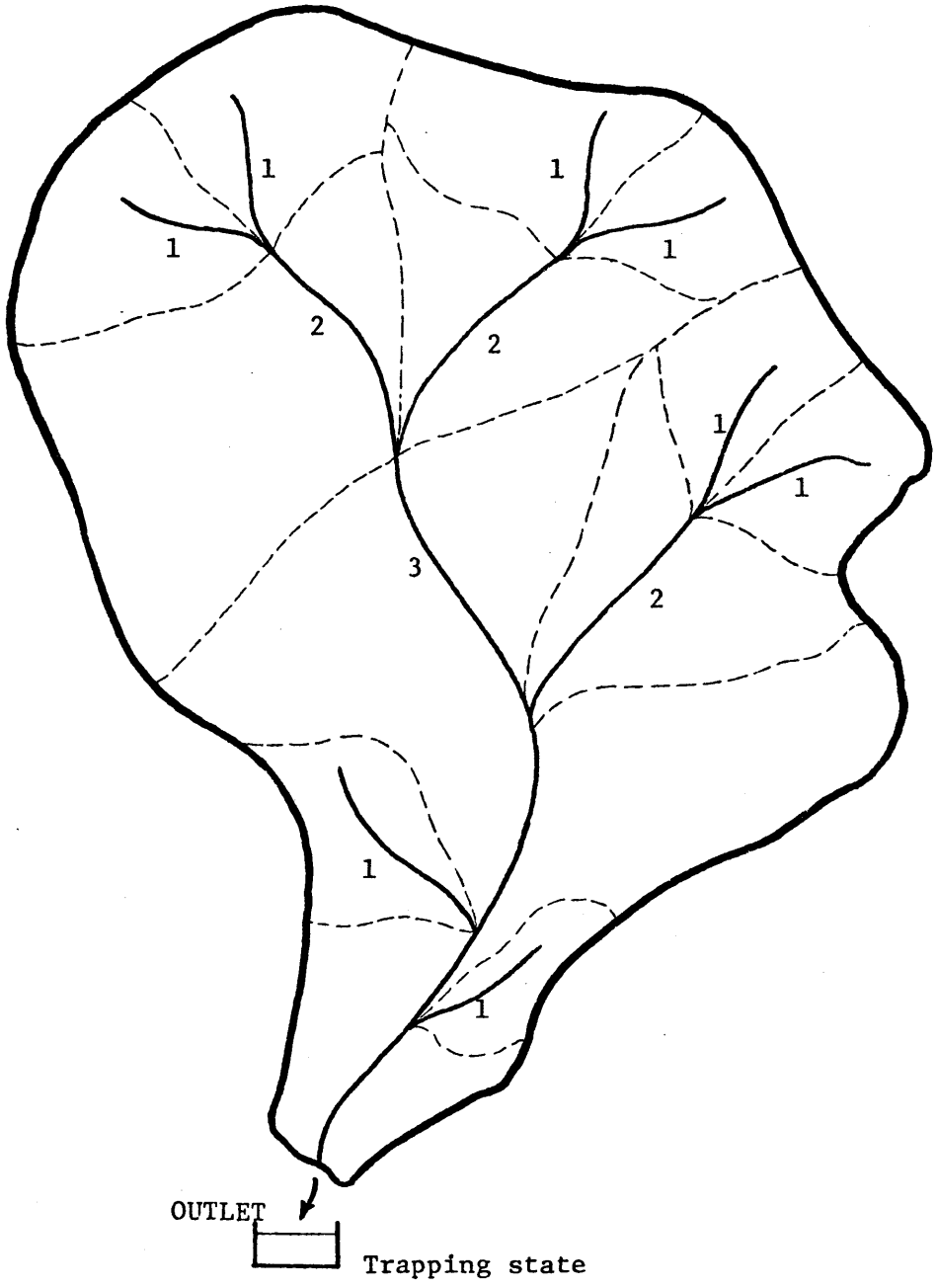

Third order basin with Strahler's ordering scheme
(From Rodriguez-Iturbe and Valdes, 1979)

Figure 2.1

3. When two streams of different order join, the channel segment immediately downstream has the higher of the orders of the two combining streams.

4. The order of the basin, Ω, is the highest stream order.

The quantitative expressions of Horton's laws are:

$$\text{Law of stream numbers:} \quad R_B = \frac{N_i}{N_{i+1}}$$

$$\text{Law of stream lengths:} \quad R_L = \frac{\bar{L}_i}{\bar{L}_{i-1}}$$

Schumm (1956) proposed a Horton-type law for drainage areas:

$$\text{Law of stream areas:} \quad R_A = \frac{\bar{A}_i}{\bar{A}_{i-1}}$$

where N_i is the number of streams of order i, L_i is the average length of a stream of order i, and A_i is the mean area of the sub-basin of order i. R_B, R_L, and R_A represent, respectively, the bifurcation, length and area ratios, which are characteristics of the geomorphology of the basin. For natural basins the normal values are between three and five for R_B, between 1.5 and 3.5 for R_L, and between three and six for R_A.

2.4 Derivation of the Geomorphologic Unit Hydrograph

A drop of water, travelling throughout a basin can make transitions from streams of lower order to streams of higher order. Assume a third order basin (Ω=3). The drop, falling randomly on the basin may follow

a finite number of paths to reach the outlet. In terms of the different orders, streams and areas, the paths may be characterized as:

$$\begin{aligned} s_1 &= a(1) \rightarrow r(1) \rightarrow r(2) \rightarrow r(3) \rightarrow \text{OUTLET} \\ s_2 &= a(1) \rightarrow r(1) \rightarrow r(3) \rightarrow \text{OUTLET} \\ s_3 &= a(2) \rightarrow r(2) \rightarrow r(3) \rightarrow \text{OUTLET} \\ s_1 &= a(3) \rightarrow r(3) \rightarrow \text{OUTLET} \end{aligned} \tag{2.2}$$

where a(i) defines the area contributing to streams of order i and r(i) represents a stream of order i.

All possible paths fall into one of the above sequences. Figure 2.2 is a representation of the basin in terms of all alternative paths.

From now on, it is assumed that the time that a drop spends as overland flow is negligible (Rodriguez-Iturbe and Valdes, 1979). Therefore, the probability that a drop reaches the outlet at a given time is a function of the probability that a drop initially falls in an area draining to a channel or order $i(i=1,\ldots,\Omega)$, the transition probabilities to channels of higher order, p_{ij}, $j=i+1,\ldots,\Omega$, and the PDF of the time spent in a channel of the corresponding order.

According to Gupta et al., (1980), the cumulative density function of the time that a drop takes to travel to the outlet of the basin is given by

$$P(T_B \leq t) = \sum_{s \in S} P\ (T_s \leq t)\ P(s) \tag{2.3}$$

where $P(\cdot)$ represents the probability of the event given in parenthesis, T_B is the travel time to the outlet of the basin, T_s is the travel time through a path s, belonging to S, the set of all possible paths.

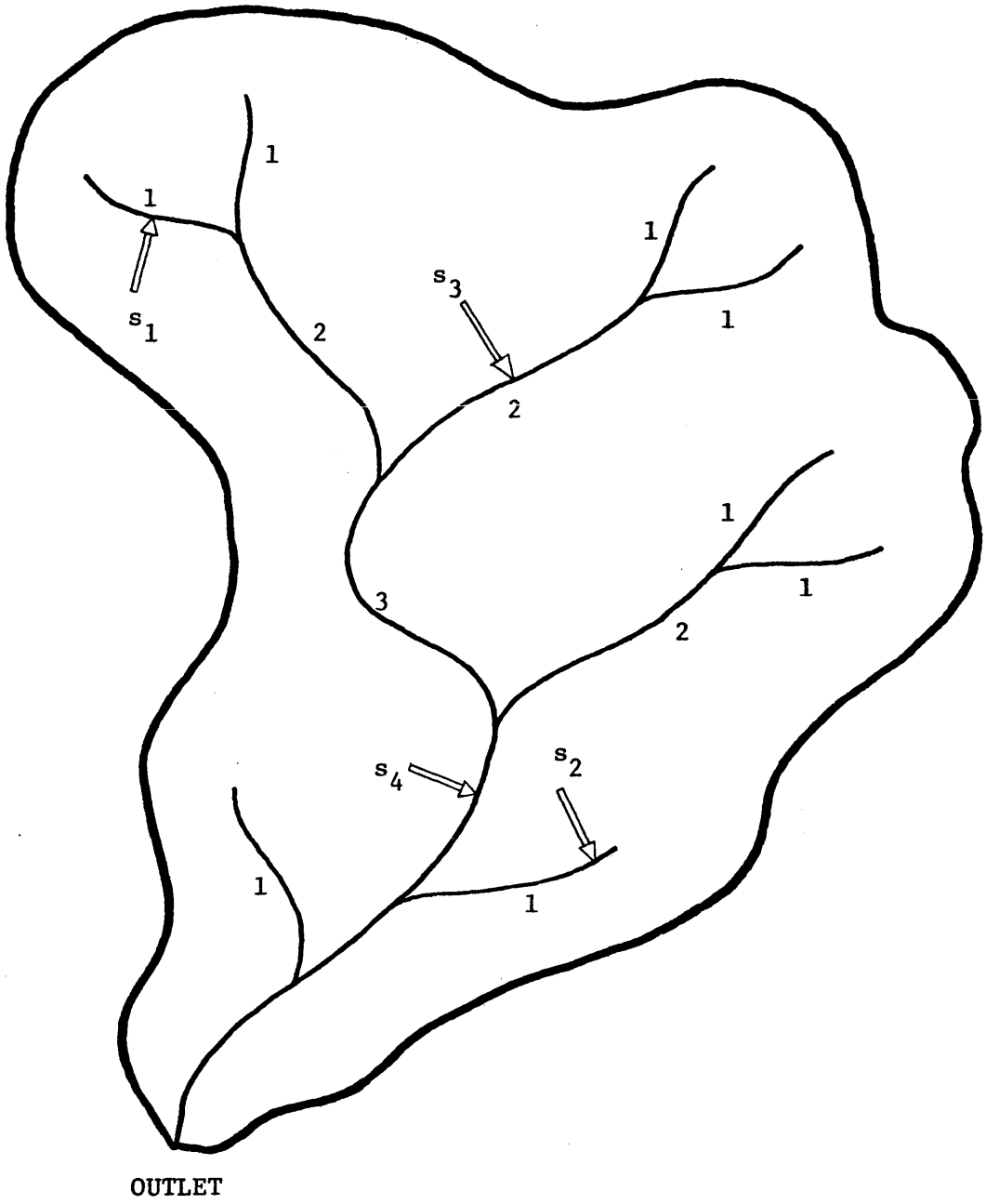

Basin representation in terms of alternative paths

Figure 2.2

The travel time, T_s, in a particular path, $a(i) \rightarrow r(i) \rightarrow \ldots \rightarrow r(\Omega) \rightarrow$ OUTLET, where $i \in \{1, \ldots \Omega\}$, must be equal to the sum of travel times in the elements of the path:

$$T_s = T_{r(i)} + \ldots + T_{r(\Omega)} \tag{2.4}$$

where $T_{r(i)}$ is the travel time in a stream of order i. It was assumed that $T_{a(i)} = 0$. Given that there exist several streams of a given order, $T_{r(i)}$ may be considered an independent random variable with a given probability density function, $f_T^{(i)}(t)$, so that the cumulative density function T_s is the convolution of the individual cumulative density functions, $F_T^{(i)}(t)$:

$$F_T^s(t) = F_T^{(1)}(t) * \ldots * F_T^{(\Omega)}(t) \tag{2.5}$$

where * indicates the convolution operation.

The probability of a given path s is:

$$P(s) = \Theta_i \cdot p_{ij} \cdots p_{k\,\Omega} \tag{2.6}$$

where Θ_i is the probability that a drop falls in an area draining to a stream of order i and p_{ij} is the transition probability from streams of order i to streams of order j. Rodriguez-Iturbe and Valdes (1979) show that the initial and transition probabilities are functions only of the geomorphology of the basin. Table 2.1 gives the expressions for a basin of order 3.

Table 2.1

Initial and Transition Probabilities
for a Basin of Order 3

$$\Theta_1 = \frac{R_B^2}{R_A^2}$$

$$\Theta_2 = \frac{R_B}{R_A} - \frac{R_B^3 + 2R_B^2 - 2R_B}{R_A^2(2R_B-1)}$$

$$\Theta_3 = 1 - \frac{R_B}{R_A} - \frac{R_B^3 - 3R_B^2 + 2R_B}{R_A^2(2R_B-1)}$$

$$P_{12} = \frac{R_B^2 + 2R_B^2 - 2}{2R_B^2 - R_B}$$

$$P_{13} = \frac{R_B^2 - 3R_B + 2}{2R_B^2 - R_B}$$

$$P_{23} = 1$$

Now that Equation 2.3 is fully defined in terms of geomorphologic parameters and the PDFs of the travel time in the different streams, the geomorphologic IUH is obtained by calculating the derivative of $P(T_B \leq t)$:

$$h(t) = \frac{dP(T_B \leq t)}{dt}$$

$$= \sum_{s \in S} f_T^{(i)}(t) * \ldots * f_T^{(\Omega)}(t) P(s) \qquad (2.7)$$

Rodriguez-Iturbe and Valdes (1979) argue for an exponential behavior of the travel time in individual channels of a given order:

$$f_T^{(i)}(t) = \lambda_i e^{-\lambda_i t} \qquad (2.8)$$

where

$$\lambda_i = v/\bar{L}_i \qquad (2.9)$$

They use the assumption that for a given rainfall-runoff event the velocity at any moment is approximately the same throughout the whole drainage network (Pilgrim 1977). For the stream of the highest order, they prefer to modify the exponential assumption, such that $f_T^{(\Omega)}(t)$ becomes:

$$f_T^{(\Omega)}(t) = \lambda_\Omega^{*2} te^{-\lambda_\Omega^* t} \qquad (2.10)$$

where

$$\lambda_\Omega^* = 2\lambda_\Omega$$

The following results correspond to a basin of order 3. Remembering the possible paths in a basin of this order and their corresponding probabilities, Equation 2.7 is:

$$h(t) = \Theta_1 P_{12} f_T^{(1)}(t) * f_T^{(2)}(t) * f_T^{(3)}(t) + \Theta_1 P_{13} f_T^{(1)}(t) * f_T^{(3)}(t)$$

$$+ \Theta_2 f_T^{(2)}(t) * f_T^{(3)}(t) + \Theta_3 f_T^{(3)}(t) \qquad (2.11)$$

where $f_T^{(1)}(t)$ and $f_T^{(2)}(t)$ are given by Equation 2.8, whereas $f_T^{(3)}(t)$ is given by Equation 2.10. These convolution operations can easily be performed using Laplace transforms:

$$\mathcal{L}\left\{\lambda_i e^{-\lambda_i t}\right\} = \frac{\lambda_i}{s+\lambda_i} \qquad (2.12)$$

$$\mathcal{L}\left\{\lambda_\Omega^{*2}\, t\, e^{-\lambda_\Omega^* t}\right\} = \frac{\lambda_\Omega^{*2}}{(s+\lambda_\Omega^*)^2} \qquad (2.13)$$

Then,

$$h(t) = \Theta_1 P_{12} \mathcal{L}^{-1}\left\{\frac{\lambda_1}{s+\lambda_1}\,\frac{\lambda_2}{s+\lambda_2}\,\frac{\lambda_3^{*2}}{(s+\lambda_3^*)^2}\right\}$$

$$+ \Theta_1 P_{13} \mathcal{L}^{-1}\left\{\frac{\lambda_1}{s+\lambda_1}\,\frac{\lambda_3^{*3}}{(s+\lambda_3^*)^2}\right\}$$

$$+ \Theta_2 \mathcal{L}^{-1}\left\{\frac{\lambda_2}{s+\lambda_2}\,\frac{\lambda_3^{*2}}{(s+\lambda_3^*)^2}\right\}$$

$$+ \Theta_3 \mathcal{L}^{-1}\left\{\frac{\lambda_3^{*2}}{(s+\lambda_3^*)^2}\right\} \qquad (2.14)$$

and after some calculations of the inverse Laplace transforms, the final expression for the geomorphologic IUH is:

$$h(t) = \Theta_1 P_{12} \lambda_1 \lambda_2 \lambda_3^{*2} \left\{ \frac{e^{-\lambda_1 t}}{(\lambda_1-\lambda_3^*)^2(\lambda_2-\lambda_1)} + \frac{e^{-\lambda_2 t}}{(\lambda_2-\lambda_3^*)^2(\lambda_1-\lambda_2)} \right.$$

$$\left. + \frac{[2\lambda_3^*-\lambda_1-\lambda_2 + (\lambda_1-\lambda_3^*)(\lambda_2-\lambda_3^*)t]e^{-\lambda_3^* t}}{(\lambda_1-\lambda_3^*)^2(\lambda_2-\lambda_3^*)^2} \right\}$$

$$+ \Theta_1 P_{13} \lambda_1 \lambda_3^* \frac{2e^{-\lambda_1 t} - [1-(\lambda_3^*-\lambda_1)t]e^{-\lambda_3^* t}}{(\lambda_3^*-\lambda_1)^2}$$

$$+ \Theta_2 \lambda_2 \lambda_3^* \frac{2e^{-\lambda_2 t} - [1-(\lambda_3^*-\lambda_2)t]e^{-\lambda_3^* t}}{(\lambda_3^*-\lambda_2)^2} + \Theta_3 \lambda_3^{*2} t e^{-\lambda_3^* t} \qquad (2.15)$$

The GIUH, h(t), can be convoluted with a specific rainfall event in order to get the discharge hydrograph. Under the assumption that the effective rainfall can be represented by an event with constant intensity i_e during a period t_e, an analytical expression for the discharge hydrograph is obtained as follows:

The expression for the rainfall event is given by:

$$i(t) = i_e[u(t) - u(t-t_e)] \qquad (2.16)$$

where u(t) is the unit step function. Given that the operation involved in Equation 2.1 is a convolution, the Laplace transforms can be used again to calculate Q(t). The Laplace transform of i(t) is:

$$\mathcal{L}\{i(t)\} = \frac{1-e^{-t_e s}}{s} i_e \qquad (2.17)$$

Therefore,

$$Q(t) = \Theta_1 P_{12} \mathcal{L}^{-1}\left\{\frac{\lambda_1}{s+\lambda_1}\,\frac{\lambda_2}{s+\lambda_2}\,\frac{\lambda_3^{*2}}{(s+\lambda_3^*)^2}\,\frac{1-e^{-t_e s}}{s}\,i_e\right\}$$

$$+ \Theta_1 P_{13} \mathcal{L}^{-1}\left\{\frac{\lambda_1}{s+\lambda_1}\,\frac{\lambda_3^{*2}}{(s+\lambda_3^*)^2}\,\frac{1-e^{-t_e s}}{s}\,i_e\right\}$$

$$+ \Theta_2 \mathcal{L}^{-1}\left\{\frac{\lambda_2}{s+\lambda_2}\,\frac{\lambda_3^{*2}}{(s+\lambda_3^*)^2}\,\frac{1-e^{-t_e s}}{s}\,i_e\right\}$$

$$+ \Theta_3 \mathcal{L}^{-1}\left\{\frac{\lambda_3^{*2}}{(s+\lambda_3^*)^2}\,\frac{1-e^{-t_e s}}{s}\,i_e\right\} \qquad (2.18)$$

After some manipulations, the expression for the discharge hydrograph becomes:

$$Q(t) = A_3 bi_e\left[\frac{\Theta_1 P_{12}\lambda_2\lambda_3^{*2}}{(\lambda_1-\lambda_3^*)^2(\lambda_2-\lambda_1)} + \frac{\Theta_1 P_{13}\lambda_3^{*2}}{(\lambda_3^*-\lambda_1)^2}\right]\left\{1 - e^{-\lambda_1 t} - \left[1-e^{-\lambda_1(t-t_e)}\right]u(t-t_e)\right\}$$

$$+ A_3 bi_e\left[\frac{\Theta_1 P_{12}\lambda_1\lambda_3^{*2}}{(\lambda_2-\lambda_3^*)^2(\lambda_1-\lambda_2)} + \frac{\Theta_2\lambda_3^{*2}}{(\lambda_3^*-\lambda_2)^2}\right]\left\{1 - e^{-\lambda_2 t} - \left[1-e^{-\lambda_2(t-t_e)}\right]u(t-t_e)\right\}$$

$$+ A_3 bi_e\left[\frac{\Theta_1 P_{12}\lambda_1\lambda_2\lambda_3^*(2\lambda_3^*-\lambda_1-\lambda_2)}{(\lambda_1-\lambda_3^*)^2(\lambda_2-\lambda_3^*)^2} - \frac{\Theta_1 P_{13}\lambda_1\lambda_3^*}{(\lambda_1-\lambda_3^*)^2} - \frac{\Theta_2\lambda_2\lambda_3^*}{(\lambda_2-\lambda_3^*)^2}\right] \cdot$$

$$\left\{1 - e^{-\lambda_2 t} - \left[1-e^{-\lambda_2(t-t_e)}\right]u(t-t_e)\right\}$$

$$+ A_3 bi_e\left[\frac{\Theta_1 P_{12}\lambda_1\lambda_2}{(\lambda_1-\lambda_3^*)(\lambda_2-\lambda_3^*)} + \frac{\Theta_1 P_{13}\lambda_1}{(\lambda_1-\lambda_3^*)} + \frac{\Theta_2\lambda_2}{(\lambda_2-\lambda_3^*)} + \Theta_3\right]\left\{1 - (\lambda_3^* t+1)e^{-\lambda_3^* t} + u(t-t_e)\right.$$

$$\left. + e^{-\lambda_3^*(t-t_e)}\,u(t-t_e) + \lambda_3^*(t-t_e)\,e^{-\lambda_3^*(t-t_e)}\,u(t-t_e)\right\} \qquad (2.19)$$

where A_3 is the area of the basin in km^2, t and t_e are given in hours, i_e in cm/hr and b is 1/0.36 in order to obtain Q(t) in m^3/sec.

2.5 The Peak and Time to Peak of the IUH

The most important characteristics of the IUH are its peak, q_p, and time to peak, t_p, the shape being less critical and adequately represented by a triangle. Unfortunately, the sum of exponential functions in the IUH expression (Equation 2.15) does not lend itself to mathematical manipulation in order to obtain the maximum of the function. Therefore, from regression analyses, Rodriguez-Iturbe and Valdes (1979) obtained the following expressions for q_p and t_p:

$$q_p = \frac{1.31}{L_\Omega} R_L^{0.43} v \tag{2.20}$$

$$t_p = \frac{0.44 L_\Omega}{v} \left(\frac{R_B}{R_A}\right)^{0.55} R_L^{-0.38} \tag{2.21}$$

where L_Ω is the length in km of the highest order stream and v is the peak velocity of the response in m/s; t_p and q_p are given in hours and inverse hours, respectively. With the definition of these two parameters, the revision of the geomorphologic theory of the instantaneous unit hydrograph has been completed.

Chapter 3

THE RESPONSE OF A CHANNEL: INFILTRATION LOSSES EFFECT

3.1 Introduction

Calculating the course of a flood wave is known in hydrology as flood routing. There are several flood routing procedures. They differ in the nature of the governing equations used to describe the wave movement, and on the assumptions and approximations introduced. In this chapter, an approximate linear solution to the one-dimensional unsteady flow equations in a wide rectangular channel (including infiltration losses) will be found. The solution will correspond to initial conditions imposed by the definition of the IUH. The first result is the response channel to an instantaneous input at the upstream end. From this solution, the response to an instantaneous uniform input along the channel will be derived.

3.2 Linear Solution to the Equations of Motion

The one-dimensional equations of motion for unsteady flow in a wide rectangular open channel including infiltration losses are given by:

Continuity:

$$\frac{\partial q}{\partial x} + \frac{\partial y}{\partial t} = -q_I(x,t) \tag{3.1}$$

Momentum:

$$\frac{\partial v}{\partial x} + \frac{v}{g}\frac{\partial v}{\partial x} + \frac{1}{g}\frac{\partial v}{\partial t} - \frac{v}{gy}q_I(x,t) = S_o - S_f \tag{3.2}$$

where

g = gravitational acceleration $[LT^{-2}]$

v = mean velocity $[LT^{-1}]$

y = depth [L]

$q \equiv vy$ = discharge per unit width $[L^2T^{-1}]$

S_o = slope of the channel bottom

S_f = friction slope

x = space coordinate, measured downstream along the channel [L]

t = time coordinate [T]

$q_I(x,t)$ = infiltration rate $[LT^{-1}]$

The Chezy formula is used to describe the frictional effects,

$$S_f \approx \frac{v^2}{C^2 y} \tag{3.3}$$

where C is the Chezy coefficient.

Eliminating the velocity from the momentum equation, retaining q and y as the dependent variables, differentiating Equation 3.1 with respect to x and Equation 3.2 with respect to t and combining them with Equation 3.3, the following second order partial differential equation of motion results:

$$(gy^3-q^2)\frac{\partial^2 q}{\partial x^2} - 2qy\frac{\partial^2 q}{\partial t \partial x} - y^2\frac{\partial^2 q}{\partial t^2} = \frac{2gq}{C^2}\frac{\partial q}{\partial t}$$

$$+ 2q\left(\frac{\partial q}{\partial x}\frac{\partial y}{\partial t} - \frac{\partial y}{\partial x}\frac{\partial q}{\partial t}\right) - (gy^3 - q^2)\frac{\partial q_I(x,t)}{\partial x}$$

$$+ 3gy^2\left(S_o - \frac{\partial y}{\partial x}\right)\frac{\partial q}{\partial x} + 3gy^2\left(S_o - \frac{\partial y}{\partial x}\right) q_I(x,t)$$

$$- 2yq_I(x,t)\frac{\partial q}{\partial t} \qquad (3.4)$$

The above equation is highly non-linear. Its linearization is performed according to the following definitions and assumptions:

$$q \equiv q_o + \delta q \qquad q_o >> \delta q$$

$$y \equiv y_o + \delta y \qquad y_o >> \delta y \qquad (3.5)$$

where q_o and y_o are a reference discharge and a reference depth, and δq and δy are perturbations about these values. Substituting Equation 3.5 into Equation 3.4 and eliminating any second order differential terms (perturbations are here assumed small), the linearized equation of motion is:

$$(gy_o^3 - q_o^2)\frac{\partial^2 \delta q}{\partial x^2} - 2q_o y_o \frac{\partial^2 \delta q}{\partial x \partial t} - y_o^2 \frac{\partial^2 \delta q}{\partial t^2} - 3gS_o y_o^2 \frac{\partial \delta q}{\partial x}$$

$$- 2gy_o^3 \frac{S_o}{q_o} \frac{\partial \delta q}{\partial t} = -(gy_o^3 - q_o^2)\left[\frac{\partial q_I(x,t)}{\partial x}\right]_L$$

$$+ 3gS_o y_o^2 [q_I(x,t)]_L - 2y_o [q_I(x,t)]_L \frac{\partial \delta q}{\partial t} \qquad (3.6)$$

where C has been assumed constant and equal to the value corresponding to the reference state, i.e.,

$$C = \frac{q_o}{S_o^{1/2} y_o^{3/2}}$$

and $[\cdot]_L$ is the linearized expression of the argument, given the specific representation of the infiltration losses. An adequate representation of these losses [Burkham (1970a, b)] is:

$$q_I(x,t) = Kq^a$$

where a is about 0.8. For tractability reasons it is assumed here that a is equal to 1, and then the dimension of K, the infiltration coefficient, is L^{-1}. Therefore,

$$[q_I(x,t)]_L = K(q_o + \delta q) \qquad (3.7)$$

$$\left[\frac{\partial}{\partial x} q_I(x,t)\right]_L = K \frac{\partial \delta q}{\partial x} \qquad (3.8)$$

Introducing Equations 3.7 and 3.8 into 3.6, the linearized equation of motion becomes:

$$(gy_o^3 - q_o^2)\frac{\partial^2\delta q}{\partial x^2} - 2q_o y_o \frac{\partial^2\delta q}{\partial x \partial t} - y_o^2 \frac{\partial^2\delta q}{\partial t^2} - 3gS_o y_o^2 \frac{\partial \delta q}{\partial x}$$

$$- 3gy_o^2 \frac{S_o}{q_o}\frac{\partial \delta q}{\partial t} = -(gy_o^3 - q_o^2)\, K \frac{\partial \delta q}{\partial x} + 3gS_o y_o^2 K q_o$$

$$+ 3gS_o y_o^2 K\delta q - 2y_o K q_o \frac{\partial \delta q}{\partial t} \qquad (3.9)$$

For given initial and boundary conditions, analytical solutions of this equation may be obtained. In this study, the interest is on the response of a channel to a drop entering anywhere along its length. This will be found by first using the response of the channel to an input at its most upstream point.

3.3 Channel's Response to a Pulsed Upstream Inflow

The purpose of the derivation of the response of a channel to a drop entering anywhere along its length is its posterior utilization in the geomorphologic IUH. Therefore, the response of the channel will be obtained for using boundary conditions implied by the definition of the IUH:

$$\delta q(0,t) = \delta(t)$$

where $\delta(t)$ is the delta function:

Before the application of the delta function, the flow is in steady state. It may be expressed as (see Appendix A):

$$q(x,t) = q_1 e^{-Kx} \qquad t \leq 0$$

where q_1 is the flow at x=0. Then, in terms of the linearization scheme, there exists a perturbation about q_o. Recalling Equation 3.5a and the above expression, $\delta q(x,t)$ is:

$$\delta q(x,t) = q(x,t)-q_o = q_1 e^{-Kx} - q_o \qquad t \leq 0$$

As explained in Appendix A, the reference flow q_o is assumed equal to q_1. Therefore, the initial conditions for solving Equation 3.9 are:

$$\delta q(x,0) = q_o e^{-Kx} - q_o$$

and

$$\left.\frac{\partial \delta q(x,t)}{\partial t}\right|_{t=0} = 0$$

The solution of Equation 3.9 is based on the Laplace transform method. Harley (1967), O'Meara (1969), Dahl (1981), and Kirshen and Bras (1982) among others, have used the Laplace transform method to solve problems of unsteady flow in open channels. A detailed description of the solution procedure is presented in Appendix A. The solution has the following form:

$$\delta q(x,t) = q_o e^{-Kx} - q_o + w(x,t)e^{-Kx}$$

The first two terms of the above equation correspond to the value of the perturbation before the application of the delta function, and the third term represents the effect of the latter, which is the main interest here. Therefore, the net response of the infiltration channel to an instantaneous input at its most upstream point, at time t and at a distance x is:

$$h(x,t) = w(x,t)e^{-Kx}$$

or,

$$h(x,t) = \exp(-px)\delta(t-x/c_1) + \exp(-rt+zx)(d/a)^{\frac{1}{2}}x \frac{I_1[d^{\frac{1}{2}}((t-x/c_1)(t-x/c_2))^{\frac{1}{2}}/a]}{((t-x/c_1)(t-x/c_2))^{\frac{1}{2}}} u(t-x/c_1) \qquad (3.10)$$

where

$$a = \frac{1}{gy_o(1-F_o^2)^2}$$

$$c_1 = v_o + (gy_o)^{\frac{1}{2}}$$

$$c_2 = v_o - (gy_o)^{\frac{1}{2}}$$

$$d = \frac{b^2}{4} - ac$$

$$b = \frac{S_o}{y_o v_o} \frac{2+F_o^2}{(1+F_o^2)^2} + \frac{K}{v_o} \frac{F_o^2}{1-F_o^2}$$

$$c = \frac{K^2}{4} + \frac{3}{2} K \frac{S_o}{y_o} \frac{1}{1-F_o^2} + \frac{9}{4} \frac{S_o^2}{y_o^2} \frac{1}{(1-F_o^2)^2}$$

$$p = \frac{S_o}{2y_o} \frac{2-F_o}{(1+F_o)F_o} - \frac{3}{2}KF_o + \frac{K}{2}$$

$$r = g \frac{S_o}{v_o} + \frac{gS_oF_o^2}{2v_o} - \frac{3}{2} Kv_o(1-F_o^2)$$

$$z = \frac{S_o}{2y_o} - \frac{K}{2} + \frac{3}{2} KF_o^2$$

$v_o = \frac{q_o}{y_o}$ = reference velocity

$F_o = \frac{v_o}{(gy_o)^{\frac{1}{2}}}$ = reference Froude number

$I_1[\cdot]$ = first order modified Bessel function of the the first kind.

$u(\cdot)$ = unit step function.

This solution is valid for Froude numbers less than 1. For Froude numbers between 1 and 2 the first order modified Bessel function of the first kind, I[•], will change to the first order Bessel function of the first kind, J[•], whose solution will contain imaginary terms, implying oscillations in the discharge and water surface.

It is important to note that when K=0, Equation 3.10 reduces to the same solution obtained by Harley (1967) and used later by Kirshen and Bras (1982).

For a fixed value of x, the area under h(x,t), denoted A_h, is equal to e^{-Kt}, as it is shown in Appendix A. It represents the fraction of the perturbation that reaches point x. By definition of the delta function, $1-A_h$ is the fraction of it that infiltrates along the interval [0, x]; if K = 0, A_h = 1. In the special case in which x=L, where L is the length of the channel, h(L,t) will be referred to as the upstream inflow IUH and will be denoted as:

$$u(t) \equiv h(L,t) \tag{3.11}$$

If I is the infiltrated percentage of the flow in a channel of length L, the infiltration coefficient may be expressed as a function of I and L:

$$K = -\frac{\ln(1-I/100)}{L} \tag{3.12}$$

As a result, for a given value of the infiltration coefficient, the losses will be larger as the length of the channel increases.

Figures 3.1 to 3.4 show the upstream inflow IUH for different infiltration losses and different characteristics of the channel. The slope of the bottom of the channel and the reference depth and velocity were chosen such that the implicit Manning's roughness coefficient was between

0.030 and 0.065, a reasonable range for natural channels. As it can be seen, the reduction in the value of the peak is almost proportional to I, and the time to peak does not change. If the length of the channel is increased by a factor of two, as it is the case in Figures 3.1 and 3.2, the form of u(t) changes from a very rapid response to a relatively slow one, indicating that the wave was attenuated in the second half of the channel. Kirshen and Bras (1982) give a physical interpretation of Equation 3.10: the first term represents the dynamic component of the wave and occurs at time $t=L/c_1$, time when the wavefront, moving with a dynamic propagation speed $c_1= v_o + (gy_o)$, reaches the downstream end of the channel; the second term, constitutes the kinematic component, whose center of mass is moving with a mean velocity equal to $1.5v_o$, indicating that it dissipates slower than the dynamic component. As one could expect, both components are affected by infiltration losses. Looking at the expression for the parameter p in Equation 3.10, if F_o is less than 1/3, the infiltion reduces the dynamic part of the response. For F_o greater than 1/3 the dynamic response is enhanced. Given the complicated expression for the kinematic component, no general relationship with K can be inferred.

Finally, note that in order to make the values of I equal, the corresponding values of K in Figure 3.2 had to be reduced to half of those in Figure 3.1.

The response of the channel to an instantaneous input at its most upstream point h(x,t), can be interpreted as the conditional PDF of the time that a drop entering at the upstream extreme of the channel spends travelling a given distance x, $f_{T|X}(x,t)$. This PDF is a mixed type distribution: a continuous part defined by h(x,t) itself, with an area

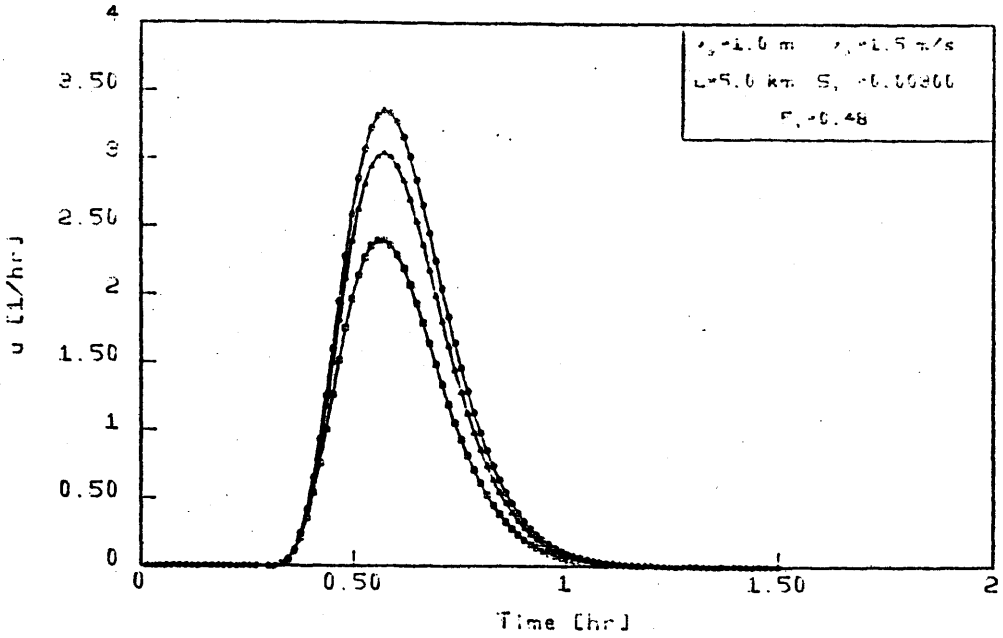

Upstream inflow response for different infiltration losses
○ I=0.0% △ I=10.0% □ I=30.0%

Figure 3.1

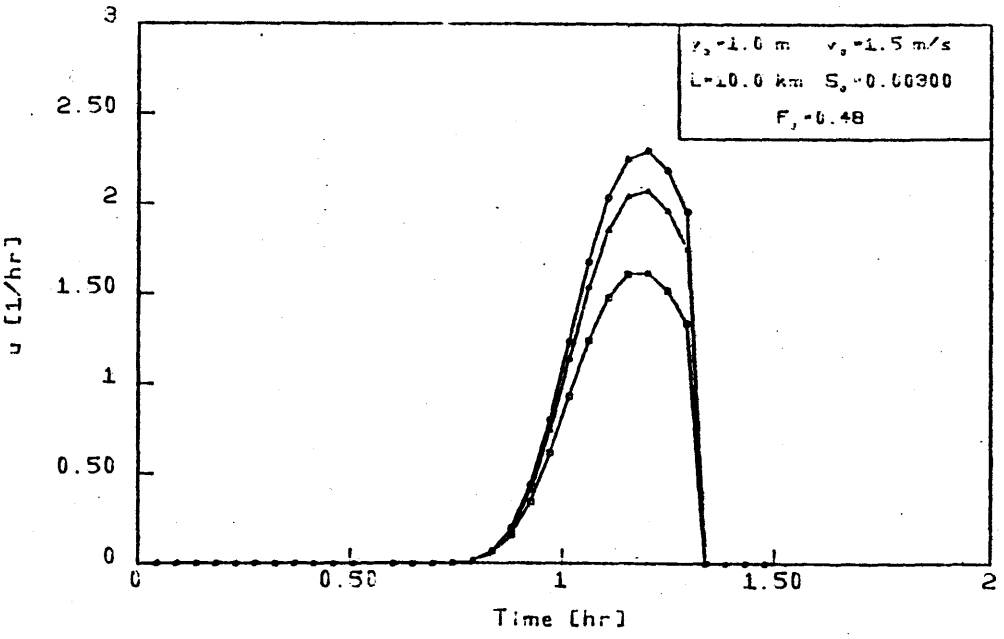

Upstream inflow response for different infiltration losses
○ I=0.0% △ I=10.0% □ I=30.0%

Figure 3.2

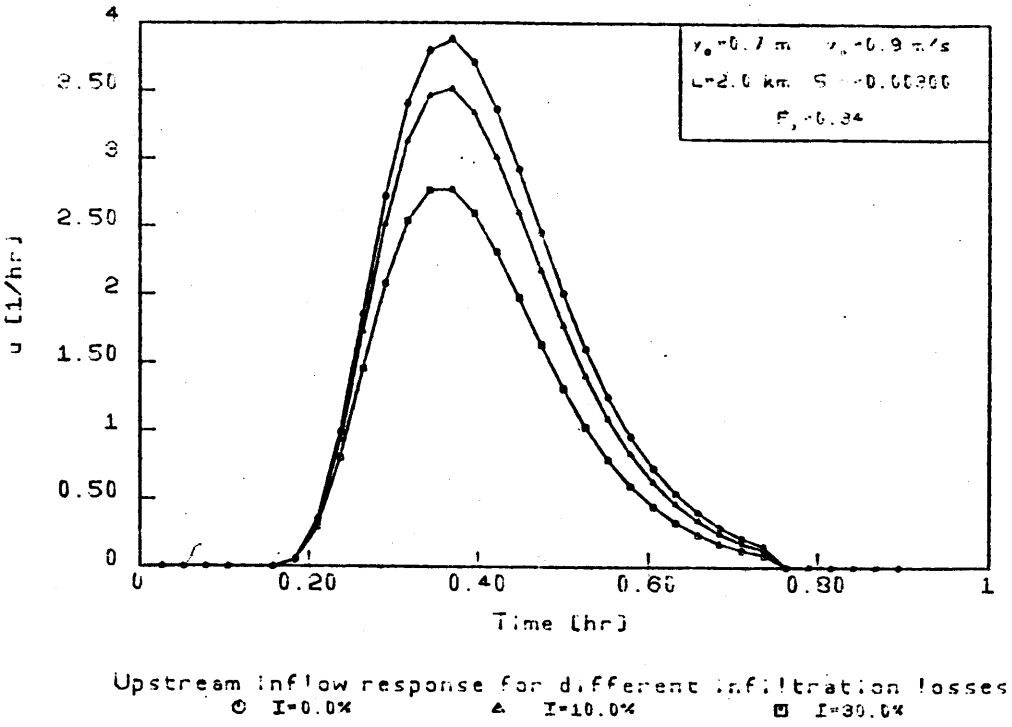

Upstream inflow response for different infiltration losses
© I=0.0% △ I=10.0% □ I=30.0%

Figure 3.3

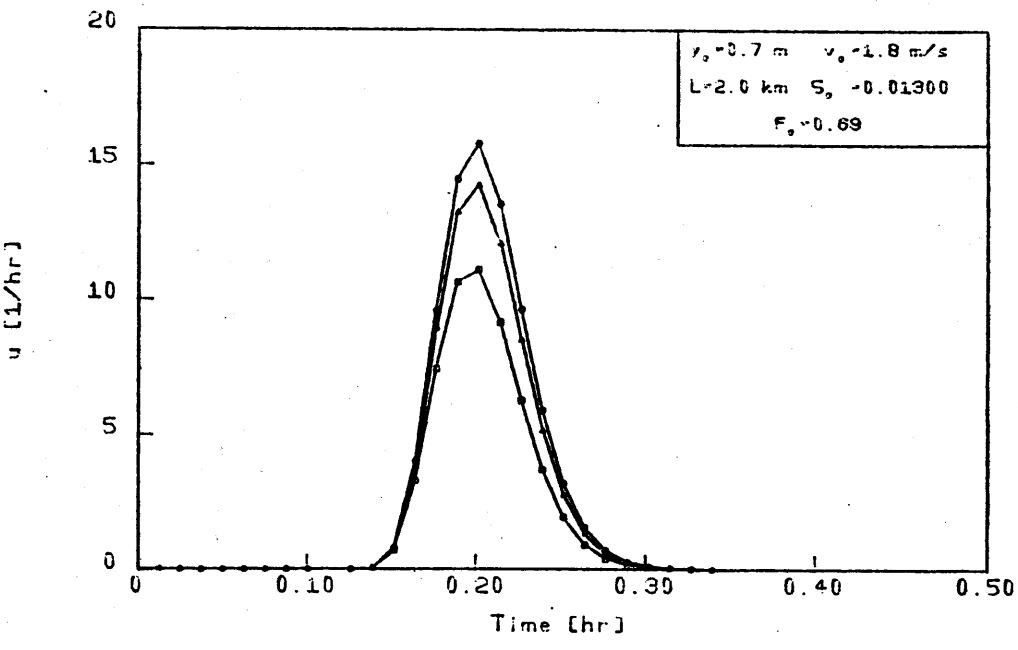

Upstream inflow response for different infiltration losses
© I=0.0% △ I=10.0% □ I=30.0%

Figure 3.4

equal to e^{-Kx} and a discrete part given by a spike at infinity with a value of $1-e^{-Kx}$. Formally,

$$f_{T|X} = \begin{cases} h(x,t) & t \geq 0 \\ P_{T|X}(x,t) = 1-e^{-Kx} & t = \infty \end{cases} \tag{3.13}$$

The continuous part involves the travel time of those drops that reach point x, whereas the spike represents the travel time that a drop that infiltrates along the interval [0,x] takes to reach x(i.e., the infiltration event constitutes an absorbing state). The probabilistic interpretation of the upstream inflow IUH, u(t), where x=L, beomes:

$$f_T^u(t) = \begin{cases} h(L,t) & t \geq 0 \\ P_T^u(t) = 1-e^{-KL} & t = \infty \end{cases} \tag{3.14}$$

Figure 3.5 shows $f_T^u(t)$.

3.4 The Lateral Inflow Response

Recalling the derivation of the geomorphologic IUH, the PDF of the travel time of a drop entering anywhere in the channel and travelling to its outlet is required. Kirshen and Bras (1982) derived this PDF for the case of no infiltration losses. This section will present its derivation considering these losses.

For a given channel of length L, the landing spot y of the drop must be between 0, the upstream end, and L, the outlet of the channel. The probability that the drop lands at y is the same for all y within the interval [0,L]. Let x=L-y be defined as the distance between the landing spot and the outlet. Therefore, the following PDF of x may be established:

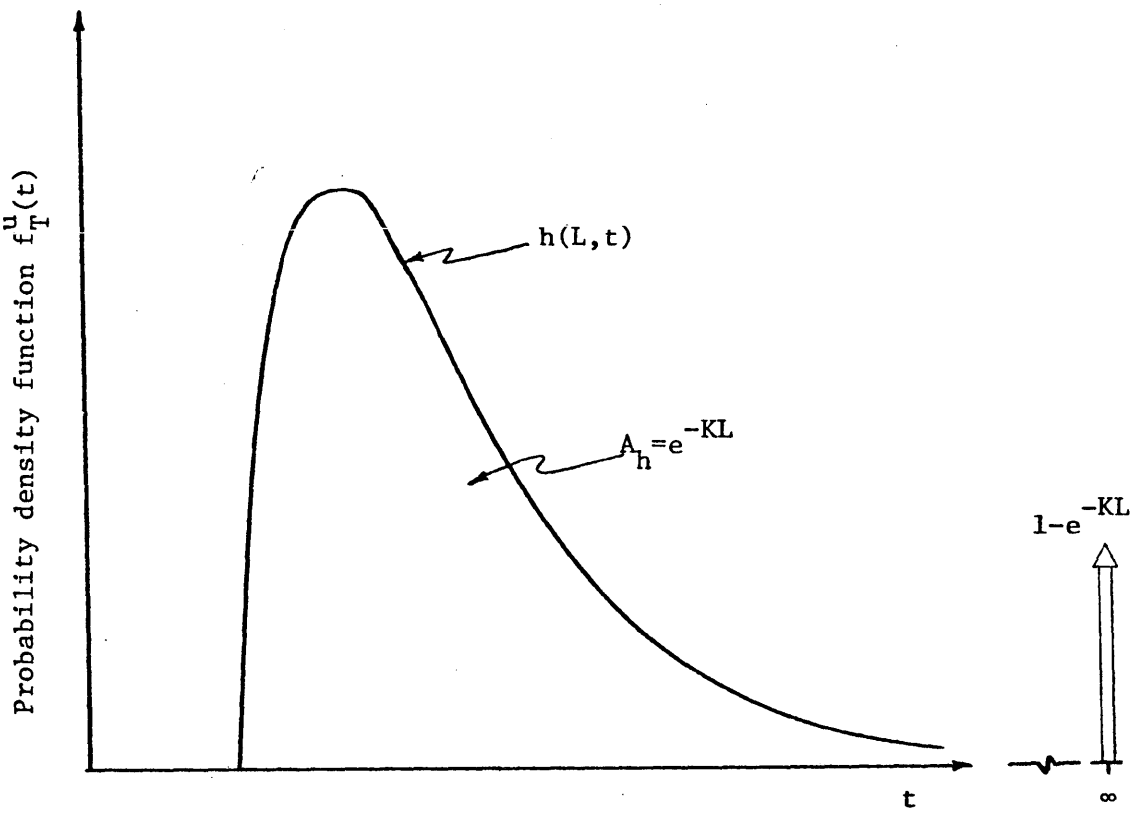

Probabilistic interpretation of the upstream inflow IUH

Figure 3.5

$$f_X(x) = \begin{cases} \frac{1}{L} & 0 \leq x \leq L \\ 0 & \text{otherwise} \end{cases} \tag{3.15a}$$

In the previous section, the conditional PDF of a drop's travel time along a given distance x, $f_{T|X}(x,t)$, was given. The interest here is the PDF of the travel time of a drop landing anywhere along the length of the channel, which is given by the unconditional PDF corresponding to $f_{T|X}(x,t)$, denoted $f_T^r(t)$:

$$f_T^r(t) = \int_o^L f_{T|X}(x,t) f_X(x) dx$$

or using Equation 3.13:

$$f_T^r(t) = \begin{cases} \int_o^L h(x,t) f_X(x) dx & t \geq 0 \\ \int_o^L P_{T|X}(x,t) f_X(x) dx & t = \infty \end{cases} \tag{3.15b}$$

In the above equation, the first term constitutes the continuous part of $f_T^r(t)$, and the second one the discrete part with a spike at infinity. Introducing Equation 3.15a, $f_T^r(t)$ becomes:

$$f_T^r(t) = \begin{cases} \frac{1}{L}\int_o^L h(x,t) dx & t \geq 0 \\ \frac{1}{L}\int_o^L P_{T|X}(x,t) dx & t = \infty \end{cases} \tag{3.16}$$

Evaluation of the first term of this equation, in which h(x,t) is given by Equation 3.10, yields:

$$r(t) = \frac{1}{L} \int_o^L h(x,t)dx = g_1(t) + g_2(t) \tag{3.17}$$

where

$$g_1(t) = \begin{cases} \frac{c_1}{L} \exp(-pc_1t) & t \leq L/c_1 \\ 0 & t > L/c_1 \end{cases} \tag{3.18}$$

and

$$g_2(t) = \frac{(d/a)^{\frac{1}{2}}\exp(-rt)}{L} \int_o^{L_1} x\exp(zx) \frac{I_1[d^{\frac{1}{2}}((t-x/c_1)(t-x/c_2))^{\frac{1}{2}}/a]}{((t-x/c_1)(t-x/c_2))^{\frac{1}{2}}}dx \tag{3.19}$$

where $$\begin{cases} L_1 = c_1t & t \leq L/c_1 \\ L_1 = L & t > L/c_1 \end{cases}$$

Since a closed form solution of the above integral does not exist, it must be evaluated numerically.

On the other hand, the second term of Equation 3.16 is:

$$\frac{1}{L} \int_o^L P_{T|X}(t,x)\, dx$$

$$= \frac{1}{L} \int_o^L (1-e^{-Kx})\, dx = 1 - \frac{1}{KL}(1-e^{-KL}) \tag{3.20}$$

Therefore,

$$f_T^r(t) = \begin{cases} r(t) & t \geq 0 \\ p_T^r(t) = 1 - (1-e^{-KL})/KL & t = \infty \end{cases} \qquad (3.21)$$

where Equations 3.18 and 3.19 define the expression for r(t). Figure 3.6 shows this PDF. The continuous part involves the travel time of a drop that enters the channel anywhere and reaches the outlet, while the value of the spike is the probability that a drop landing anywhere infiltrates before the outlet. The area under the continuous part, A_r, is equal to $(1-e^{-KL})/KL$, as it is proven in Appendix A. This quantity added to the value of the spike at infinity results a total area of 1, a property of any probability density function. Besides, A_r represents the fraction of the water that enters along the channel and reaches the outlet.

The term r(t) may be interpreted as the lateral inflow response, i.e., the response of the channel to an instantaneous input at every point along its length. As a result, an individual wave will be originated at each point. The total response due to the wave fronts is given by Equation 3.18. This response is zero after $t=L/c_1$ since at this time all the wave fronts, travelling at the dynamic velocity $c_1 = v_o + (gy_o)^{\frac{1}{2}}$, have reached the outlet of the channel. The total response due to the wave bodies is given by Equation 3.19. In this equation, for $t \leq L/c_1$, the upper integration limit is $L_1 = c_1 t$, which means that waves originating between the outlet and L_1 can contribute to the response at the outlet at time t; however, those waves starting beyond L_1 cannot yet contribute. For $t > L/c_1$, all waves are contributing to the response and the upper limit changes to $L_1 = L$. Figure 3.7 shows the relative contributions of wave fronts and wave bodies to the lateral inflow response, for a fixed value of the infiltration coefficient.

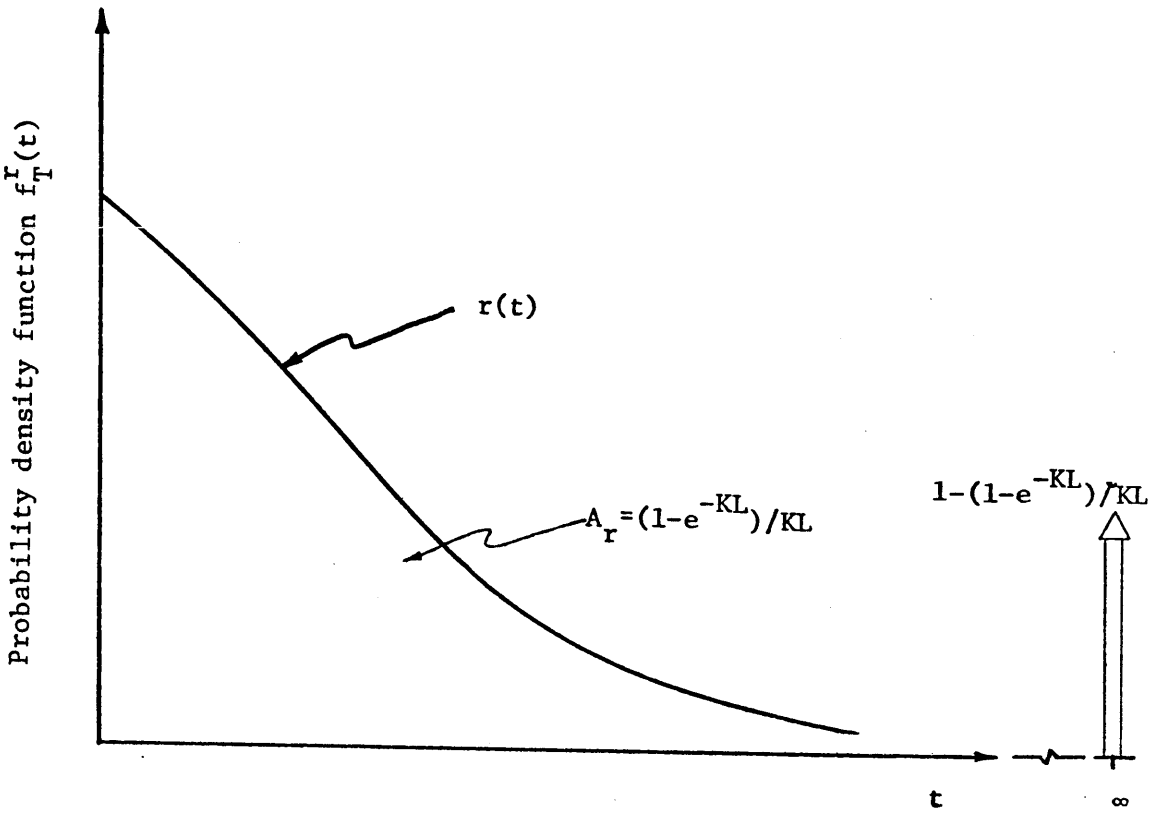

Probabilistic interpretation of the lateral IUH

Figure 3.6

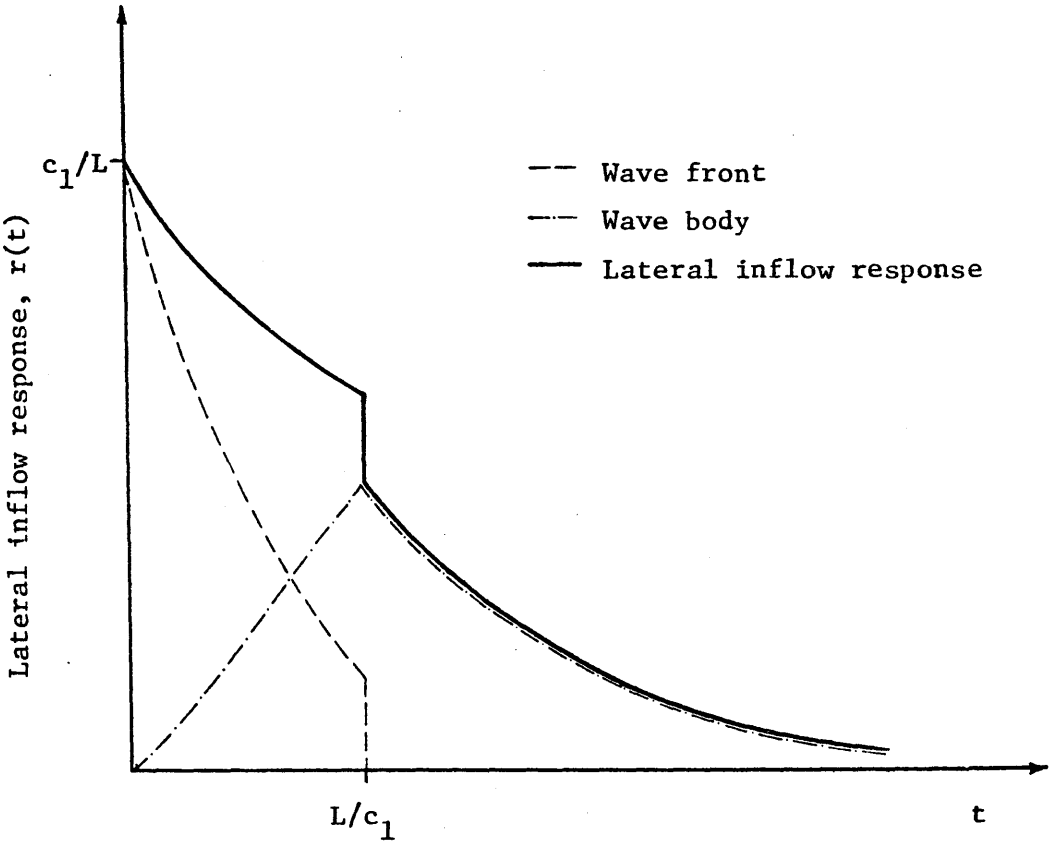

Contribution to the wave front and wave body to the lateral inflow response (From Kirshen and Bras, 1982)

Figure 3.7

Similarly to the upstream inflow response, if I is the infiltrated percentage of the flow in a channel of length L, the corresponding infiltration coefficient can be expressed as an implicit function of I and L (see Equation 3.21):

$$KL = \frac{1 - e^{-KL}}{1-I/100} \tag{3.22}$$

Plots of r(t) for infiltration losses of 0, 10 and 30 percent, and different characteristics of the channel are presented in Figures 3.8 to 3.11. As it can be observed, the ordinate of each curve starts at the corresponding value of c_1/L (see Equation 3.17), independent of the infiltration losses. Figures 3.8 and 3.9 correspond to a very steep channel (the reference Froude number is 0.95), for two values of its length, i.e., 1 and 2 km. respectively. In both the response is very fast, and a high percentage of the drops respond before $t=c_1/L$; for I=0, the shape of the response is basically rectangular; however, as I increases, it tends to decay. Figure 3.10 shows the responses for a channel of lesser slope with a length of 1 km. and reference depth and velocity of 1.0 m and 1.5m/s., respectively. In this case, they follow closely the shape of an exponential decay. Finally, in Figure 3.11, the lateral inflow responses are plotted for a longer channel and less rapid reference flow. Their shape lie between that of Figure 3.10 and those of Figures 3.8 and 3.9.

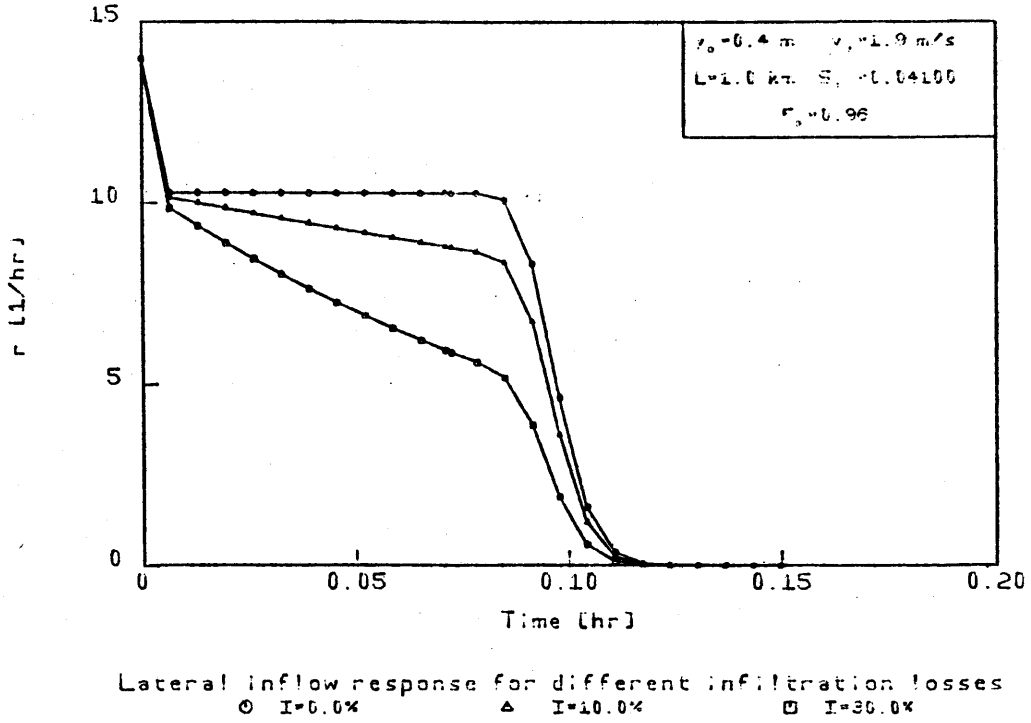

Figure 3.8

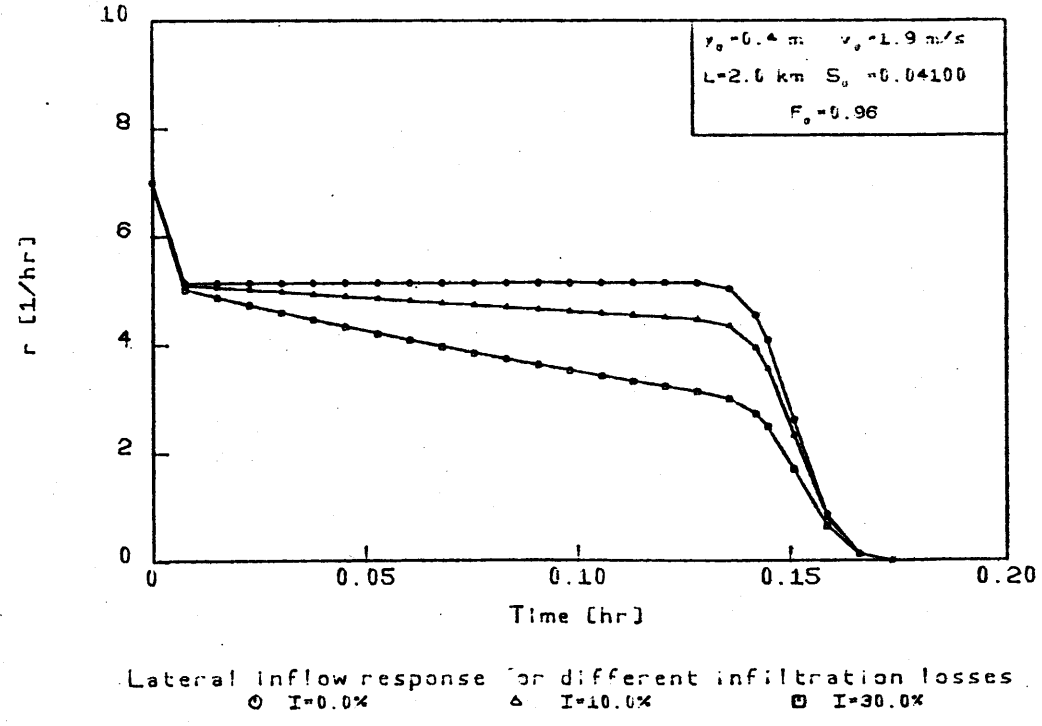

Figure 3.9

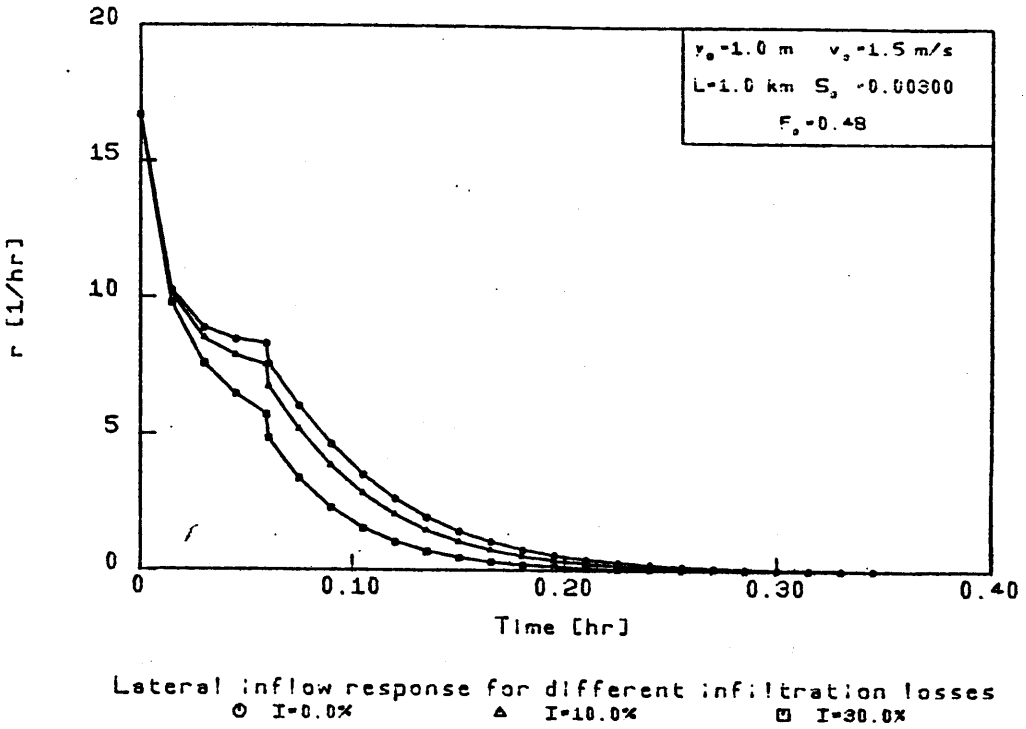

Figure 3.10

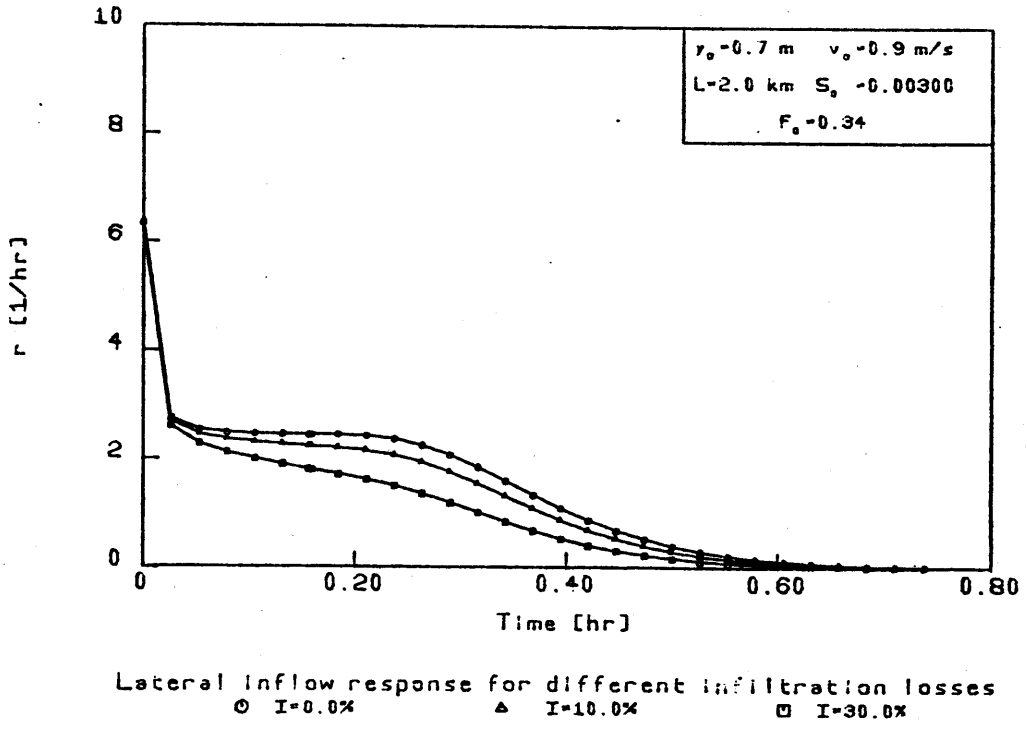

Figure 3.11

The fact that the ordinate of r(t) starts at the value c_1/L, independent of I, along with the shape similitude, in some cases, of the lateral inflow response with an exponential decay, suggests a modification to the linear reservoir response, assumed in the geomorphologic IUH by Rodriguez-Iturbe and Valdes (1979). In order to take into account the infiltration losses the following distribution time in channels may be assumed:

$$r_e(t) = \mu e^{-\lambda t} \tag{3.23}$$

where,

$$\mu = \frac{c_1}{L}$$

and λ is computed such that the are under $r_e(t)$ is 1-I:

$$\lambda = \frac{c_1}{L(1-I/100)}$$

Figures 3.12 to 3.17 present some comparisons between the linearized solution r(t), and the exponential approximation $r_e(t)$, of the lateral inflow response. Figures 3.12 and 3.13 show the comparison for a channel with a length of 5 km, a bottom slope of 3 m/km and reference depth and velocity of 1 m and 1.5 m/s, respectively. Infiltration losses of 0 and 30 percent are used, respectively. As can be seen, the linearized solution responds slower at the beginning, but after approximately 0.2 hours, it becomes faster. In the case of the infiltration losses of 30 percent, the two curves are closer than for zero losses. In Figures 3.14 and 3.15, the responses are plotted for the same channel but with a length of 1 km only. The comparison shows similar results as before, but now the curves are much closer. Figure 3.16 plots r(t) and $r_e(t)$ for the same

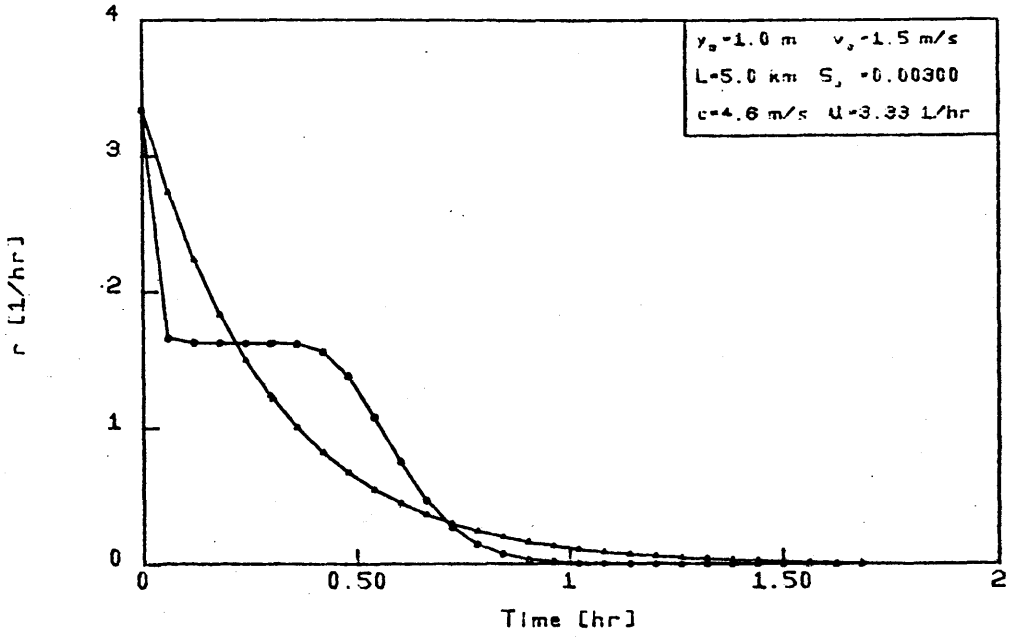

Exponential assumption vs Linearized solution
for the lateral channel response
⊙ Linearized solution ▲ Exponential assumption
I=0.0%

Figure 3.12

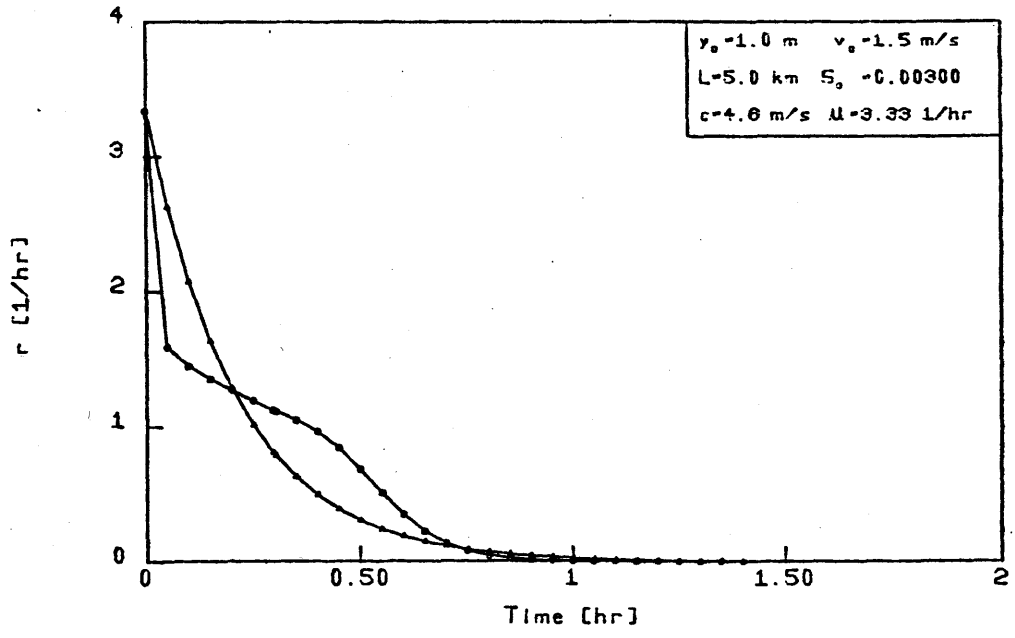

Exponential assumption vs Linearized solution
for the lateral channel response
⊙ Linearized solution ▲ Exponential assumption
I=30.0%

Figure 3.13

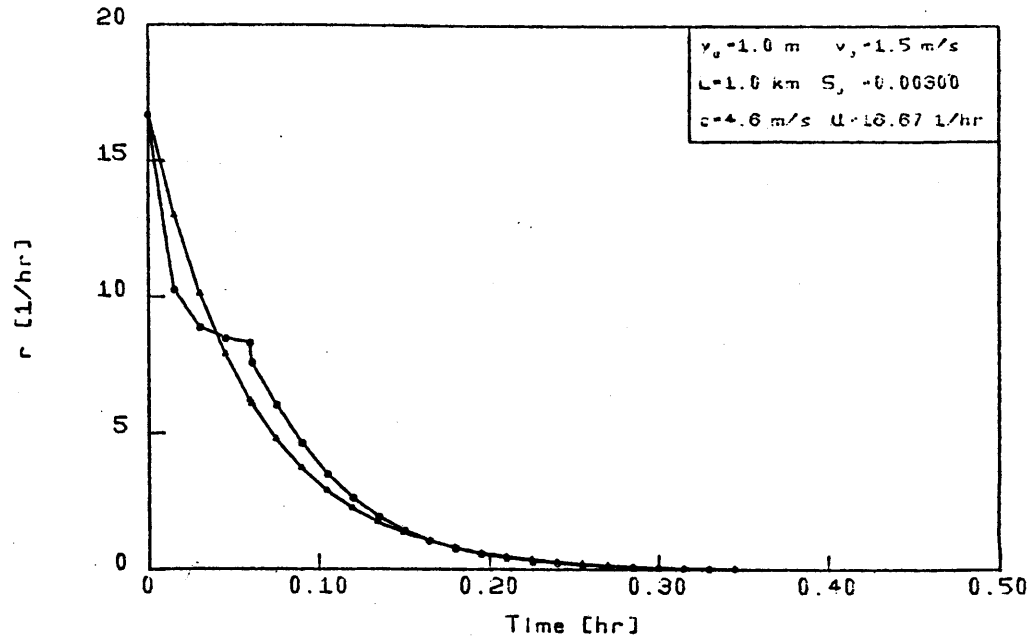

Exponential assumption vs Linearized solution
for the lateral channel response
○ Linearized solution △ Exponential assumption
I=0.0%

Figure 3.14

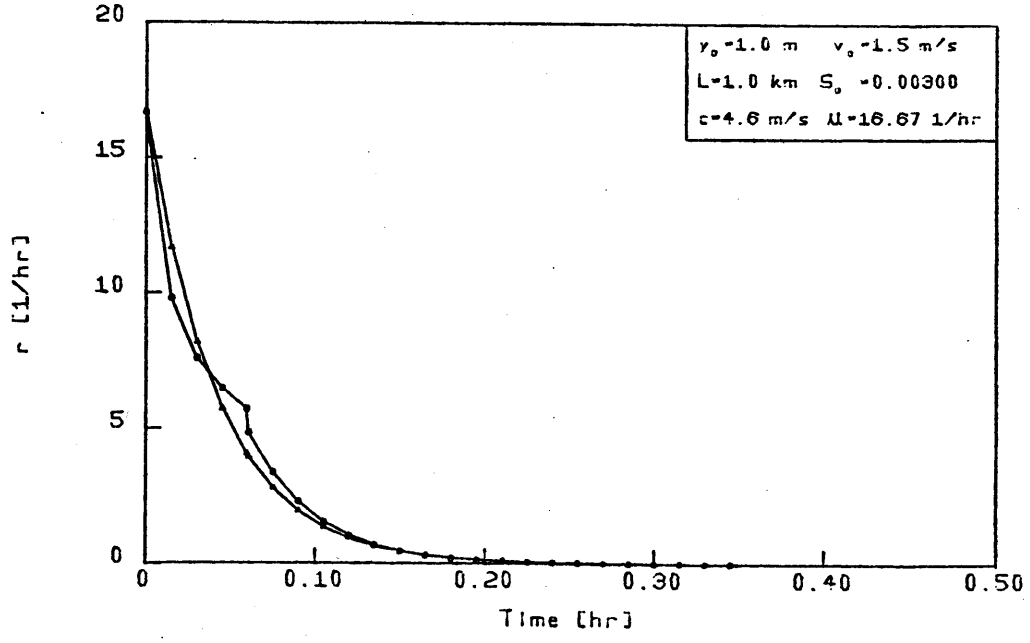

Exponential assumption vs Linearized solution
for the lateral channel response
○ Linearized solution △ Exponential assumption
I=30.0%

Figure 3.15

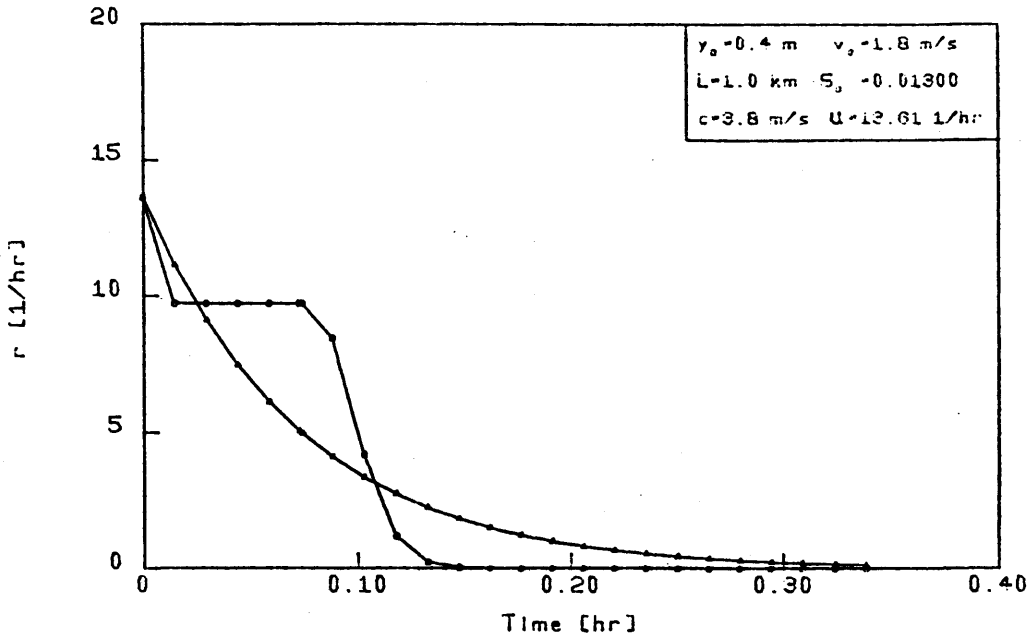

Exponential assumption vs Linearized solution
for the lateral channel response
⊙ Linearized solution ▲ Exponential assumption
I=0.0%

Figure 3.16

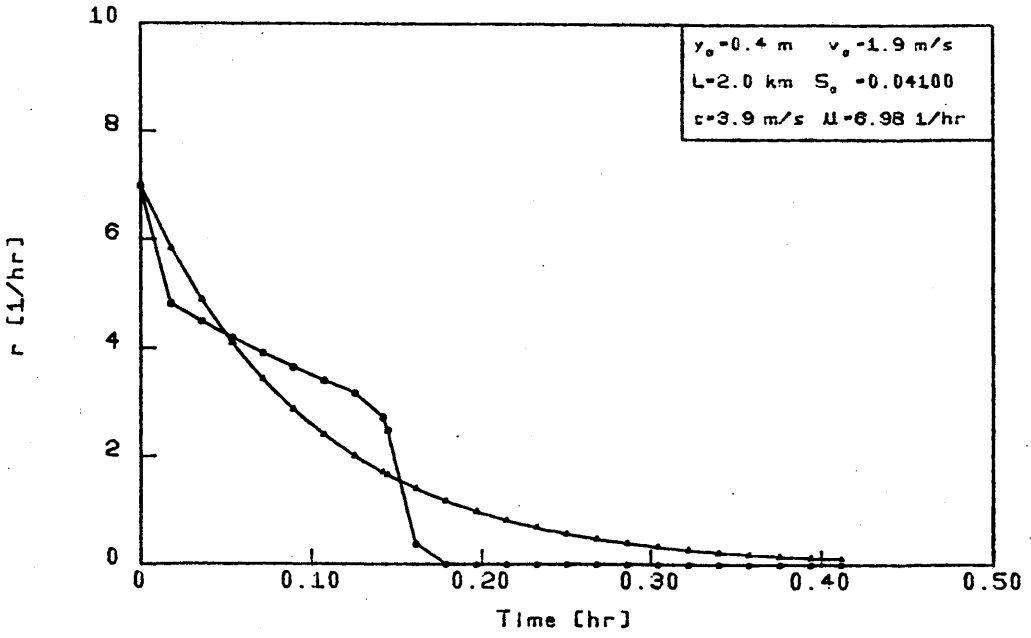

Exponential assumption vs Linearized solution
for the lateral channel response
⊙ Linearized solution ▲ Exponential assumption
I=30.0%

Figure 3.17

channel of Figure 3.8 with no infiltration losses, whereas Figure 3.17 presents the comparison for the channel of Figure 3.9 with I=30 percent. In general, the shorter for channel and the bigger the losses, the similarity of r(t) and $r_e(t)$ increases.

3.5 Summary

This chapter presents the derivation of two analytical expressions for the approximated linear response of a channel with infiltration losses. The first one corresponds to the response to an instantaneous input at the upstream of the channel, denoted u(t). The other response constitutes that to an instantaneous input originating anywhere along the channel, r(t). Both of them are functions of the infiltration coefficient, the channel slope and length, and the reference depth and velocity. From the characteristics of r(t), a modification to the conceptual linear reservoir response, was proposed in order to take into account the infiltration losses.

The responses, which describe the movement of the flood wave along the channel, are interpreted as the PDFs of the time that a drop spends travelling to reach the outlet of the channel. These PDFs will be used in the next chapter to determine the IUH and the discharge hydrograph of a given basin.

Chapter 4

THE BASIN IUH AND DISCHARGE HYDROGRAPH

4.1 Introduction

Chapter 2 presented the derivation of the geomorphologic IUH, and the resulting expression for the discharge hydrograph when the GIUH is convoluted with a rainfall input of constant effective intensity and given duration. In Chapter 3, a physically based linear channel respone was obtained from the equations of motion for unsteady flow, including infiltration losses. The response of the channel was interpreted as the probability density function of the amount of time that an individual drop of water takes to travel to the outlet of the channel. This chapter utilizes this PDF, which is more physically based than the linear reservoir assumption, in the expressions for the geomorphologic IUH.

4.2 The Basin IUH and Discharge Hydrograph-Linearized Solution

Equation 3.21 gives the analytical expression for the PDF of the travel time needed by a drop entering anywhere along the channel to reach the outlet, $f_T^r(t)$, which results from the linearized solution of the equations of motion. Replacing $f_T^r(t)$ in Equation 2.11, the IUH becomes:

$$h(t) = \Theta_1 P_{12} f_T^{r(1)}(t) * f_T^{r(2)}(t) * f_T^{r(3)}(t) + \Theta_1 P_{13} f_T^{r(1)}(t) * f_T^{r(3)}(t) + \Theta_2 f_T^{r(2)}(t) * f_T^{r(3)}(t) + \Theta_3 f_T^{r(3)}(t) \quad (4.1)$$

As in Equation 2.11, the solution of this equation may be calculated using Laplace transforms. The Laplace transform of $f_T^{r(i)}(t)$ is (see Equation A.23):

$$\mathcal{L}\left\{f_T^{r(i)}(t)\right\} = \frac{1}{L_i}\int_o^{L_i} e^{-K_i x} W_i(x,s)\,dx$$

$$= \frac{1}{B_i L_i}\left[e^{B_i L_i} - 1\right] \qquad (4.2)$$

where

$$B_i = -(a_i s^2 + b_i s + c_i) + e_i s + f_i + K_i \qquad (4.3)$$

In the above expressions, the subscript i indicates the order of the channel, W(x, s) is the Laplace transform of $f_T^u(t)$, L is the length of the channel, K is the infiltration factor, a, b, c are defined in Equation 3.10, and e and f are:

$$e = \frac{v_o}{g y_o (1-F_o^2)}$$

$$f = \frac{K}{2} + \frac{3}{2}\frac{S_o}{y_o}\frac{1}{(1-F_o^2)}$$

where the right hand side parameters have been defined previously. Proceeding in a similar manner as in Chapter 2, the basin IUH is then:

$$h(t) = \Theta_1 P_{12} \mathcal{L}^{-1} \left\{ \frac{1}{B_1 L_1} \left(e^{B_1 L_1} - 1 \right) \frac{1}{B_2 L_2} \left(e^{B_2 L_2} - 1 \right) \frac{1}{B_3 L_3} \left(e^{B_3 L_3} - 1 \right) \right\}$$

$$+ \Theta_1 P_{13} \mathcal{L}^{-1} \left\{ \frac{1}{B_1 L_1} \left(e^{B_1 L_1} - 1 \right) \frac{1}{B_3 L_3} \left(e^{B_3 L_3} - 1 \right) \right\}$$

$$+ \Theta_2 \mathcal{L}^{-1} \left\{ \frac{1}{B_2 L_2} \left(e^{B_2 L_2} - 1 \right) \frac{1}{B_3 L_3} \left(e^{B_3 L_3} - 1 \right) \right\}$$

$$+ \Theta_3 \mathcal{L}^{-1} \left\{ \frac{1}{B_3 L_3} \left(e^{B_3 L_3} - 1 \right) \right\} \qquad (4.4)$$

Unfortunately, the above equation cannot be solved analytically, and a subroutine (IMSL, 1980) is used to solve it numerically. The same occurs with the discharge hydrograph Q(t), which results from the convolution of h(t), as given by Equation 4.4, with a rainfall event, represented by Equation 2.16. The corresponding expression for Q(t) is

$$Q(t) = \frac{\Theta_1 P_{12} A_3}{b} \mathcal{L}^{-1} \left\{ \frac{1}{B_1 L_1} \left(e^{B_1 L_1} - 1 \right) \frac{1}{B_2 L_2} \left(e^{B_2 L_2} - 1 \right) \cdot \right.$$

$$\left. \frac{1}{B_3 L_3} \left(e^{B_3 L_3} - 1 \right) \frac{1 - e^{-t_e s}}{s} i_e \right\}$$

$$+ \frac{\Theta_1 P_{13} A_3}{b} \mathcal{L}^{-1} \left\{ \frac{1}{B_1 L_1} \left(e^{B_1 L_1} - 1 \right) \frac{1}{B_3 L_3} \left(e^{B_3 L_3} - 1 \right) \frac{1 - e^{-t_e s}}{s} i_e \right\}$$

$$+ \frac{\Theta_2 A_3}{b} \mathcal{L}^{-1} \left\{ \frac{1}{B_2 L_2} \left(e^{B_2 L_2} - 1 \right) \frac{1}{B_3 L_3} \left(e^{B_3 L_3} - 1 \right) \frac{1 - e^{-t_e s}}{s} i_e \right\}$$

$$+ \frac{\Theta_3 A_3}{b} \mathcal{L}^{-1} \left\{ \frac{1}{B_3 L_3} \left(e^{B_3 L_3} - 1 \right) \frac{1 - e^{-t_e s}}{s} i_e \right\} \qquad (4.5)$$

where A_3 is the area of the basin, t_e is given in hr., i_e in cm/hr. and b is a conversion factor equal to 0.36 in order to obtain Q(t) in m^3/sec.

Before further discussion of h(t) and Q(t), the following subsection deals with the estimation of the parameters involved in Equation 4.4.

4.2.1 Parameter Estimation

In order to calculate the IUH derived from the linearized solution, for a given basin, two sets of parameters must be estimated: parameters representing the physiographic characteristics of the basin and individual channels, and parameter representing the dynamic component of the response.

The physiographic characteristics of the basin are expressed in terms of the Horton's numbers, R_A, R_B and R_L. The characteristics of the individual channels are lumped according to stream order. The average channel length and the geometric mean of the slope are used to represent the channel's physiographic characteristics. All the above parameters may be estimated easily from topographic maps, aerial photographs, or satellite imagery.

The reference depth y_o, reference velocity v_o and the infiltration factor, K, represent the dynamic component of the response. These parameters, are also lumped according to the order of the stream, and their estimation may involve field inspections and some engineering judgement. Following is a proposed procedure to estimate y_o and v_o based on Manning's equation, and on the expressions $c_1 = v_o + (gy_o)^{\frac{1}{2}}$ and $F_o = v_o/(gy_o)^{\frac{1}{2}}$:

1. From visual inspection, estimate, for each order stream i, the average Manning's roughness coefficient n and the Froude number under steady state conditions, F_o.
2. Using the estimated values of S_o for each order, calculate the respective values of the celerity of the wave flood as

$$c_1 = n^3 \, F_o^3 \, g^2(1+F_o)/S_o^{1.5} \tag{4.6}$$

3. Calculate y_o and v_o for each order stream.

$$y_o = \frac{c_1}{g(1+F_o)^2} \tag{4.7}$$

$$v_o = \frac{c_1 F_o}{1+F_o} \tag{4.8}$$

where g is the gravitational acceleration in m/sec^2, and the units of c_1 and v_o are m/sec, and y_o is given in m.

The procedure can be modified slightly, in case another estimate of the celerity of the wave is available. In step 2, instead of calculating c_1, Equation 4.6 can be solved for F_o by trial and error.

If one assumes that c_1 is related somehow to the specific rainfall event for which the IUH is being calculated (greater the intensity, greater the velocity of the flood wave), then there does not exist an unique IUH characteristic of the basin. This means that the nonlinearities present in the rainfall-runoff process are reflected in such a way that the IUH would be a function of both the rainfall input and the geomorphology, as Rodriguez-Iturbe et al., (1982) recognize. However, no attempt is made here to relate the celerity of the flood wave to the rainfall input characteristics.

Finally the infiltration factor, K, may be estimated from isolated streamflow measurements performed in reaches where no inflows from tributaries are present. From these measurements, the percentage of the flow infiltrated can be evaluated and introduced in Equation 3.12 to obtain an estimate of K.

4.2.2 Hydrographs for Three Basins

In this sub-section the IUHs and discharge hydrographs for three basins are presented. The first two correspond to sub-basins of the Indio basin, located in Puerto Rico, namely Morovis and Unibon basins, which have been studied in the context of the geomorphologic IUH by Valdes et al., (1979) and Kirshen and Bras (1982). For these basins Rodriguez-Iturbe et al. (1979) give the parameters and the discharge hydrographs resulting from a kinematic wave rainfall-runoff model. Some of these results will be used to check the hydrographs obtained here. Figure 4.1 shows the general layout of the Morovis and Unibon basins.

The third basin is Wadi Umm Salam, also studied by Kirshen and Bras (1982). This is a sub-basin of Wadi Abad, one of the largest wadis in Upper Egypt. Wadis like Wadi Umm Salam are subject to occasional flash floods, which cause damages to the downstream villages. Usually there are no rainfall or streamflow measurements at any location within the wadi. Thus, the geomorphologic IUH constitutes a useful tool to estimate the discharge due to specific storms in these wadis. In concept, only a topographic map or aerial photograph, estimation of the storm charcteristics, and perhaps a field inspection are required. Figure 4.2 presents the general layout of Wadi Umm Salam.

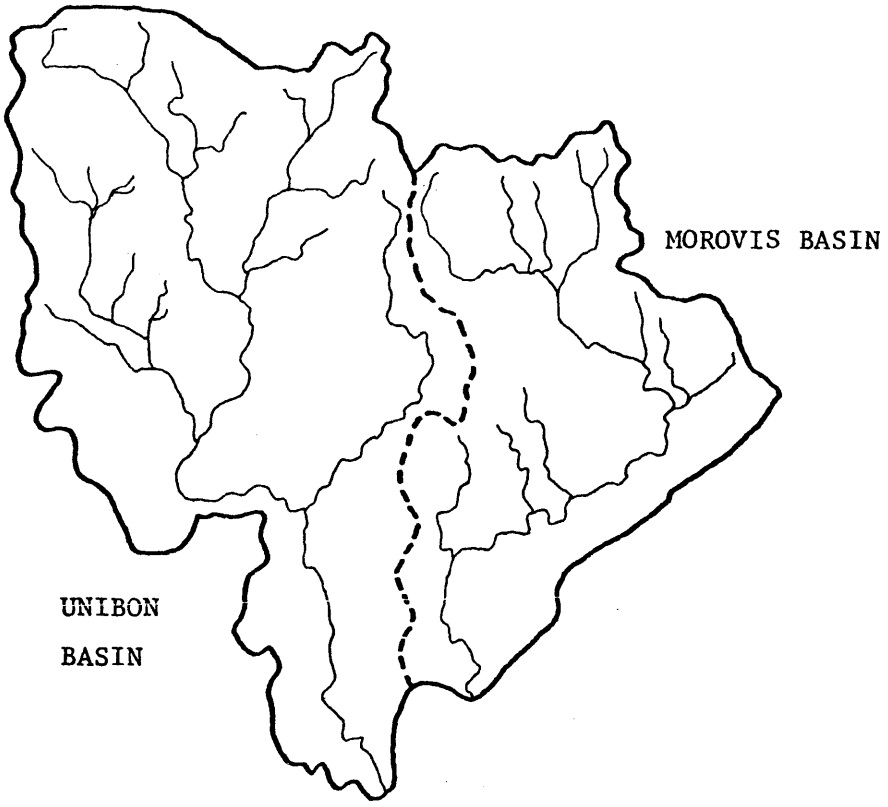

Figure 4.1 General layout of Morovis and Unibon basins

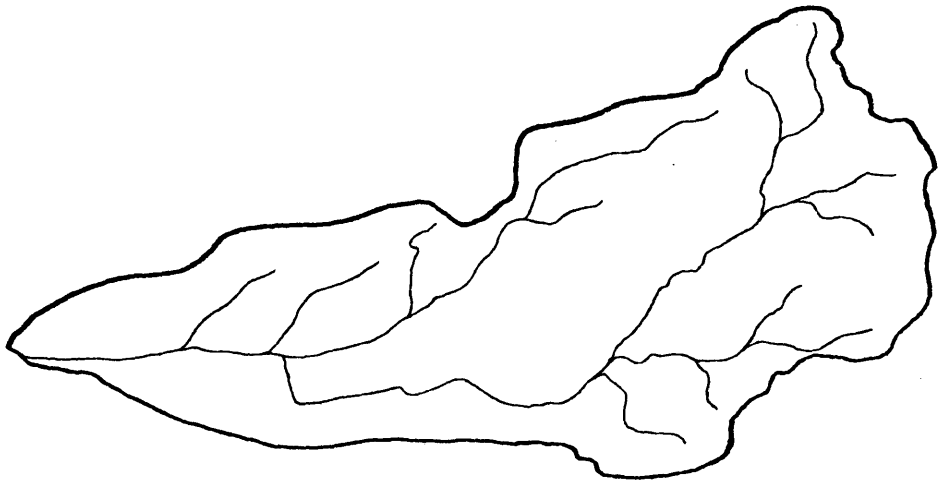

Figure 4.2 General layout of Wadi Umm Salam

TABLE 4.1

Comparisons Between the Rainfall-Runoff Model and the Linearized Solution

Basin	i_e (cm/hr)	t_e (hr)	Rainfall-Runoff Model Q_p (m^3/s)	Rainfall-Runoff Model T_p (hr)	Linearized Solution Q_p (m^3/s)	Linearized Solution T_p (hr)
Morovis	3	2	103	2.2	103	1.5
	3	3	112	3.0	106	1.5
Unibon	3	3	188	2.0	181	1.6
	3	3	194	3.0	183	1.7

Figures 4.3, 4.4, and 4.5 show the IUHs for the above basins using different combinations of the infiltration losses in the channels. Each figure contains the information on the values of I and the physiographic characteristics of the basin and the channels. The values of v_o and y_o were estimated according to the modified procedure proposed in sub-section 4.2.1, assuming a velocity of the wave flood of 3 m/sec. and an estimated value of the Manning's coefficient of about 0.067 for Morovis and Unibon (very steep channels, presumably with big rocks in the bed), and about 0.045 for Wadi Umm Salam. The responses of Morovis and Unibon are very similar, Morovis responding faster. The response of Wadi Umm Salam is slower, since it is not as mountainous as the others. The effect of the infiltration losses is clearly illustrated with the differences in the height and area under the IUHs.

Figures 4.6 and 4.7 present the discharge hydrographs for Morovis and Unibon basins when the IUHs of Figures 4.3 and 4.4 are convoluted with an effective rainfall of 3 cm/hr intensity and a duration of 2 hours. Similar hydrographs were obtained for a three-hour assumption. Table 4.1 compares the main characteristics of the discharge hydrographs obtained here for the Unibon and Morovis basins (I=0 percent) and those obtained by Rodriguez-Iturbe et al., (1979) using a rainfall-runoff model. As it can be seen, the agreement in the peaks is good, although in the case of Unibon, the peak velocity given by the rainfall-runoff model was 4 m/sec, greater than the 3 m/sec used for the velocity of the wave in the linearized solution. It is important to note that no adjustement of the linearized solution hydrographs, modifying v_o and y_o, was made. This means that

if the estimation of n was correct, the proposed procedure to estimate v_o and y_o is adequate.

There are no rainfall-runoff results in Wadi Umm Salam to which the hydrographs obtained here can be compared. However, Figures 4.8 to 4.11 present the hydrographs corresponding to rainfall with a return period of 100 years, for storm durations of 2.0, 1.5, 1.0 and 0.5 hours, and intensities of 1.8, 2.4, 3.7, and 7.3 cm/hr respectively (Kirshen and Bras, 1982). Again, the effect of the channel infiltration losses is significant.

An interesting exercise would be the comparison between the IUHs and discharge hydrographs obtained by Equations 4.4 and 4.5 and those produced by Equations 2.15 and 2.19. However, these comparisons would be valid only for I=0 percent. Therefore, Equations 2.15 and 2.19 must be modified slightly to allow comparisons for I greater than zero. This is done in the next section.

4.3 Linearized Solution vs. Exponential Assumption: A Comparison

Equations 2.15 and 2.19 give the IUH and the discharge hydrographs, when the linear reservoir assumption is used to represent the behavior of the channels forming the drainage network. These expressions are valid when no infiltration losses are considered. However, in Chapter 3, a modification to the linear reservoir response was proposed to account for infiltration. It is given by Equation 3.23. Its probabilistic interpretation is:

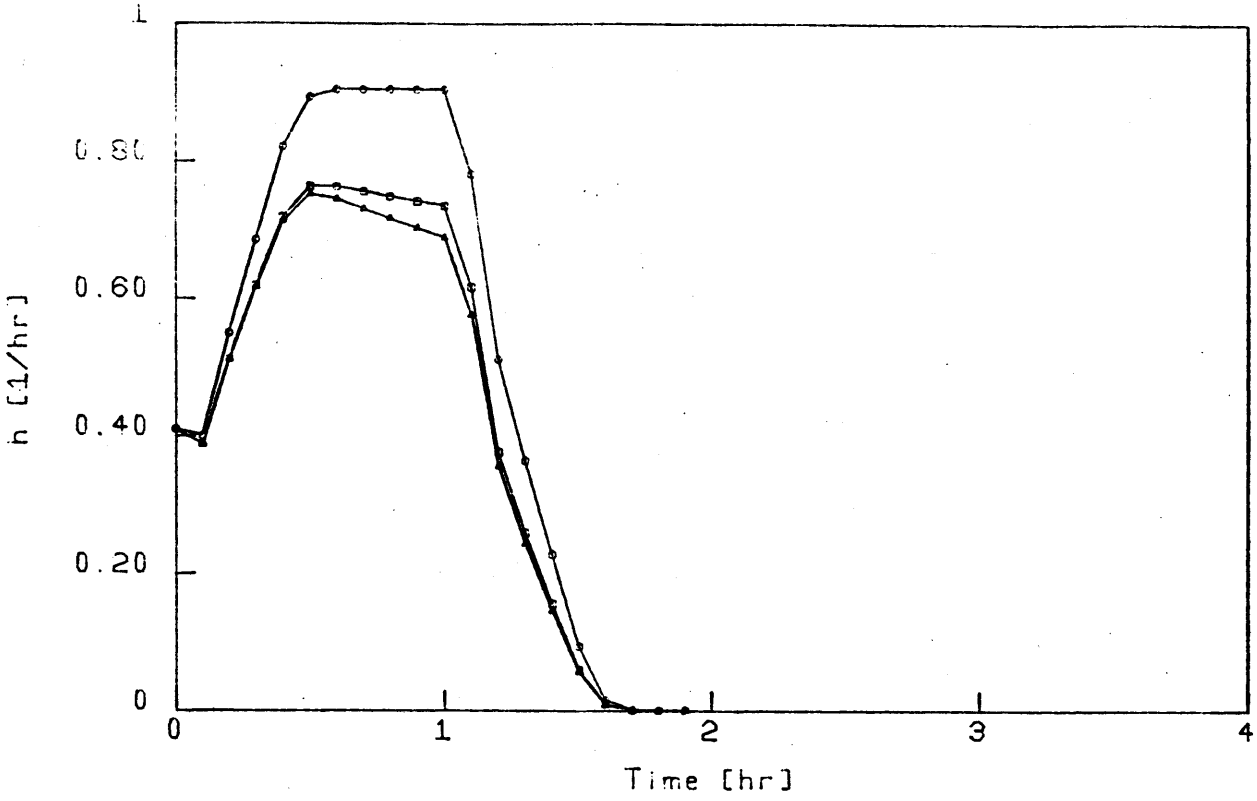

MOROVIS BASIN

Basin iuh for different infiltration losses

(Basin representation 1)

Characteristics:

	I(%)						
Order	1	2	3	Order	1	2	3
○	0.0	0.0	0.0	y_o (m)	0.25	0.30	0.30
△	10.0	10.0	10.0	v_o (m/s)	1.47	1.31	1.34
□	15.0	10.0	5.0	F_o	0.94	0.76	0.78
				S_o (m/km)	71.90	32.10	39.20
R_A=5.00	R_B=3.20	R_L=2.70		L (km)	1.10	3.00	8.00

p12=0.85 p13=0.15

Θ1=0.41 Θ2=0.29 Θ3=0.30

p(s1)=0.35 p(s2)=0.06 p(s3)=0.29 p(s4)=0.30

Figure 4.3

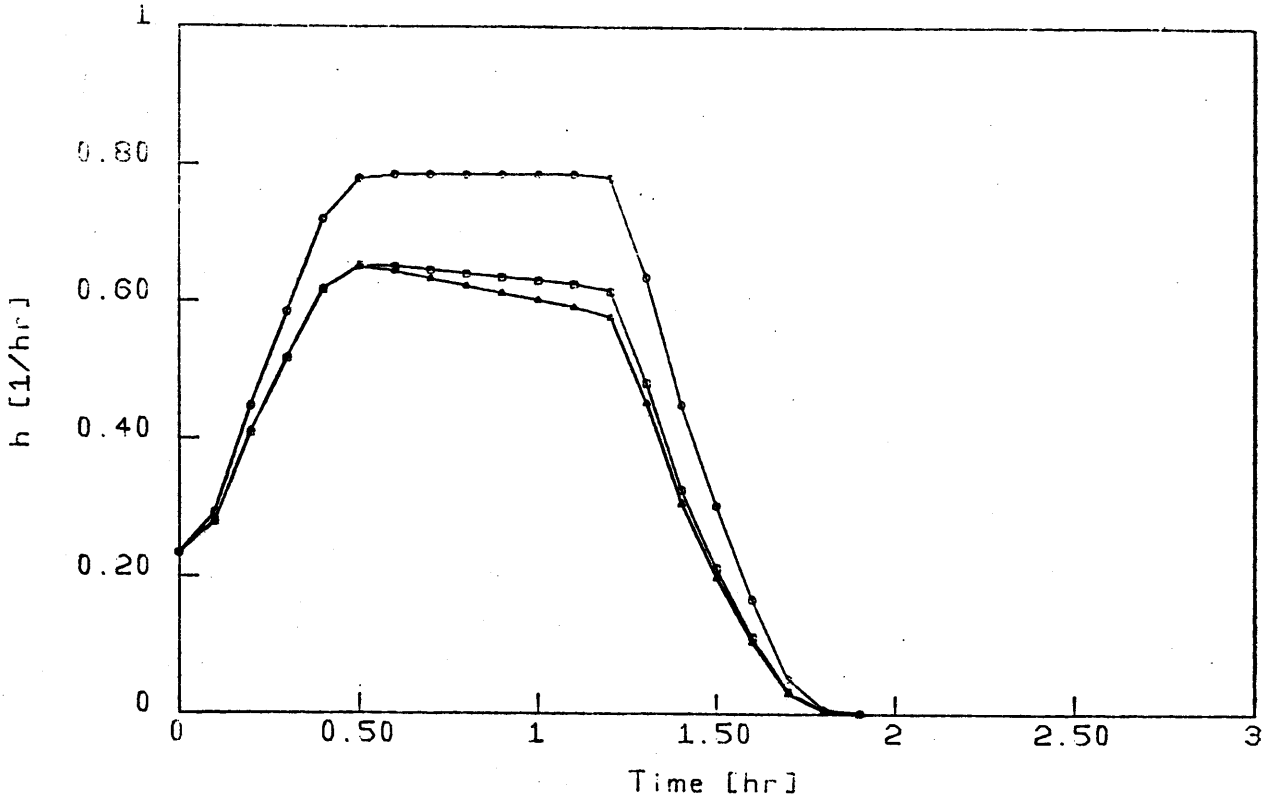

UNIBON BASIN

Basin iuh for different infiltration losses

(Basin representation 1)

Characteristics:

	I(%)						
Order	1	2	3	Order	1	2	3
○	0.0	0.0	0.0	y_o (m)	0.24	0.28	0.37
△	10.0	10.0	10.0	v_o (m/s)	1.50	1.40	1.25
□	15.0	10.0	5.0	F_o	0.98	0.85	0.66
				S_o (m/km)	82.70	46.60	23.30
R_A=5.60	R_B=4.00	R_L=2.80		L (km)	1.10	3.10	8.60

p12=0.79 p13=0.21

Θ1=0.51 Θ2=0.31 Θ3=0.18

p(s1)=0.40 p(s2)=0.11 p(s3)=0.31 p(s4)=0.18

Figure 4.4

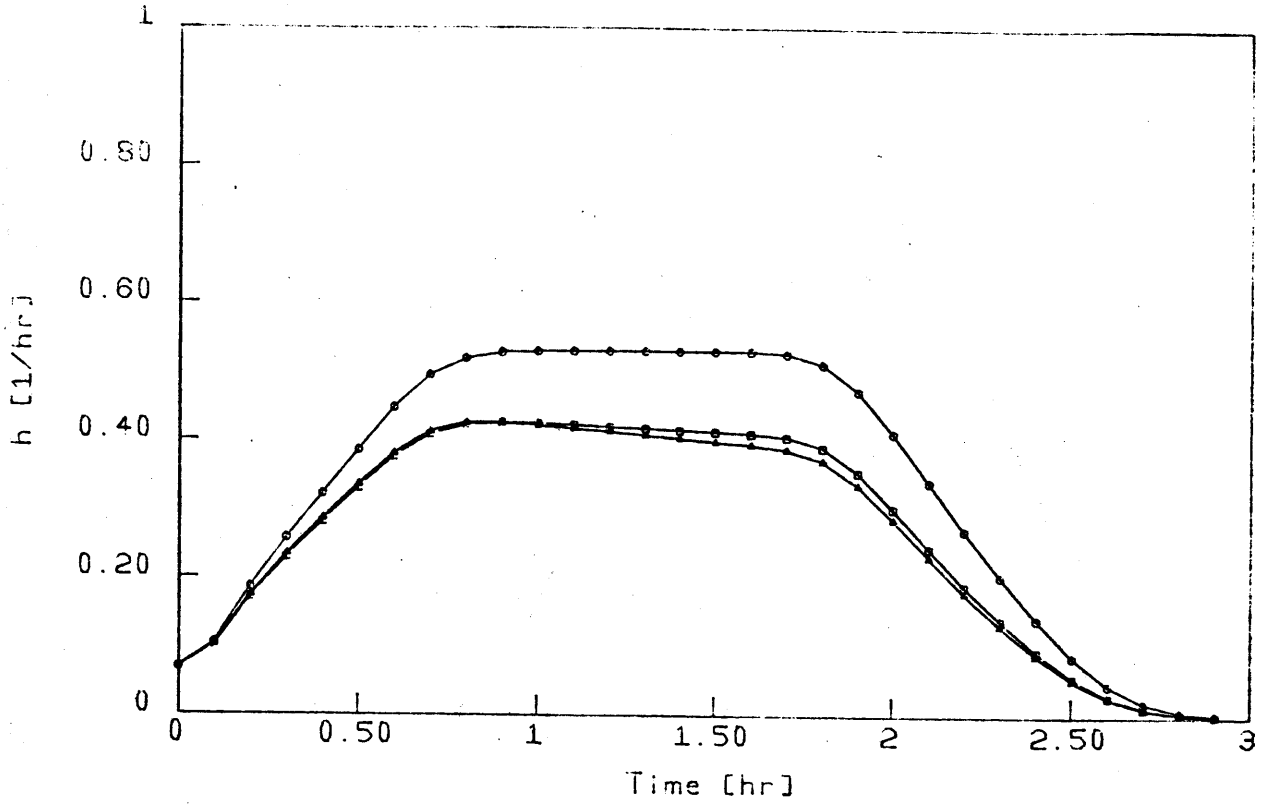

WADI UMM SALAM

Basin iuh for different infiltration losses

(Basin representation 1)

Characteristics:

	I(%)						
Order	1	2	3	Order	1	2	3
⏲	0.0	0.0	0.0	y_o (m)	0.39	0.40	0.41
△	10.0	10.0	10.0	v_o (m/s)	1.05	1.01	0.98
⏲	15.0	10.0	5.0	F_o	0.54	0.51	0.49
				S_o (m/km)	8.00	7.00	6.50
R_A=5.00	R_B=4.00		R_L=2.80	L (km)	1.30	3.60	10.00

p12=0.79 p13=0.21

Θ1=0.64 Θ2=0.30 Θ3=0.06

p(s1)=0.50 p(s2)=0.14 p(s3)=0.30 p(s4)=0.06

Figure 4.5

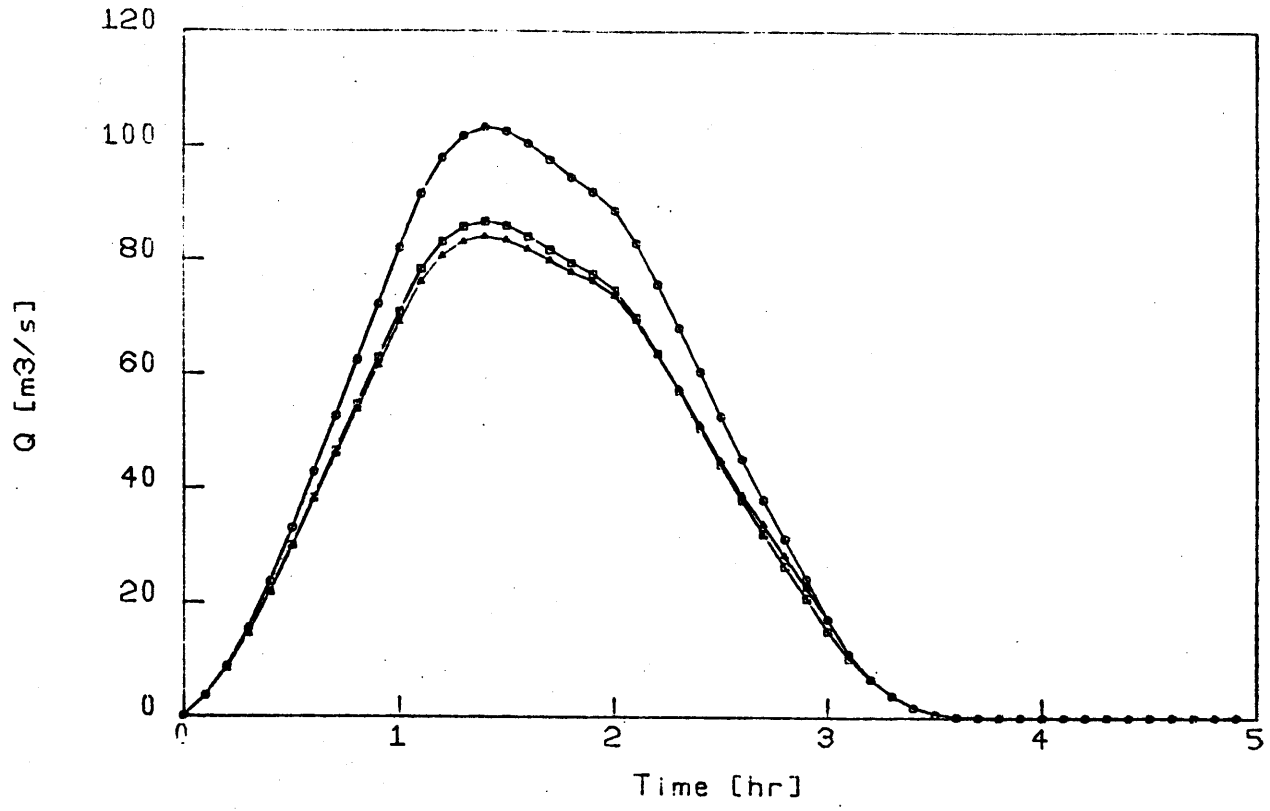

MOROVIS BASIN

Discharge hydrographs using different infiltration losses

(Basin representation 1)

Characteristics:

i=3.0 cm/hr t=2.0 hr A=13.0 km²

Order	I(%) 1	2	3	Order	1	2	3
○	0.0	0.0	0.0	y_o (m)	0.25	0.30	0.30
△	10.0	10.0	10.0	v_o (m/s)	1.47	1.31	1.34
□	15.0	10.0	5.0	F_o	0.94	0.76	0.78
				S_o (m/km)	71.90	32.10	39.20
				L (km)	1.10	3.00	8.00

R_A=5.00 R_B=3.20 R_L=2.70

p12=0.85 p13=0.15

Θ1=0.41 Θ2=0.29 Θ3=0.30

p(s1)=0.35 p(s2)=0.06 p(s3)=0.29 p(s4)=0.30

Figure 4.6

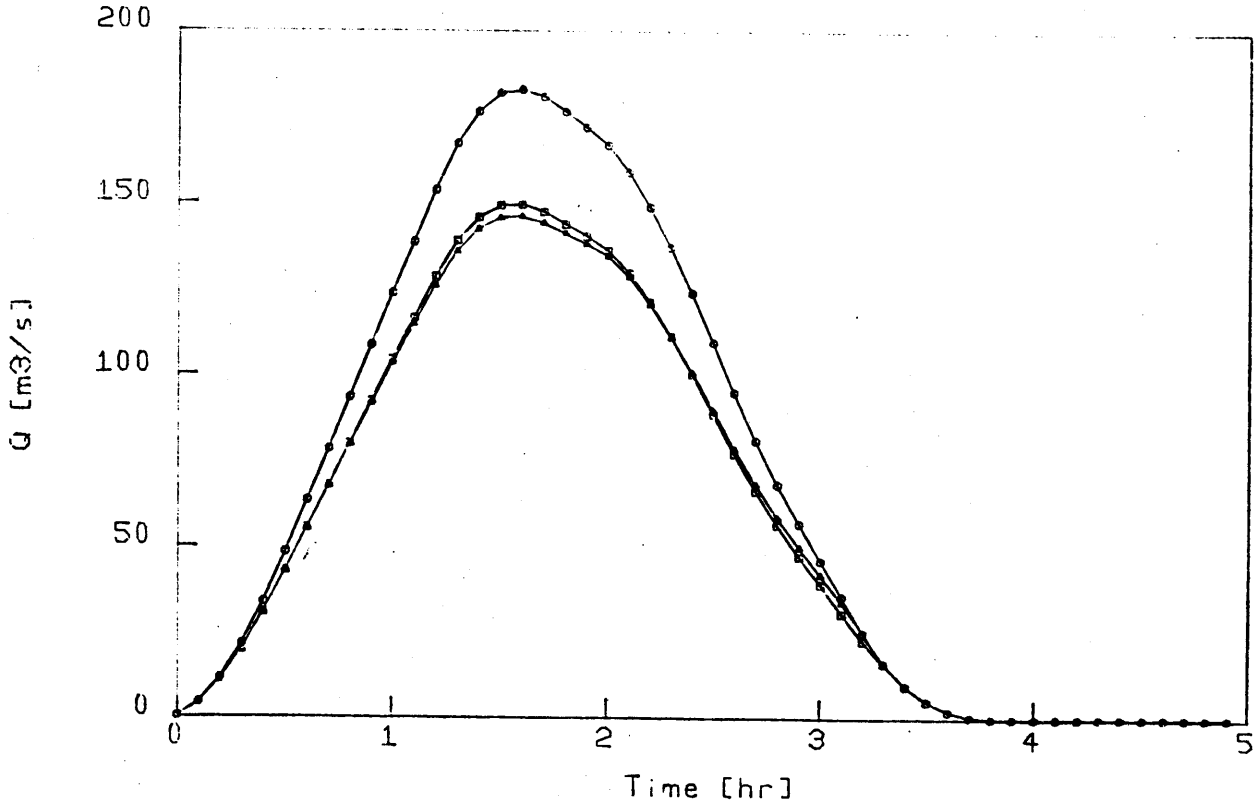

UNIBON BASIN

Discharge hydrographs using different infiltration losses

(Basin representation 1)

Characteristics:

i=3.0 cm/hr t=2.0 hr A=23.0 km²

Order	I(%) 1	2	3	Order	1	2	3
⏲	0.0	0.0	0.0	y_o (m)	0.24	0.28	0.37
△	10.0	10.0	10.0	v_o (m/s)	1.50	1.40	1.25
⊡	15.0	10.0	5.0	F_o	0.98	0.85	0.66
				S_o (m/km)	82.70	46.60	23.30
R_A=5.60	R_B=4.00	R_L=2.80		L (km)	1.10	3.10	8.60

p12=0.79 p13=0.21

Θ1=0.51 Θ2=0.31 Θ3=0.18

p(s1)=0.40 p(s2)=0.11 p(s3)=0.31 p(s4)=0.18

Figure 4.7

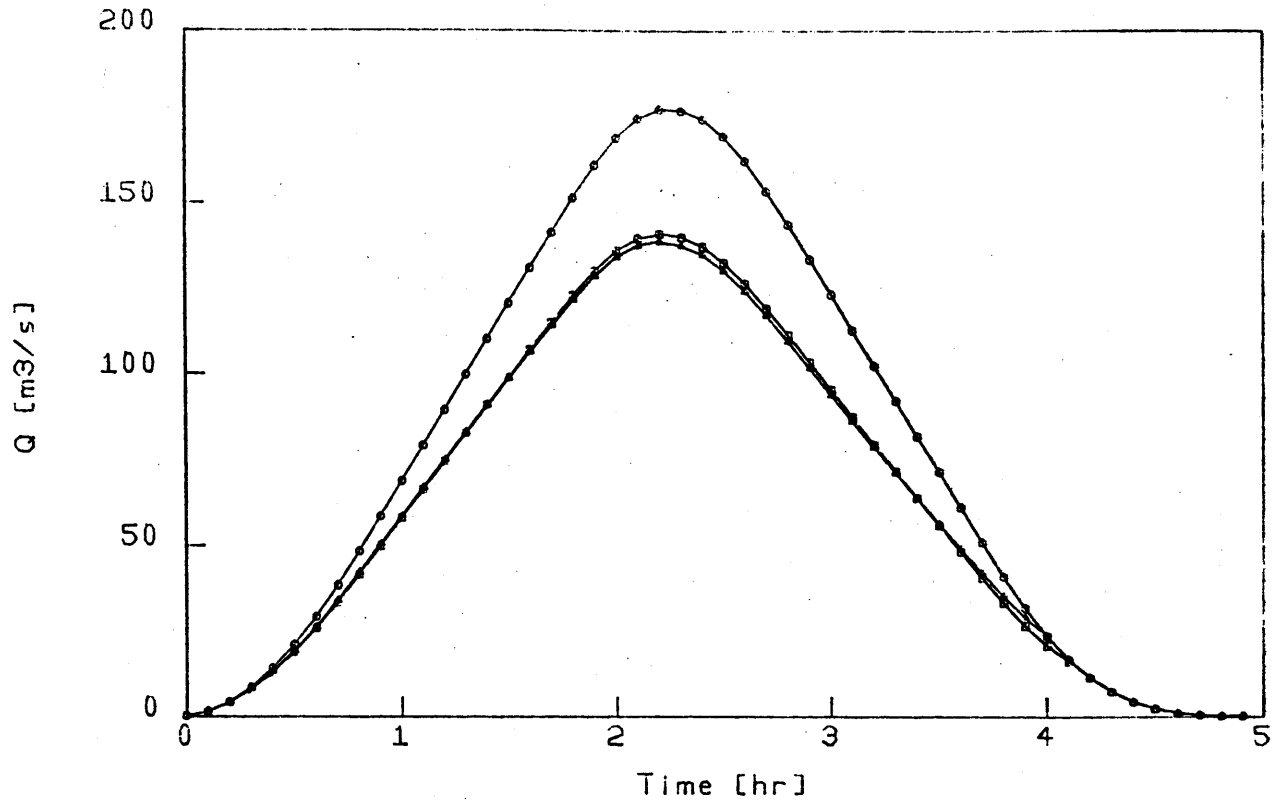

WADI UMM SALAM

Discharge hydrographs using different infiltration losses

(Basin representation 1)

Characteristics:

i=1.8 cm/hr t=2.0 hr A=39.0 km²

Order	I(%) 1	2	3	Order	1	2	3
⏲	0.0	0.0	0.0	y_o (m)	0.39	0.40	0.41
△	10.0	10.0	10.0	v_o (m/s)	1.05	1.01	0.98
⏍	15.0	10.0	5.0	F_o	0.54	0.51	0.49
				S_o (m/km)	8.00	7.00	6.50
R_A=5.00	R_B=4.00	R_L=2.80		L (km)	1.30	3.60	10.00

p12=0.79 p13=0.21

Θ1=0.64 Θ2=0.30 Θ3=0.06

p(s1)=0.50 p(s2)=0.14 p(s3)=0.30 p(s4)=0.06

Figure 4.8

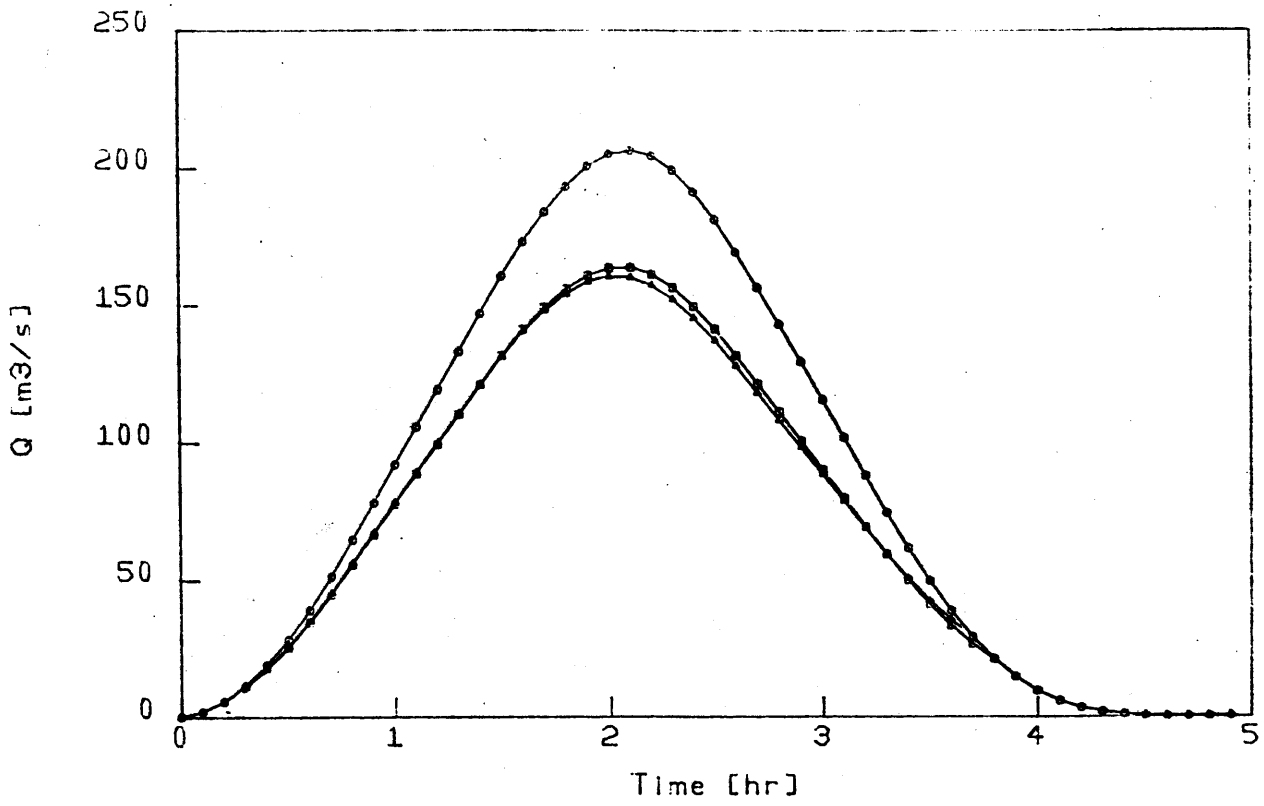

WADI UMM SALAM

Discharge hydrographs using different infiltration losses

(Basin representation 1)

Characteristics:

i=2.4 cm/hr t=1.5 hr A=39.0 km²

Order	I(%) 1	2	3	Order	1	2	3
⊙	0.0	0.0	0.0	y_o (m)	0.39	0.40	0.41
△	10.0	10.0	10.0	v_o (m/s)	1.05	1.01	0.98
⊡	15.0	10.0	5.0	F_o	0.54	0.51	0.49
				S_o (m/km)	8.00	7.00	6.50
R_A=5.00	R_B=4.00	R_L=2.80		L (km)	1.30	3.60	10.00

p12=0.79 p13=0.21

Θ1=0.64 Θ2=0.30 Θ3=0.06

p(s1)=0.50 p(s2)=0.14 p(s3)=0.30 p(s4)=0.06

Figure 4.9

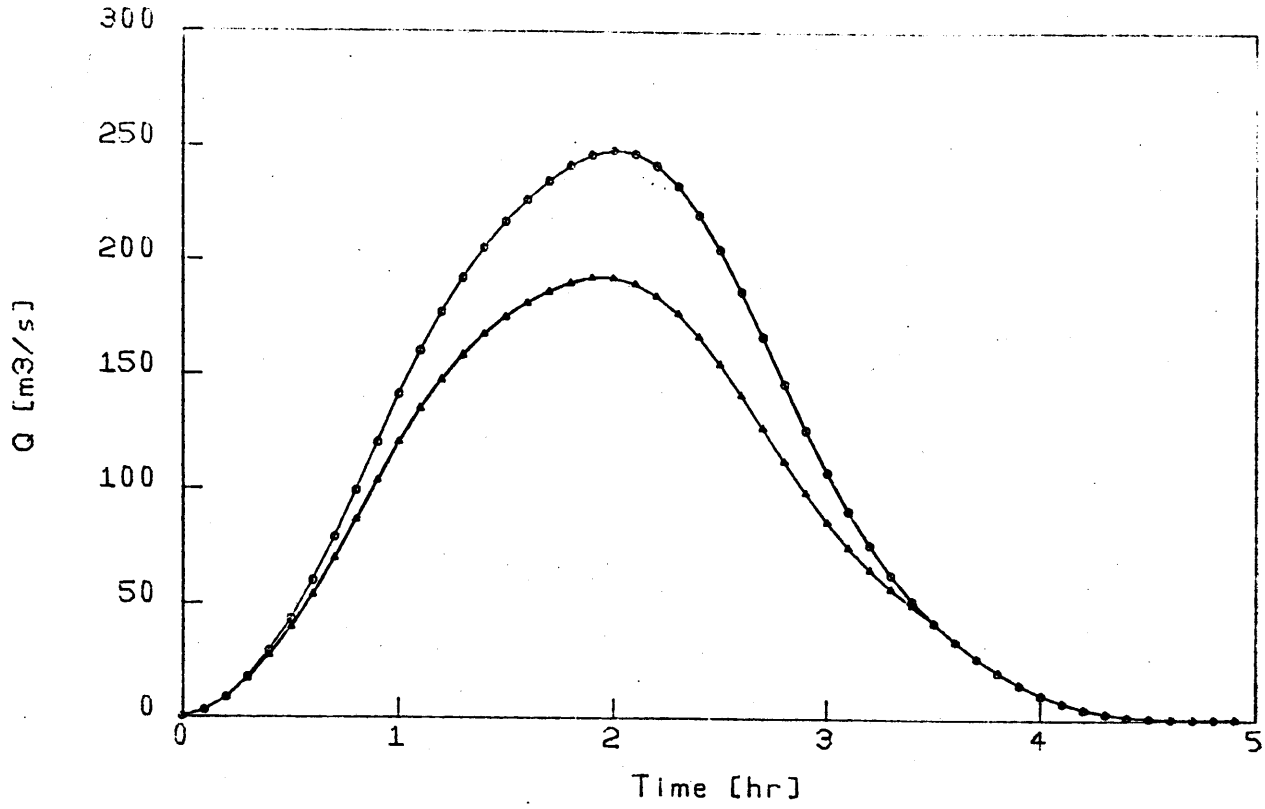

WADI UMM SALAM

Discharge hydrographs using different infiltration losses

(Basin representation 1)

Characteristics:

i=3.7 cm/hr t=1.0 hr A=39.0 km²

	I(%)						
Order	1	2	3	Order	1	2	3
⏲	0.0	0.0	0.0	y_o (m)	0.39	0.40	0.41
△	10.0	10.0	10.0	v_o (m/s)	1.05	1.01	0.98
				F_o	0.54	0.51	0.49
				S_o (m/km)	8.00	7.00	6.50
R_A=5.00	R_B=4.00	R_L=2.80		L (km)	1.30	3.60	10.00

p12=0.79 p13=0.21

Θ1=0.64 Θ2=0.30 Θ3=0.06

p(s1)=0.50 p(s2)=0.14 p(s3)=0.30 p(s4)=0.06

Figure 4.10

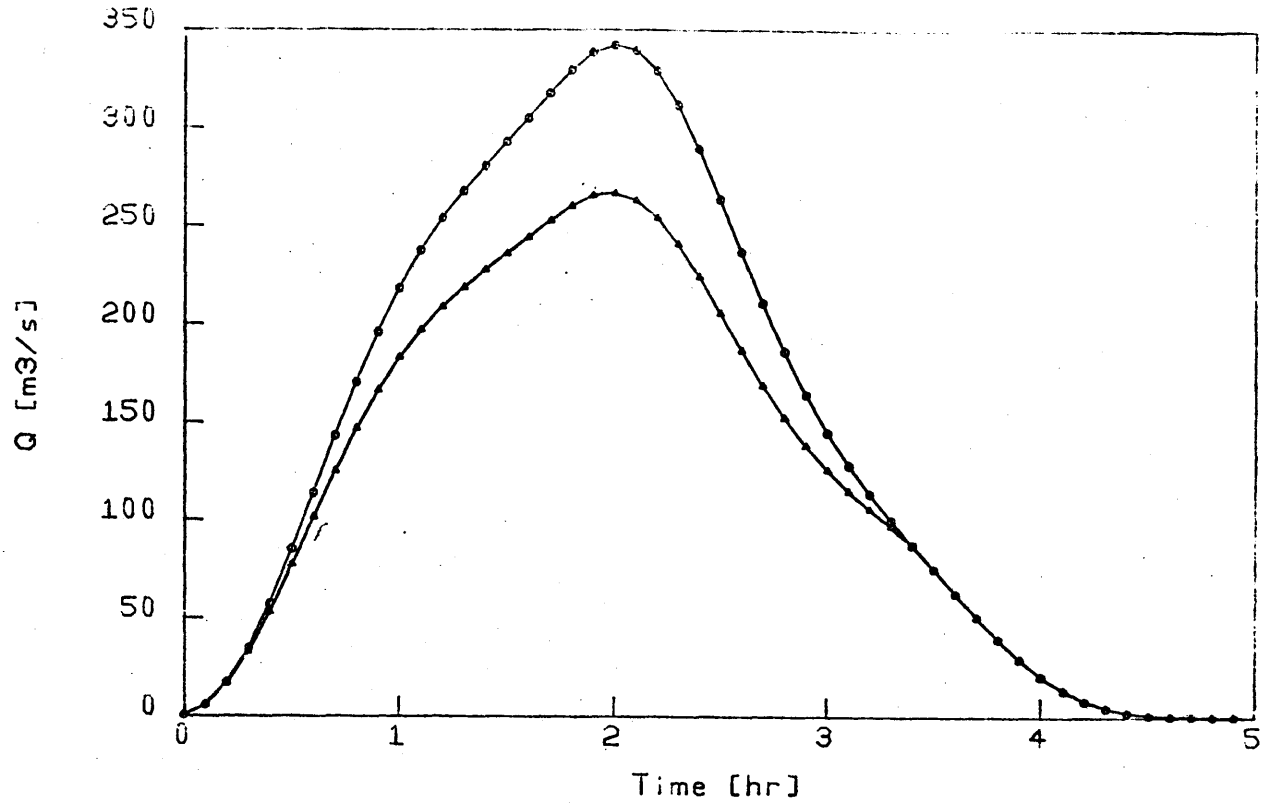

WADI UMM SALAM

Discharge hydrographs using different infiltration losses

(Basin representation 1)

Characteristics:

i=7.3 cm/hr t=0.5 hr A=39.0 km²

Order	I(%) 1	2	3	Order	1	2	3
⊙	0.0	0.0	0.0	y_o (m)	0.39	0.40	0.41
△	10.0	10.0	10.0	v_o (m/s)	1.05	1.01	0.98
				F_o	0.54	0.51	0.49
				S_o (m/km)	8.00	7.00	6.50
R_A=5.00	R_B=4.00	R_L=2.80		L (km)	1.30	3.60	10.00

p12=0.79 p13=0.21

Θ1=0.64 Θ2=0.30 Θ3=0.06

p(s1)=0.50 p(s2)=0.14 p(s3)=0.30 p(s4)=0.06

Figure 4.11

$$f_T^{(i)}(t) = \begin{cases} \mu_i e^{-\lambda_i t} & t \geq 0 \\ p_T(t) = 1-(1-e^{-K_i L_i})/K_i L_i & t = \infty \end{cases} \tag{4.9}$$

where,

$$\mu = \frac{c_{l_i}}{L_i} \tag{4.10}$$

and

$$\lambda_i = \frac{c_{l_i}}{L_i(1-I_i/100)} \tag{4.11}$$

Rodriguez-Iturbe and Valdes (1979) used Equation 2.10 to represent the PDF of the travel time in the streams of highest order. This equation also has to be modified for infiltration losses, i.e.,

$$f_T^{(\Omega)}(t) = \begin{cases} \mu_\Omega^{*2} t e^{-\lambda_\Omega^* t} & t \geq 0 \\ p_T(t) = 1-(1-e^{-K_\Omega L_\Omega})/K_\Omega L_\Omega & t = \infty \end{cases} \tag{4.12}$$

where the following criteria are used to calculate μ_Ω^* and λ_Ω^* (Ω)

- The mean waiting time of the continuous part of $f_T(t)$ as given by Equation 4.9 must be equal to the mean waiting time of the continuous part of $f_T^{(\Omega)}(t)$ as given by Equation 4.12 (this was the criterion used by Rodriguez-Iturbe and Valdes, 1979):

$$\mu_\Omega \int_o^\infty t e^{-\lambda_\Omega t} dt = \mu_\Omega^{*2} \int_o^\infty t^2 e^{-\lambda_\Omega^* t} dt$$

or

$$\frac{\mu_\Omega}{\lambda_\Omega^2} = \frac{2\mu_\Omega^{*2}}{\lambda_\Omega^{*3}} \tag{4.13}$$

- The area under the continuous part of $f_T^{(\Omega)}(t)$ as given by Equation 4.9 must be equal to the area under the continuous part of $f_T^{(\Omega)}(t)$ as given by Equation 4.12.

$$\mu_\Omega \int_o^\infty e^{-\lambda_\Omega t} dt = \mu_\Omega^{*2} \int_o^\infty te^{-\lambda_\Omega^* t}$$

or

$$\frac{\mu_\Omega}{\lambda_\Omega} = \frac{\mu_\Omega^{*2}}{\lambda_\Omega^{*2}} \tag{4.14}$$

Then, from Equations 4.13 and 4.14, μ_Ω^* and λ_Ω^{*2} may be calculated as:

$$\lambda_\Omega^* = 2\lambda_\Omega \tag{4.15}$$

$$\mu_\Omega^{*2} = 4\mu_\Omega\lambda_\Omega \tag{4.16}$$

Therefore, the expressions for the IUH and the discharge hydrograph with the modified linear assumption which takes into account infiltration losses in the channels are (third order basin):

$$h(t) = \Theta_1 P_{12}\mu_1\mu_2\mu_3^{*2}\left\{\frac{e^{-\lambda_1 t}}{(\lambda_1-\lambda_3^*)^2(\lambda_2-\lambda_1)} + \frac{e^{-\lambda_2 t}}{(\lambda_2-\lambda_3^*)^2(\lambda_1-\lambda_2)}\right.$$

$$\left. + \frac{[2\lambda_3^*-\lambda_1-\lambda_2+(\lambda_1-\lambda_3^*)(\lambda_2-\lambda_3^*)t]e^{-\lambda_3^* t}}{(\lambda_1-\lambda_3^*)^2(\lambda_2-\lambda_3^*)^2}\right\}$$

$$+ \Theta_1 P_{13}\mu_1\mu_3^{*2}\frac{e^{-\lambda_1 t} - [1-(\lambda_3^*-\lambda_1)t]e^{-\lambda_3^* t}}{(\lambda_3^*-\lambda_1)^2}$$

$$+ \Theta_2\mu_2\mu_3^{*2}\frac{e^{-\lambda_2 t} - [1-(\lambda_3^*-\lambda_2)t]e^{-\lambda_3^* t}}{(\lambda_3^*-\lambda_2)}$$

$$+ \Theta_3\mu_3^{*2}\, te^{-\lambda_3^* t} \qquad (4.17)$$

and,

$$Q(t) = A_3 bi_e\left[\frac{\Theta_1 P_{12}\mu_1\mu_2\mu_3^{*2}}{(\lambda_1-\lambda_3^*)^2(\lambda_2-\lambda_1)\lambda_1} + \frac{\Theta_1 P_{13}\mu_1\mu_3^{*2}}{(\lambda_3^*-\lambda_1)^2\lambda_1}\right]\left\{1-e^{-\lambda_1 t}\left[1-e^{-\lambda_1(t-t_e)}\right]u(t-t_e)\right\}$$

$$+ A_3 bi_e\left[\frac{\Theta_1 P_{12}\mu_1\mu_2\mu_3^{*2}}{(\lambda_2-\lambda_3^*)^2(\lambda_1-\lambda_2)\lambda_2} + \frac{\Theta_2\mu_2\mu_3^{*2}}{(\lambda_3^*-\lambda_2)^2\lambda_2}\right]\left\{1-e^{-\lambda_2 t}-\left[1-e^{-\lambda_2(t-t_e)}\right]u(t-t_e)\right\}$$

$$+ A_3 bi_e\left[\frac{\Theta_1 P_{12}\mu_1\mu_2\mu_3^{*2}(2\lambda_3^*-\lambda_1-\lambda_2)}{(\lambda_1-\lambda_3^*)^2(\lambda_2-\lambda_3^*)\lambda_3^*} - \frac{\Theta_1 P_{13}\mu_1\mu_3^{*2}}{(\lambda_1-\lambda_3^*)^2\lambda_3^*} - \frac{\Theta_2\mu_2\mu_3^{*2}}{(\lambda_2-\lambda_3^*)^2\lambda_3^*}\right]$$

$$\left\{1-e^{-\lambda_3^* t}-\left[1-e^{-\lambda_3^*(t-t_e)}\right]u(t-t_e)\right\}$$

$$+ A_3 bi_e\left[\frac{\Theta_1 P_{12}\mu_1\mu_2\mu_3^{*2}}{(\lambda_1-\lambda_3^*)(\lambda_1-\lambda_3^*)} + \frac{\Theta_1 P_{13}\mu_1\mu_3^{*2}}{(\lambda_1-\lambda_3^*)} + \frac{\Theta_2\mu_2\mu_3^{*2}}{(\lambda_2-\lambda_3^*)} + \Theta_3\mu_3^{*2}\right]\left\{1-(\lambda_3^* t+1)e^{-\lambda_3^* t}\right.$$

$$\left. + \left[1-e^{-\lambda_3^*(t-t_e)}\right]u(t-t_e) + \lambda_3^*(t-t_e)e^{-\lambda_3^*(t-t_e)}u(t-t_e)\right\} \qquad (4.18)$$

Figures 4.12 to 4.15 show some comparisons between IUHs based on the linearized solution (Equation 4.4) and IUHs based on the modified linear reservoir assumption (Equation 4.17). Figures 4.12 and 4.13 correspond to Morovis and Unibon basins for the case of no infiltration losses. As it can be seen, the linearized solution is "more rectangular" than the exponential, which is smoother, but in general terms, the agreement is good. Figures 4.14 and 4.15 show the IUH's for Unibon basin and Wadi Umm Salam, when the percentage of infiltration losses are 15, 10, and 5 percent for streams of order 1, 2, and 3 respectively. The Unibon results show a better agreement than Wadi Umm Salam. Figures 4.16 to 4.19 present comparisons of discharges from the three basins studied here. As it is shown in these figures, both solutions give similar hydrographs, in terms of shape, peak discharge and time to peak, which permit conclude that both the linearized solution and the exponential assumption yield similar results.

4.4 Linearized Solution Hydrographs. Another Basin Representation

Kirshen and Bras (1982) used the PDFs of the travel time needed by a drop that enter the channel at its most upstream point $f_T^u(t)$ and anywhere along its length, $f_T^r(t)$, to improve the representation of the basin by increasing the possible paths that a drop can take to reach the outlet of the basin. Referring to Figure 2.1, the flow contributing to some higher order streams is in part due to flow from the junction of two

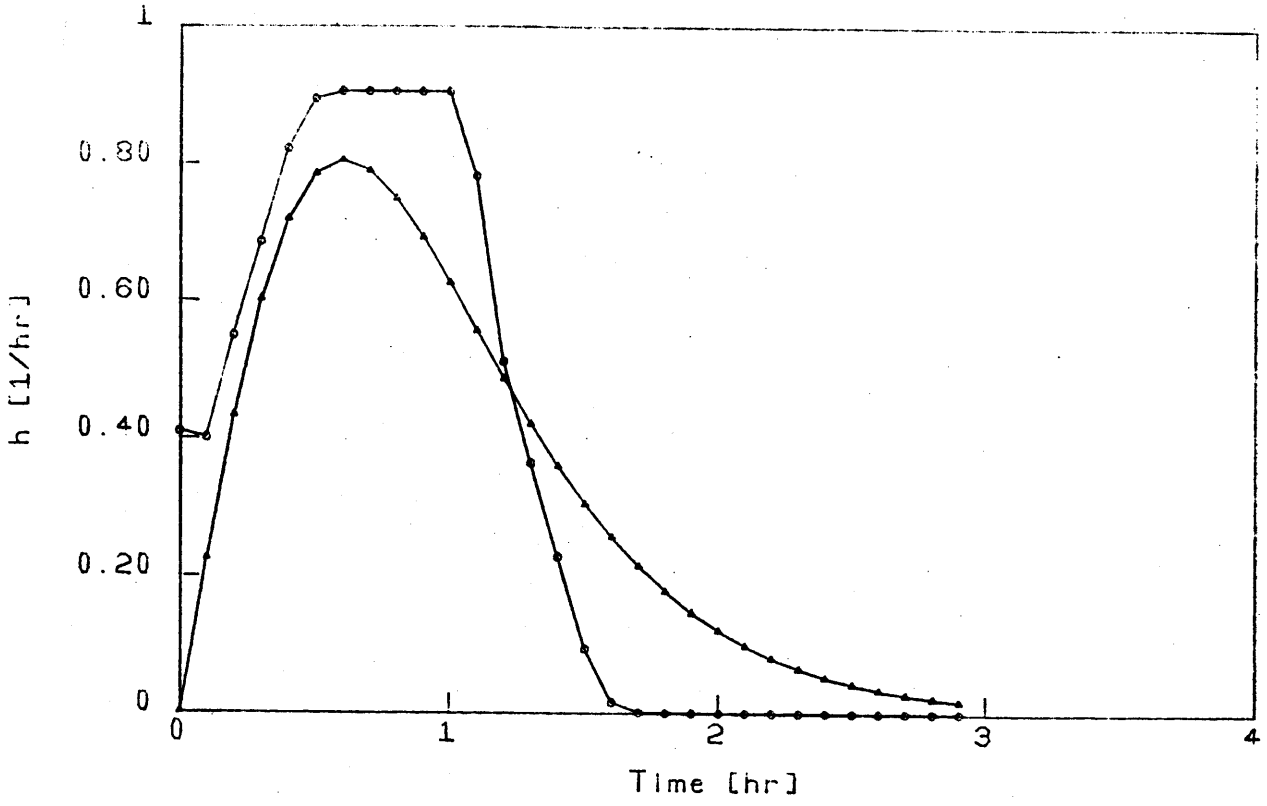

MOROVIS BASIN

Basin iuh - exponential vs linearized solution

(Basin representation 1)

Characteristics:

	I(%)						
Order	1	2	3	Order	1	2	3
	0.0	0.0	0.0	y_o (m)	0.25	0.30	0.30
⊙	Linearized solution			v_o (m/s)	1.47	1.31	1.34
△	Exponential assumption			F_o	0.94	0.76	0.78
				S_o (m/km)	71.90	32.10	39.20
R_A=5.00	R_B=3.20	R_L=2.70		L (km)	1.10	3.00	8.00

p12=0.85 p13=0.15

Θ1=0.41 Θ2=0.29 Θ3=0.30

p(s1)=0.35 p(s2)=0.06 p(s3)=0.29 p(s4)=0.30

Figure 4.12

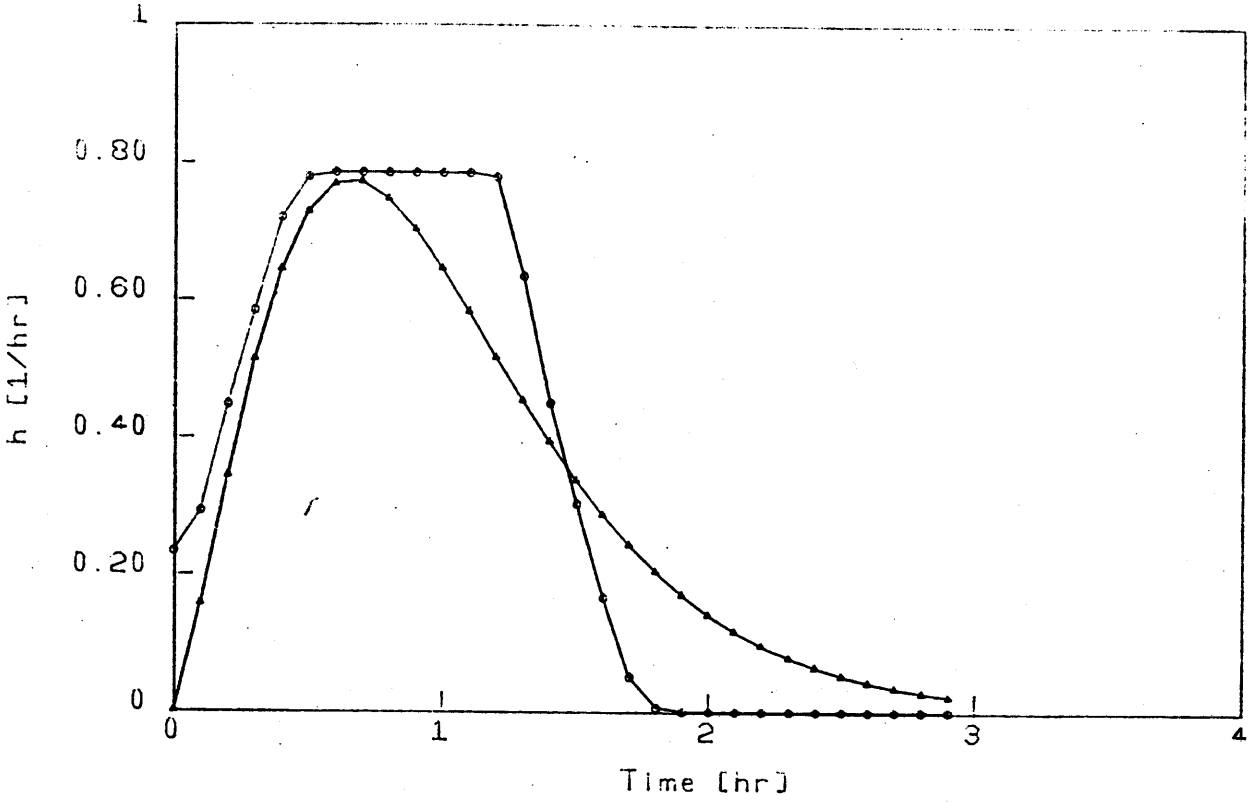

UNIBON BASIN

Basin iuh - exponential vs linearized solution

(Basin representation 1)

Characteristics:

	I(%)						
Order	1	2	3	Order	1	2	3
	0.0	0.0	0.0	y_0 (m)	0.24	0.28	0.37
⏲	Linearized solution			v_0 (m/s)	1.50	1.40	1.25
△	Exponential assumption			F_0	0.98	0.85	0.66
				S_0 (m/km)	82.70	46.60	23.30
R_A=5.60	R_B=4.00	R_L=2.80		L (km)	1.10	3.10	8.60

p12=0.79 p13=0.21

Θ1=0.51 Θ2=0.31 Θ3=0.18

p(s1)=0.40 p(s2)=0.11 p(s3)=0.31 p(s4)=0.18

Figure 4.13

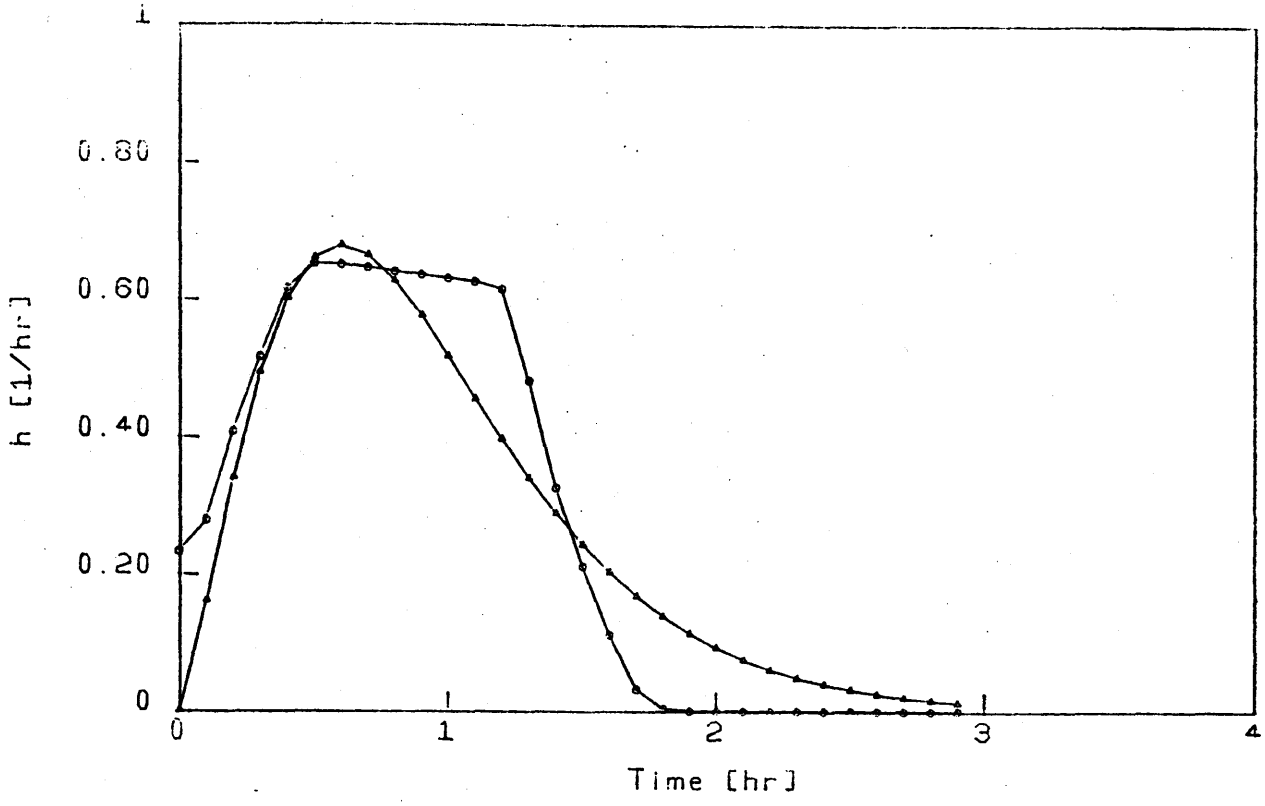

UNIBON BASIN

Basin luh - exponential vs linearized solution

(Basin representation 1)

Characteristics:

	I(%)						
Order	1	2	3	Order	1	2	3
	15.0	10.0	5.0	y_o (m)	0.24	0.28	0.37
⏀	Linearized solution			v_o (m/s)	1.50	1.40	1.25
△	Exponential assumption			F_o	0.98	0.85	0.66
				S_o (m/km)	82.70	46.60	23.30
R_A=5.60	R_B=4.00	R_L=2.80		L (km)	1.10	3.10	8.60

p12=0.79 p13=0.21

Θ1=0.51 Θ2=0.31 Θ3=0.18

p(s1)=0.40 p(s2)=0.11 p(s3)=0.31 p(s4)=0.18

Figure 4.14

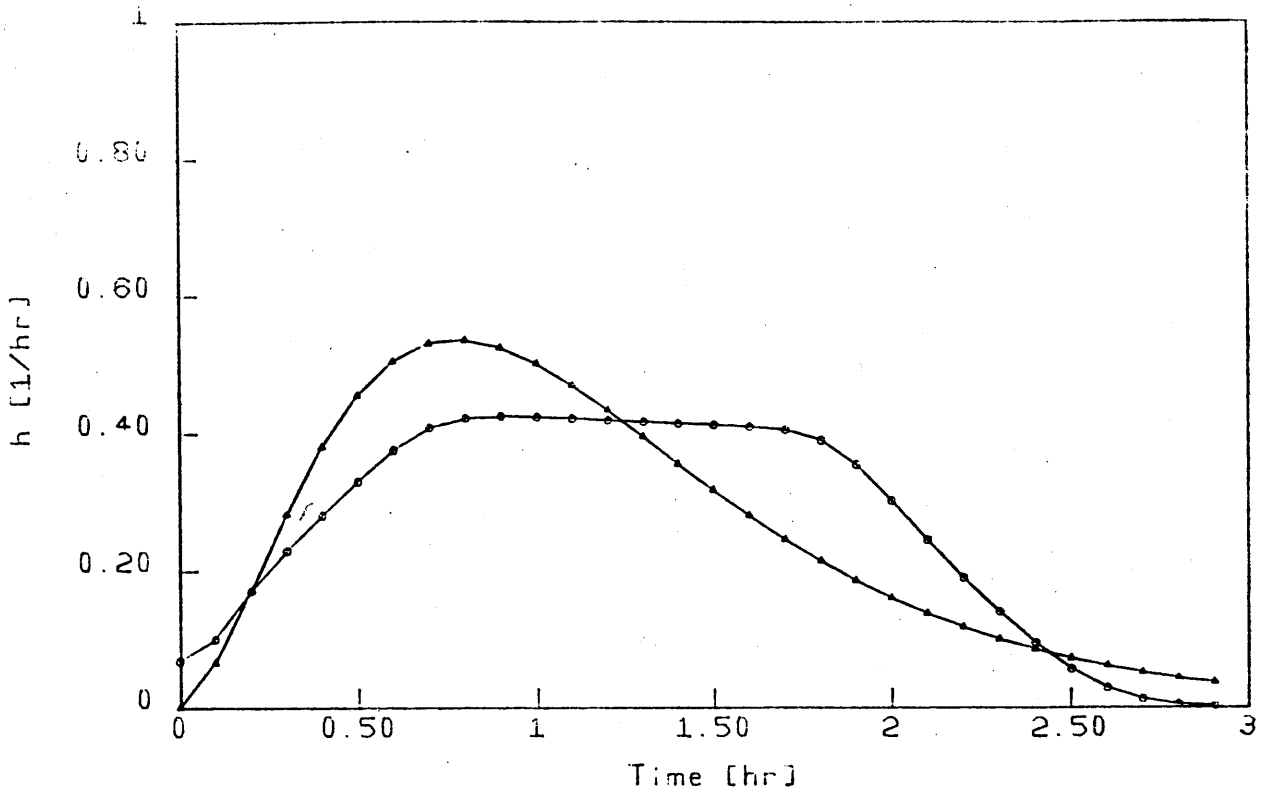

WADI UMM SALAM

Basin iuh - exponential vs linearized solution

(Basin representation 1)

Characteristics:

	I(%)						
Order	1	2	3	Order	1	2	3
	15.0	10.0	5.0	y_o (m)	0.39	0.40	0.41
⏲	Linearized solution			v_o (m/s)	1.05	1.01	0.98
△	Exponential assumption			F_o	0.54	0.51	0.49
				S_o (m/km)	8.00	7.00	6.50
R_A=5.00	R_B=4.00	R_L=2.80		L (km)	1.30	3.60	10.00

p12=0.79 p13=0.21

Θ1=0.64 Θ2=0.30 Θ3=0.06

p(s1)=0.50 p(s2)=0.14 p(s3)=0.30 p(s4)=0.06

Figure 4.15

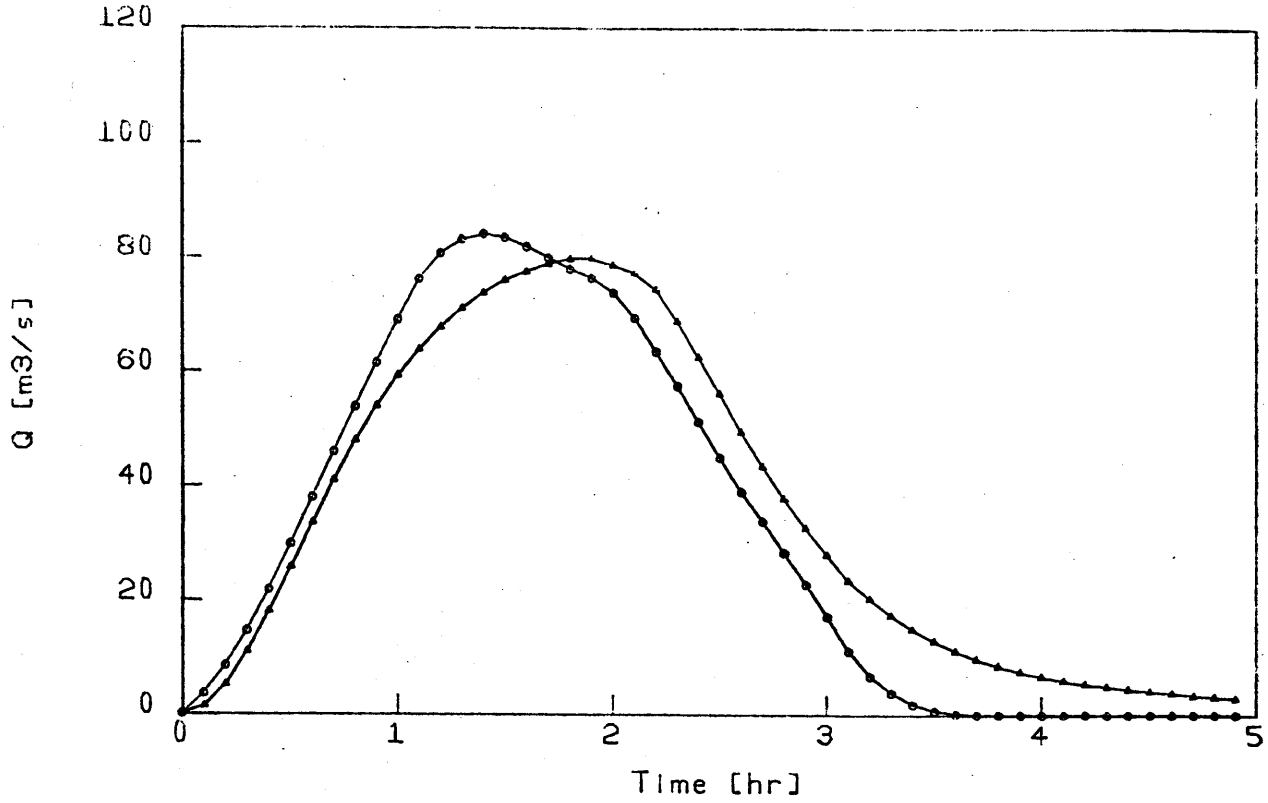

MOROVIS BASIN

Discharge hydrograph - exponential vs linearized solution

(Basin representation 1)

Characteristics:

i=3.0 cm/hr t=2.0 hr A=13.0 km²

Order	I(%) 1	2	3	Order	1	2	3
	10.0	10.0	10.0	y_0 (m)	0.25	0.30	0.30
⏲	Linearized solution			v_0 (m/s)	1.47	1.31	1.34
△	Exponential assumption			F_0	0.94	0.76	0.78
				S_0 (m/km)	71.90	32.10	39.20
R_A=5.00	R_B=3.20	R_L=2.70		L (km)	1.10	3.00	8.00

p12=0.85 p13=0.15

Θ1=0.41 Θ2=0.29 Θ3=0.30

p(s1)=0.35 p(s2)=0.06 p(s3)=0.29 p(s4)=0.30

Figure 4.16

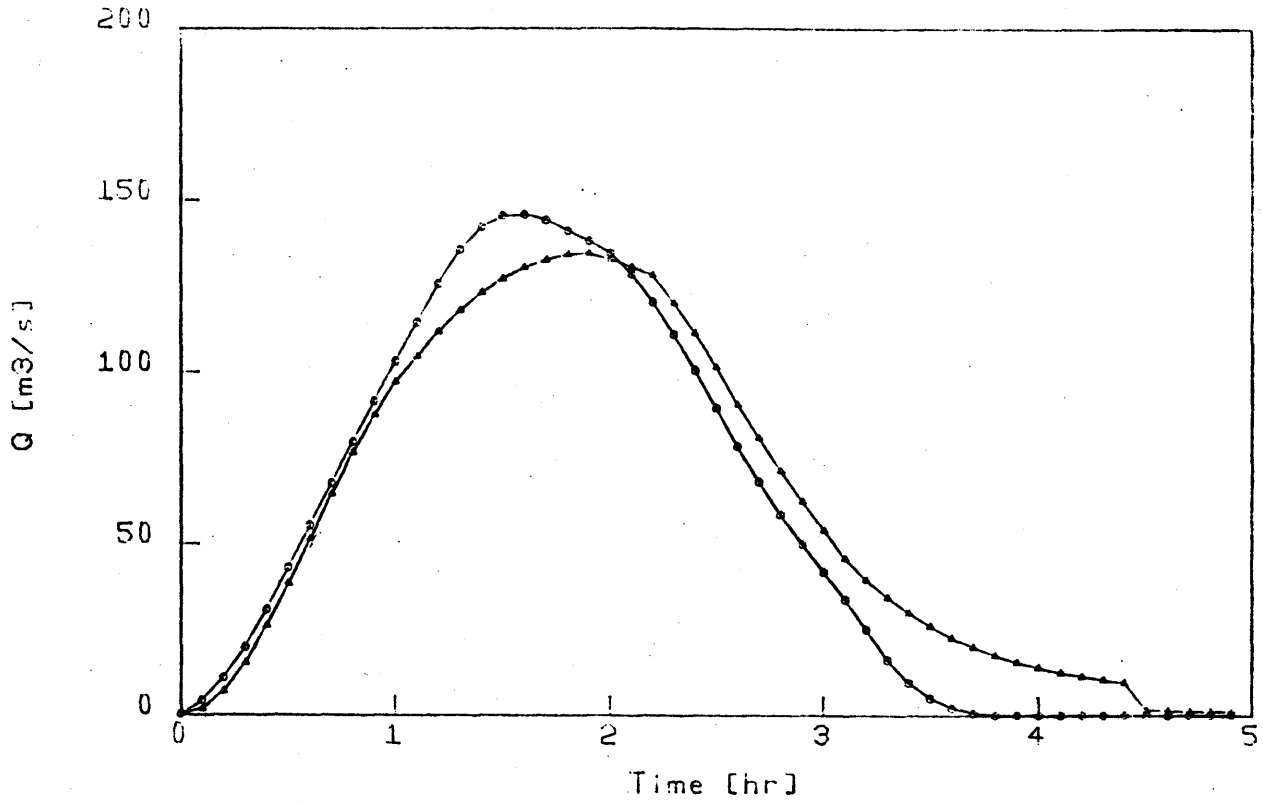

UNIBON BASIN

Discharge hydrograph - exponential vs linearized solution

(Basin representation 1)

Characteristics:

i=3.0 cm/hr t=2.0 hr A=23.0 km²

Order	I(%) 1	2	3	Order	1	2	3
	10.0	10.0	10.0	y_o (m)	0.24	0.28	0.37
⏲	Linearized solution			v_o (m/s)	1.50	1.40	1.25
△	Exponential assumption			F_o	0.98	0.85	0.66
				S_o (m/km)	82.70	46.60	23.30
R_A=5.60	R_B=4.00	R_L=2.80		L (km)	1.10	3.10	8.60

p12=0.79 p13=0.21

Θ1=0.51 Θ2=0.31 Θ3=0.18

p(s1)=0.40 p(s2)=0.11 p(s3)=0.31 p(s4)=0.18

Figure 4.17

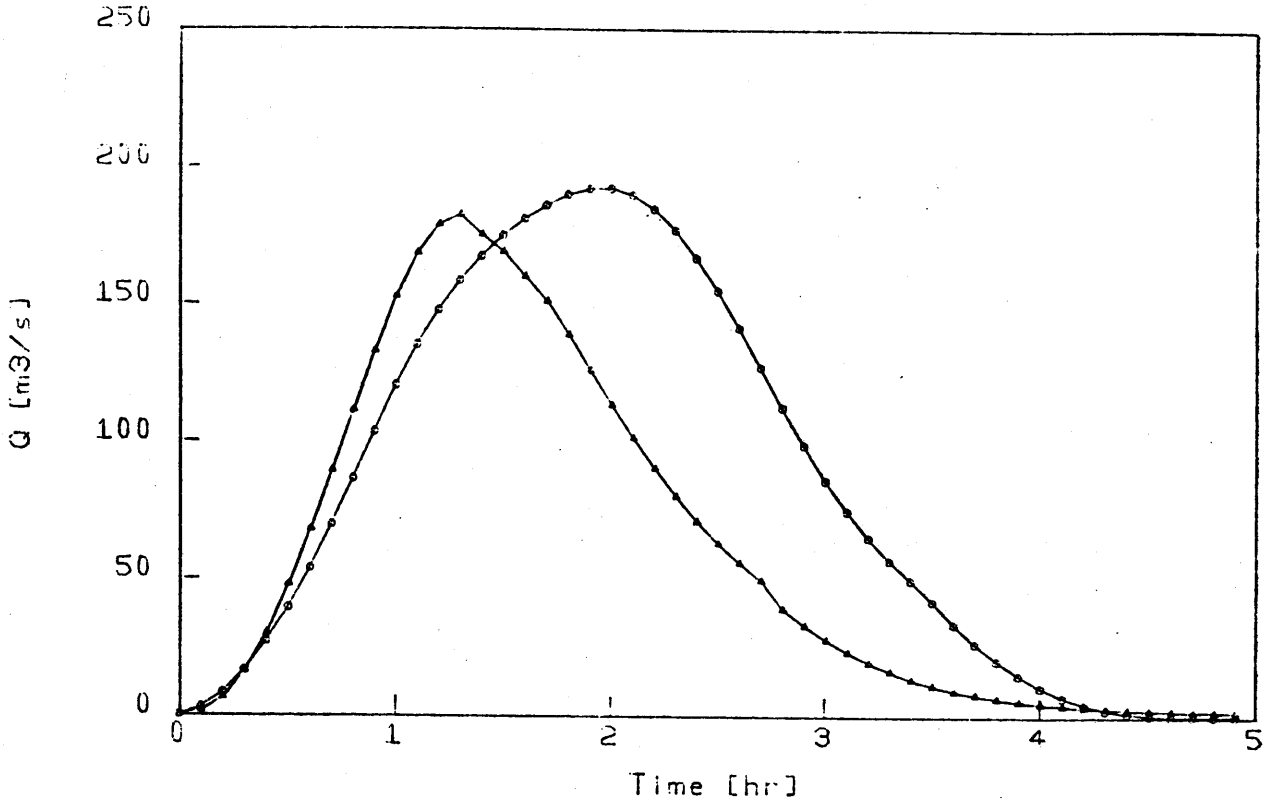

WADI UMM SALAM

Discharge hydrograph - exponential vs linearized solution

(Basin representation 1)

Characteristics:

i=3.7 cm/hr t=1.0 hr A=39.0 km²

Order	I(%) 1	2	3	Order	1	2	3
	10.0	10.0	10.0	y_o (m)	0.39	0.40	0.41
⏱	Linearized solution			v_o (m/s)	1.05	1.01	0.98
△	Exponential assumption			F_o	0.54	0.51	0.49
				S_o (m/km)	8.00	7.00	6.50
R_A=5.00	R_B=4.00	R_L=2.80		L (km)	1.30	3.60	10.00

p12=0.79 p13=0.21

Θ1=0.64 Θ2=0.30 Θ3=0.06

p(s1)=0.50 p(s2)=0.14 p(s3)=0.30 p(s4)=0.06

Figure 4.18

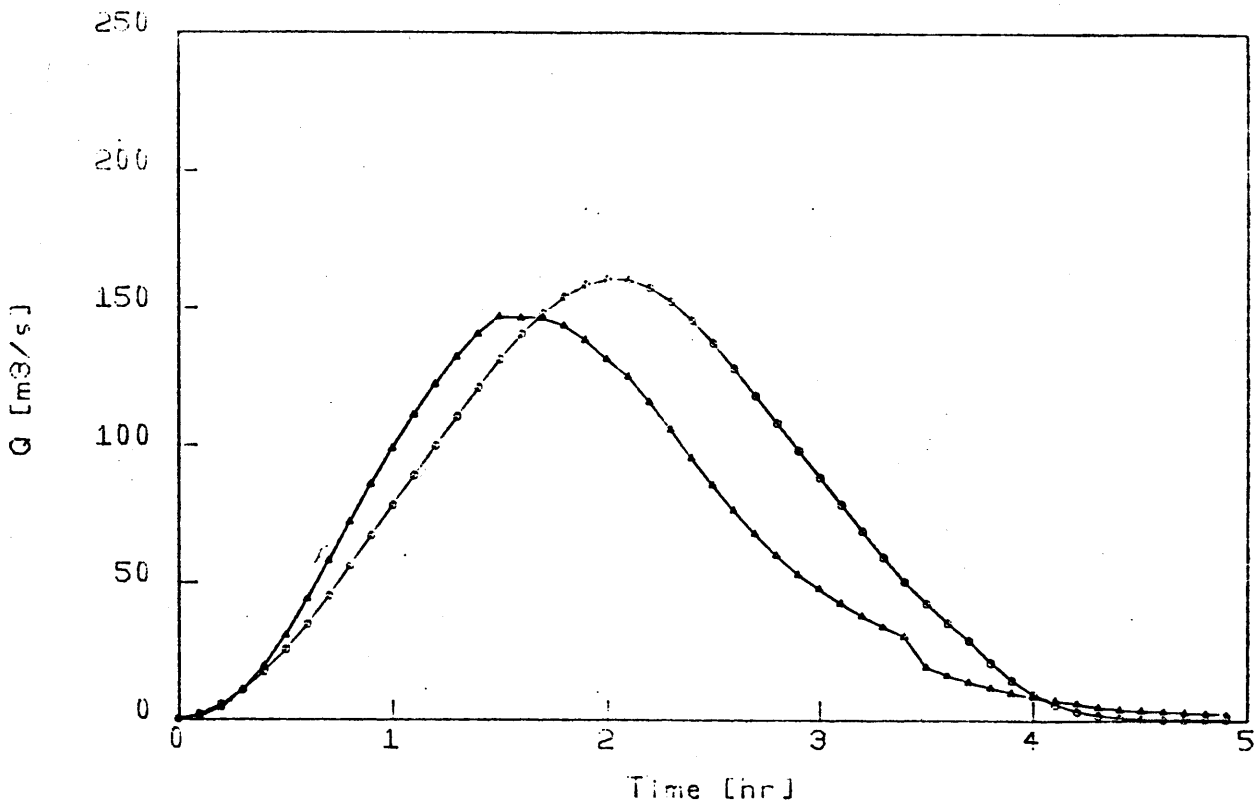

WADI UMM SALAM

Discharge hydrograph - exponential vs linearized solution

(Basin representation 1)

Characteristics:

i=2.4 cm/hr t=1.5 hr A=39.0 km²

Order	I(%) 1	2	3	Order	1	2	3
	10.0	10.0	10.0	y_o (m)	0.39	0.40	0.41
○	Linearized solution			v_o (m/s)	1.05	1.01	0.98
△	Exponential assumption			F_o	0.54	0.51	0.49
				S_o (m/km)	8.00	7.00	6.50
R_A=5.00	R_B=4.00	R_L=2.80		L (km)	1.30	3.60	10.00

p12=0.79 p13=0.21

Θ1=0.64 Θ2=0.30 Θ3=0.06

p(s1)=0.50 p(s2)=0.14 p(s3)=0.30 p(s4)=0.06

Figure 4.19

two streams of one order lower. Streams of this type respond according to the upstream inflow response. Therefore, the transitions may be differentiated in two: one representing those drops that enter along the channel laterally, r(i), and one representing those drops that enter at the channels upstream end, u(i). Then, for a third order basin, the possible paths are:

s_1 = a(1) → r(1) → r(2) → r(3) → OUTLET

s_2 = a(1) → r(1) → u(2) → r(3) → OUTLET

s_3 = a(1) → r(1) → r(2) → u(3) → OUTLET

s_4 = a(1) → r(1) → r(3) → OUTLET

s_5 = a(2) → r(2) → r(3) → OUTLET

s_6 = a(2) → r(2) → u(3) → OUTLET

s_7 = a(3) → r(3) → OUTLET

s_8 = a(1) → r(1) → u(3) → OUTLET

Figure 4.20 schematizes these paths. In order to account for the additional paths, the transition probabilities previously presented need to be modified. They are given in Table 4.2.

The extension of the expressions for h(t) and Q(t) is straigthforward. Following the definition of h(t) (see Equation 2.7) and Q(t), the summation over the eight possible paths of the convoluted terms can be easily written in a similar way as Equations 4.4 and 4.5, by using the modified transition probabilities of Table 4.2 and the Laplace transform of $f_T^{u(i)}(t)$:

$$\mathcal{L}\left\{f_T^{u(i)}(t)\right\} = e^{B_i L_i} \tag{4.19}$$

where B_i has been defined in Equation 4.3 and L_i is the length of the stream of order i.

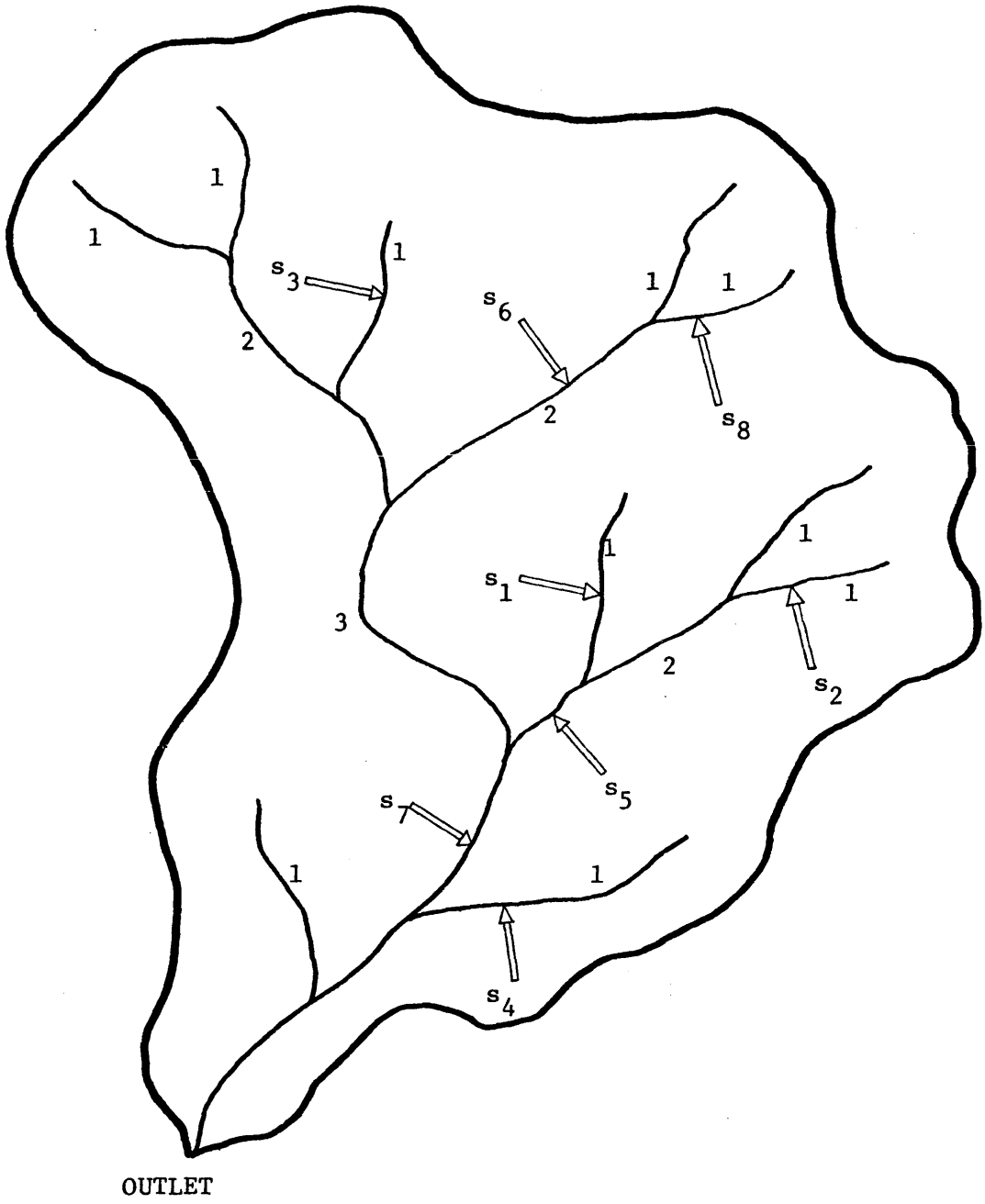

Basin representation in terms of alternative paths

Figure 4.20

TABLE 4.2

Transition Probabilities for a Third Order Basin-Basin Representation 2 (from Kirshen and Bras, 1982)

$$P_{r_1 r_2} = \frac{(R_B^2 - 2R_B)}{R_B(2R_B - 1)}$$

$$P_{r_1 u_2} = \frac{2}{R_B}$$

$$P_{r_1 r_3} = \frac{R_B^2 - 3R_B + 2}{R_B(2R_B - 1)}$$

$$P_{r_2 r_3} = \frac{R_B - 2}{R_B}$$

$$P_{r_2 u_3} = \frac{2}{R_B}$$

$$P_{u_2 r_3} = P_{r_2 r_3}$$

$$P_{u_2 u_3} = P_{r_2 u_3}$$

Figures 4.21, 4.22, and 4.23 present the IUHs resulting from this new basin representation. As it can be seen, their shape is very unusual for an instantaneous unit hydrograph. The response of the main paths can be determined from the figures.

However, when the discharge hydrographs are calculated and compared to those with the exponential assumption (Equation 4.18), the results are surprising (see Figures 4.24 to 4.31). They are very similar in the cases of Morovis and Unibon basins; for Wadi Umm Salam, the peak discharge is almost the same, although the time to peak is delayed in the linearized solution with respect to the exponential assumption.

A general conclusion from this chapter can be drawn: given that the linearized solution of the response of the channels is more physically based than the linear reservoir assumption, and given that the comparisons of h(t) and Q(t) evaluated with both of them, gave good results, then the use of linear reservoir assumption seem to be good and easy to use approximation in the h(t) and Q(t). It should be added that although the linearized solutions were obtained assuming small perturbations, the use of the results was accordingly limited. This follows general hydrologic practice.

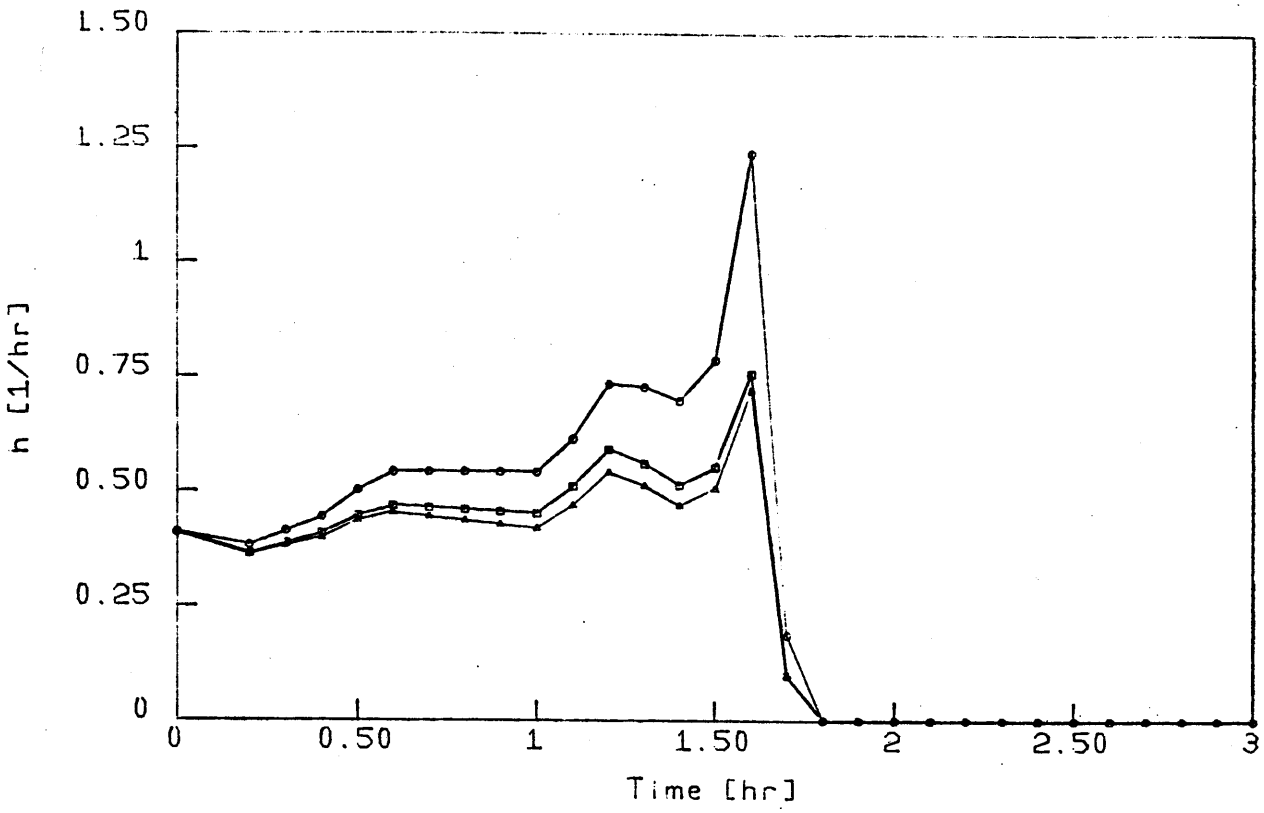

MOROVIS BASIN

Basin iuh for different infiltration losses

(Basin representation 2)

Characteristics:

	I(%)						
Order	1	2	3	Order	1	2	3
⊙	0.0	0.0	0.0	y_o (m)	0.25	0.30	0.30
△	10.0	10.0	10.0	v_o (m/s)	1.47	1.31	1.34
□	15.0	10.0	5.0	F_o	0.94	0.76	0.78
				S_o (m/km)	71.90	32.10	39.20
R_A=5.00	R_B=3.20		R_L=2.70	L (km)	1.10	3.00	8.00

Θ1=0.41 Θ2=0.29 Θ3=0.30

pr1r2=0.22 pr1u2=0.63 pr1r3=0.15 pr2r3=0.37

pr2u3=0.63 pu2r3=0.37 pu2u3=0.63

p(s1)=0.03 p(s2)=0.10 p(s3)=0.06 p(s4)=0.06

p(s5)=0.11 p(s6)=0.18 p(s7)=0.30 p(s8)=0.16

Figure 4.21

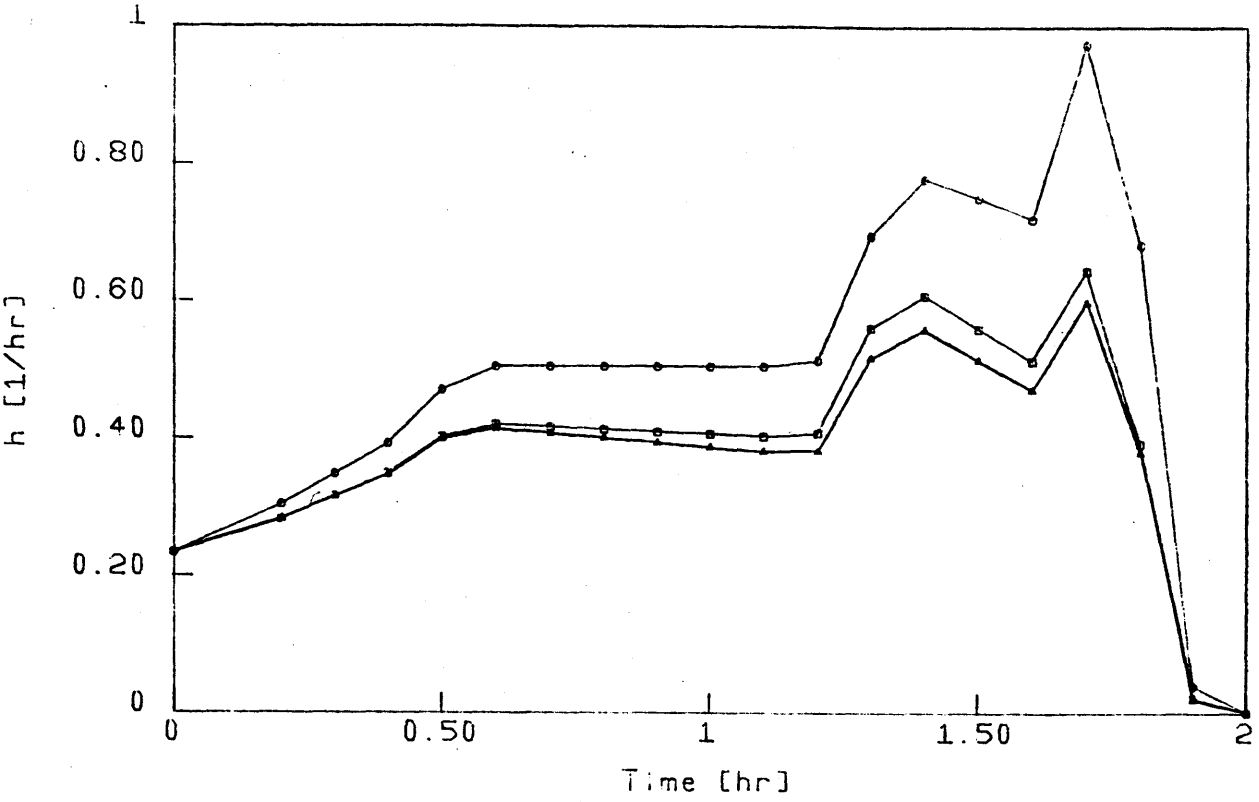

UNIBON BASIN

Basin luh for different infiltration losses

(Basin representation 2)

Characteristics:

	I(%)						
Order	1	2	3	Order	1	2	3
⊙	0.0	0.0	0.0	y_o (m)	0.24	0.28	0.37
△	10.0	10.0	10.0	v_o (m/s)	1.50	1.40	1.25
□	15.0	10.0	5.0	F_o	0.98	0.85	0.66
				S_o (m/km)	82.70	46.60	23.30
R_A=5.60	R_B=4.00	R_L=2.80		L (km)	1.10	3.10	8.60

Θ1=0.51 Θ2=0.31 Θ3=0.18

pr1r2=0.29 pr1u2=0.50 pr1r3=0.21 pr2r3=0.50

pr2u3=0.50 pu2r3=0.50 pu2u3=0.50

p(s1)=0.07 p(s2)=0.13 p(s3)=0.07 p(s4)=0.11

p(s5)=0.16 p(s6)=0.16 p(s7)=0.18 p(s8)=0.13

Figure 4.22

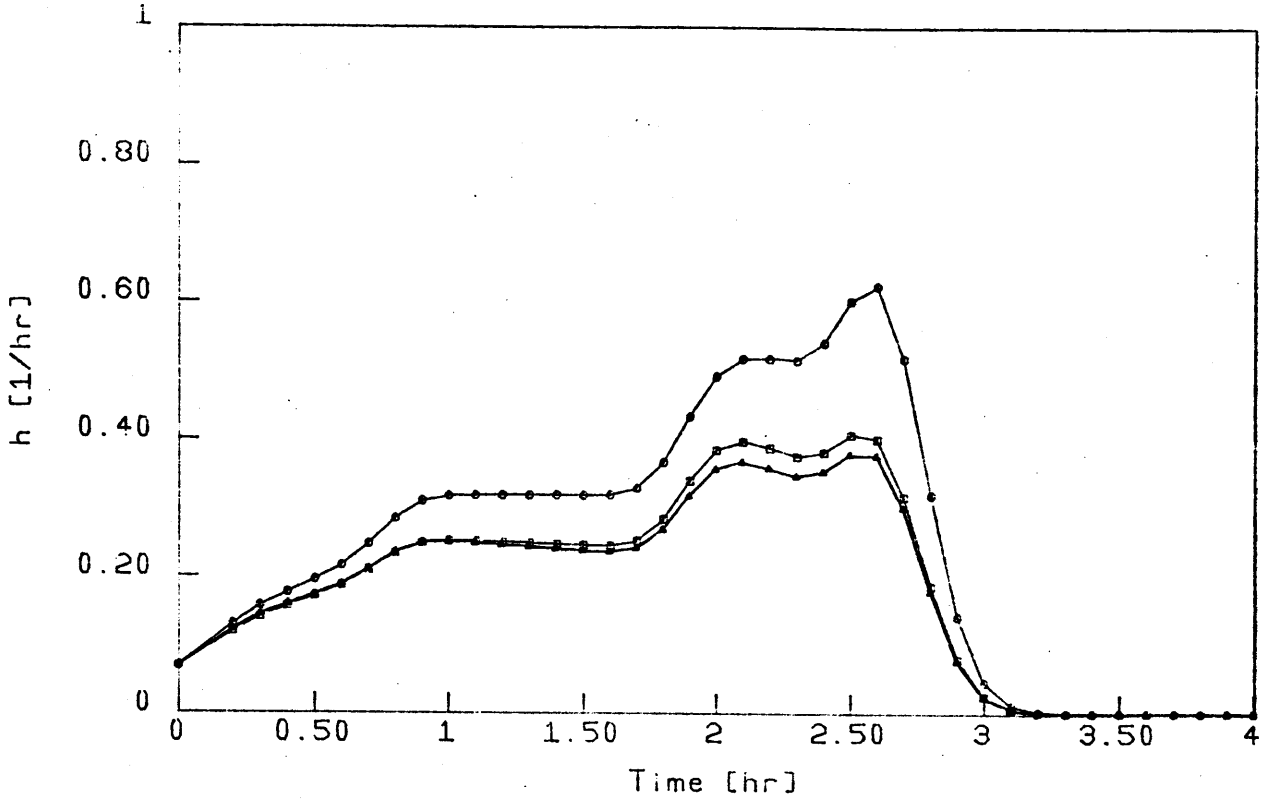

WADI UMM SALAM

Basin luh for different infiltration losses

(Basin representation 2)

Characteristics:

	I(%)						
Order	1	2	3	Order	1	2	3
⏲	0.0	0.0	0.0	y_o (m)	0.39	0.40	0.41
△	10.0	10.0	10.0	v_o (m/s)	1.05	1.01	0.98
⏍	15.0	10.0	5.0	F_o	0.54	0.51	0.49
				S_o (m/km)	8.00	7.00	6.50
R_A=5.00	R_B=4.00	R_L=2.80		L (km)	1.30	3.60	10.00

Θ1=0.64 Θ2=0.30 Θ3=0.06

pr1r2=0.29 pr1u2=0.50 pr1r3=0.21 pr2r3=0.50

pr2u3=0.50 pu2r3=0.50 pu2u3=0.50

p(s1)=0.09 p(s2)=0.16 p(s3)=0.09 p(s4)=0.14

p(s5)=0.15 p(s6)=0.15 p(s7)=0.06 p(s8)=0.16

Figure 4.23

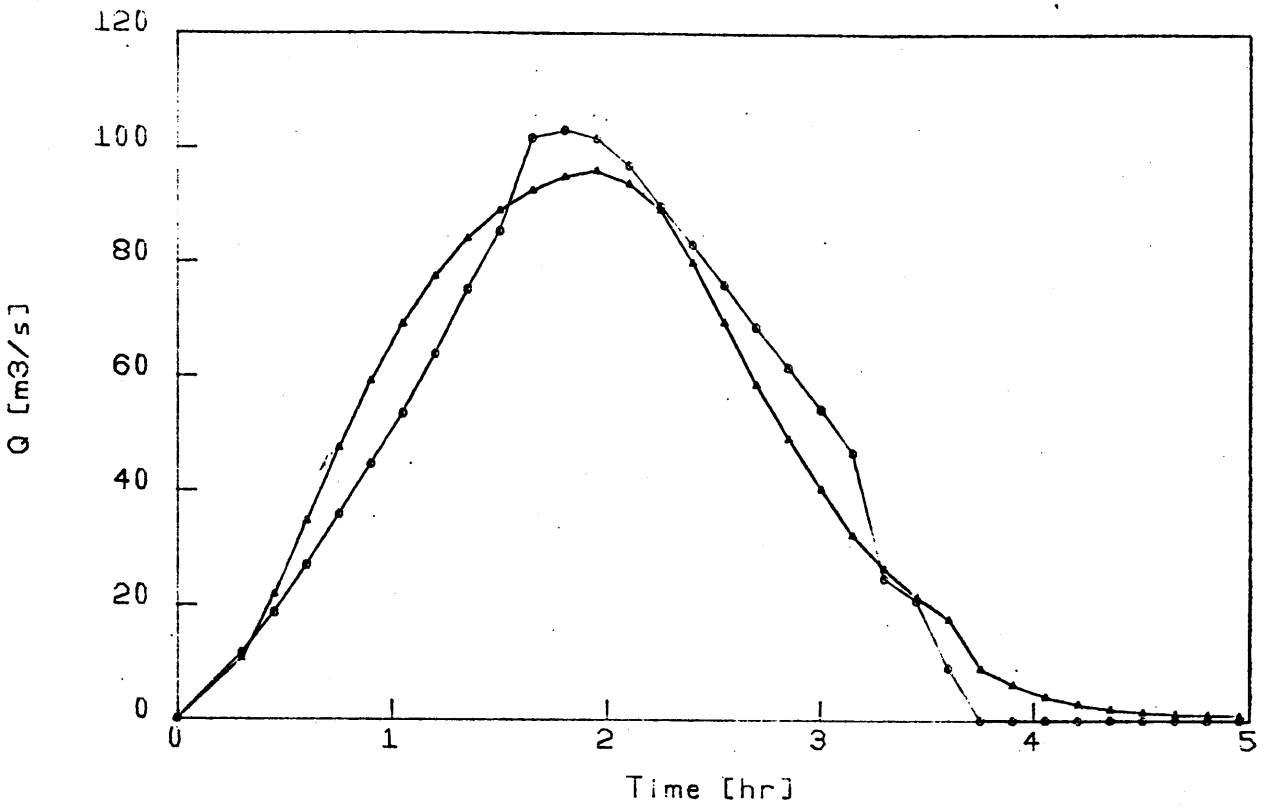

MOROVIS BASIN

Discharge hydrograph - exponential vs linearized solution

(Basin representation 2)

Characteristics:

i=3.0 cm/hr t=2.0 hr A=13.0 km²

Order	I(%) 1	2	3	Order	1	2	3
	0.0	0.0	0.0	y_o (m)	0.25	0.30	0.30
⊙	Linearized solution			v_o (m/s)	1.47	1.31	1.34
△	Exponential assumption			F_o	0.94	0.76	0.78
				S_o (m/km)	71.90	32.10	39.20
A	R =5.00	R_B=3.20	R_L=2.70	L (km)	1.10	3.00	8.00

Θ1=0.41 Θ2=0.29 Θ3=0.30

pr1r2=0.22 pr1u2=0.63 pr1r3=0.15 pr2r3=0.37

pr2u3=0.63 pu2r3=0.37 pu2u3=0.63

p(s1)=0.03 p(s2)=0.10 p(s3)=0.06 p(s4)=0.06

p(s5)=0.11 p(s6)=0.18 p(s7)=0.30 p(s8)=0.16

Figure 4.24

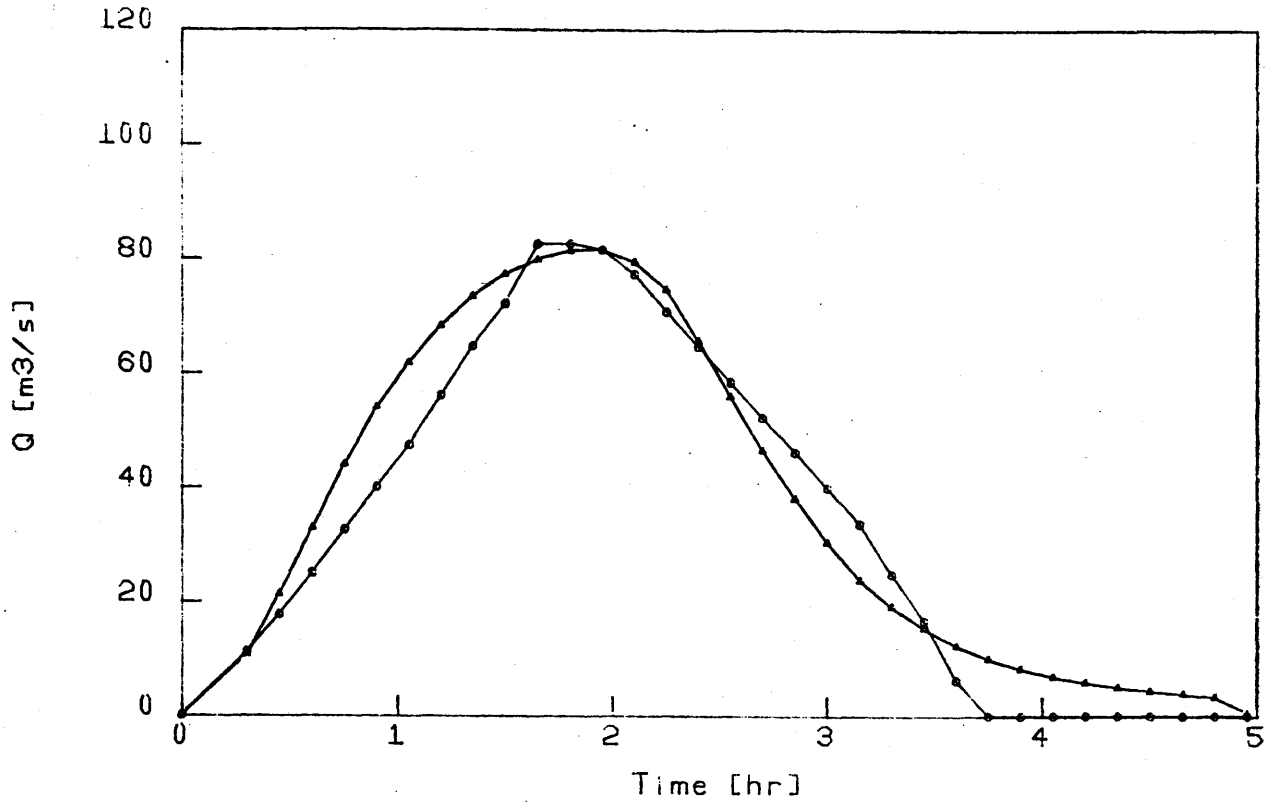

MOROVIS BASIN

Discharge hydrograph - exponential vs linearized solution

(Basin representation 2)

Characteristics:

i=3.0 cm/hr t=2.0 hr A=13.0 km²

Order	I(%) 1	2	3	Order	1	2	3
	15.0	10.0	5.0	y_o (m)	0.25	0.30	0.30
⏲	Linearized solution			v_o (m/s)	1.47	1.31	1.34
△	Exponential assumption			F_o	0.94	0.76	0.78
				S_o (m/km)	71.90	32.10	39.20
A	R =5.00	R_B=3.20	R_L=2.70	L (km)	1.10	3.00	8.00

Θ1=0.41 Θ2=0.29 Θ3=0.30

pr1r2=0.22 pr1u2=0.63 pr1r3=0.15 pr2r3=0.37

pr2u3=0.63 pu2r3=0.37 pu2u3=0.63

p(s1)=0.03 p(s2)=0.10 p(s3)=0.06 p(s4)=0.06

p(s5)=0.11 p(s6)=0.18 p(s7)=0.30 p(s8)=0.16

Figure 4.25

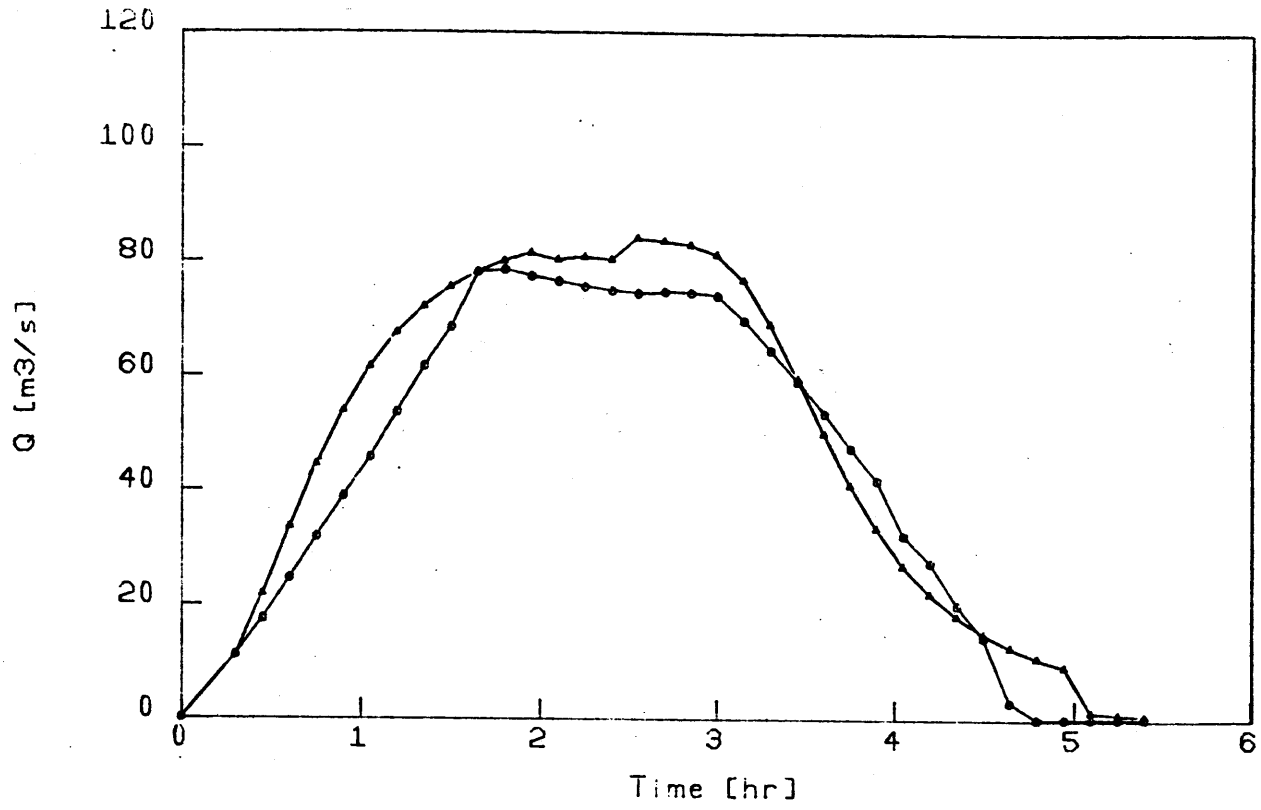

MOROVIS BASIN

Discharge hydrograph - exponential vs linearized solution

(Basin representation 2)

Characteristics:

i=3.0 cm/hr t=3.0 hr A=13.0 km²

Order	I(%) 1	2	3	Order	1	2	3
	10.0	10.0	10.0	y_o (m)	0.25	0.30	0.30
⊙	Linearized solution			v_o (m/s)	1.47	1.31	1.34
△	Exponential assumption			F_o	0.94	0.76	0.78
				S_o (m/km)	71.90	32.10	39.20
A	R =5.00	R_B=3.20	R_L=2.70	L (km)	1.10	3.00	8.00

Θ1=0.41 Θ2=0.29 Θ3=0.30

pr1r2=0.22 pr1u2=0.63 pr1r3=0.15 pr2r3=0.37

pr2u3=0.63 pu2r3=0.37 pu2u3=0.63

p(s1)=0.03 p(s2)=0.10 p(s3)=0.06 p(s4)=0.06

p(s5)=0.11 p(s6)=0.18 p(s7)=0.30 p(s8)=0.16

Figure 4.26

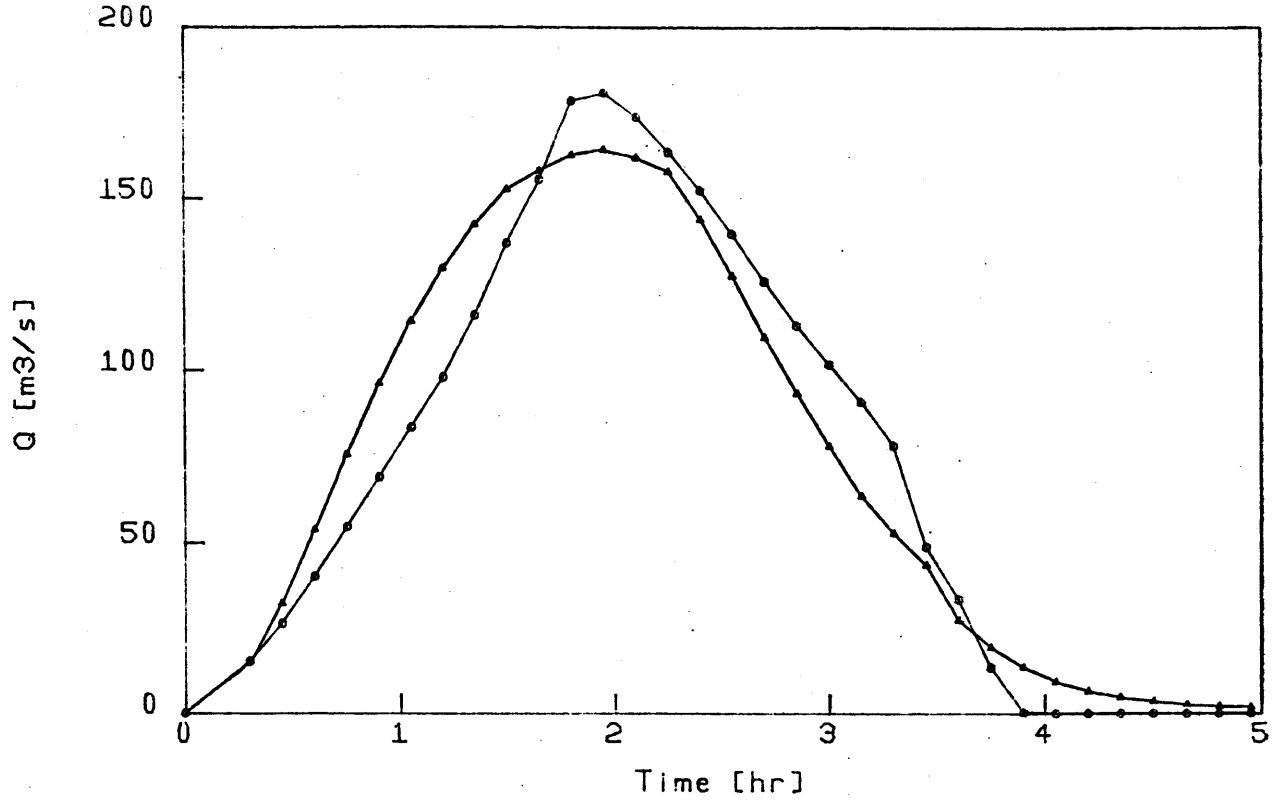

UNIBON BASIN

Discharge hydrograph - exponential vs linearized solution

(Basin representation 2)

Characteristics:

i=3.0 cm/hr t=2.0 hr A=23.0 km²

Order	I(%) 1	2	3	Order	1	2	3
	0.0	0.0	0.0	y_o (m)	0.24	0.28	0.37
⊙	Linearized solution			v_o (m/s)	1.50	1.40	1.25
△	Exponential assumption			F_o	0.98	0.85	0.66
				S_o (m/km)	82.70	46.60	23.30
R_A=5.60	R_B=4.00	R_L=2.80		L (km)	1.10	3.10	8.60

Θ1=0.51 Θ2=0.31 Θ3=0.18

pr1r2=0.29 pr1u2=0.50 pr1r3=0.21 pr2r3=0.50

pr2u3=0.50 pu2r3=0.50 pu2u3=0.50

p(s1)=0.07 p(s2)=0.13 p(s3)=0.07 p(s4)=0.11

p(s5)=0.16 p(s6)=0.16 p(s7)=0.18 p(s8)=0.13

Figure 4.27

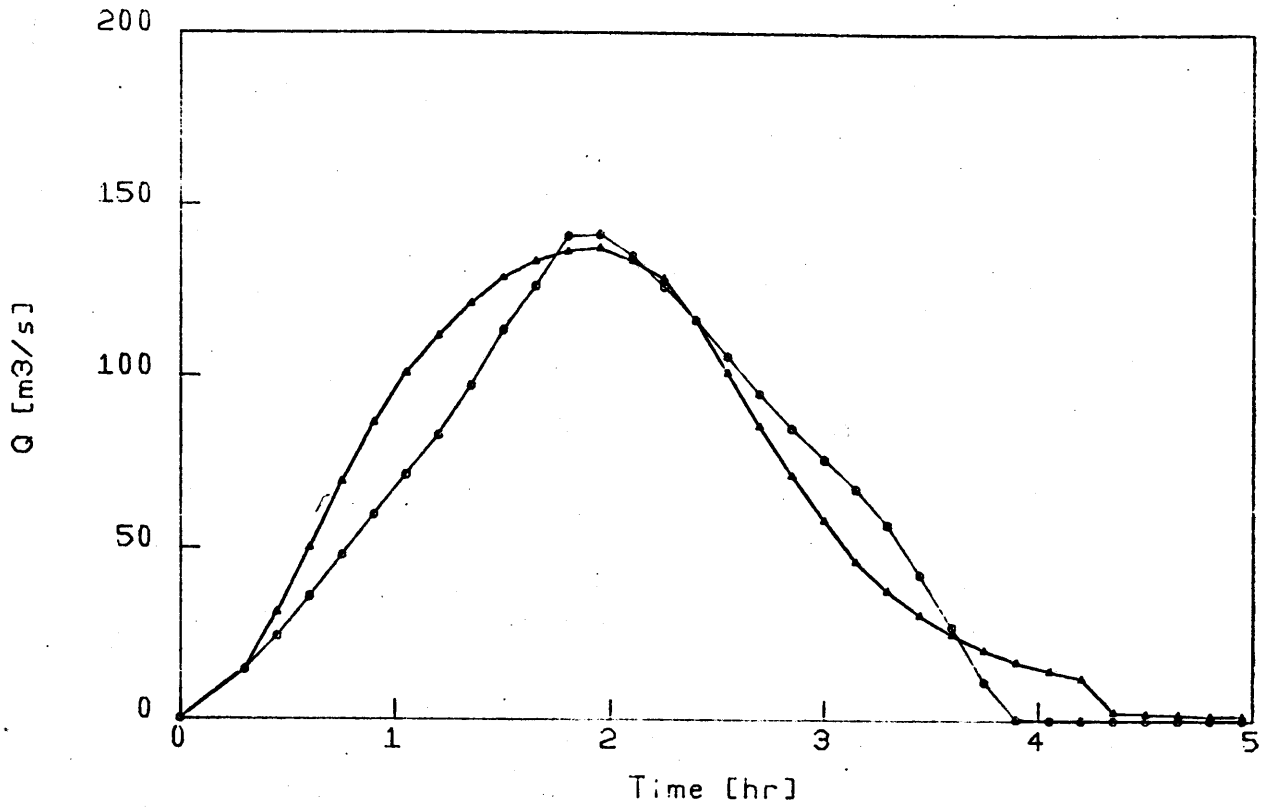

UNIBON BASIN

Discharge hydrograph - exponential vs linearized solution

(Basin representation 2)

Characteristics:

i=3.0 cm/hr t=2.0 hr A=23.0 km²

Order	I(%) 1	2	3	Order	1	2	3
	15.0	10.0	5.0	y_o (m)	0.24	0.28	0.37
⊙	Linearized solution			v_o (m/s)	1.50	1.40	1.25
△	Exponential assumption			F_o	0.98	0.85	0.66
				S_o (m/km)	82.70	46.60	23.30
R_A=5.60	R_B=4.00	R_L=2.80		L (km)	1.10	3.10	8.60

Θ1=0.51 Θ2=0.31 Θ3=0.18

pr1r2=0.29 pr1u2=0.50 pr1r3=0.21 pr2r3=0.50

pr2u3=0.50 pu2r3=0.50 pu2u3=0.50

p(s1)=0.07 p(s2)=0.13 p(s3)=0.07 p(s4)=0.11

p(s5)=0.16 p(s6)=0.16 p(s7)=0.18 p(s8)=0.13

Figure 4.28

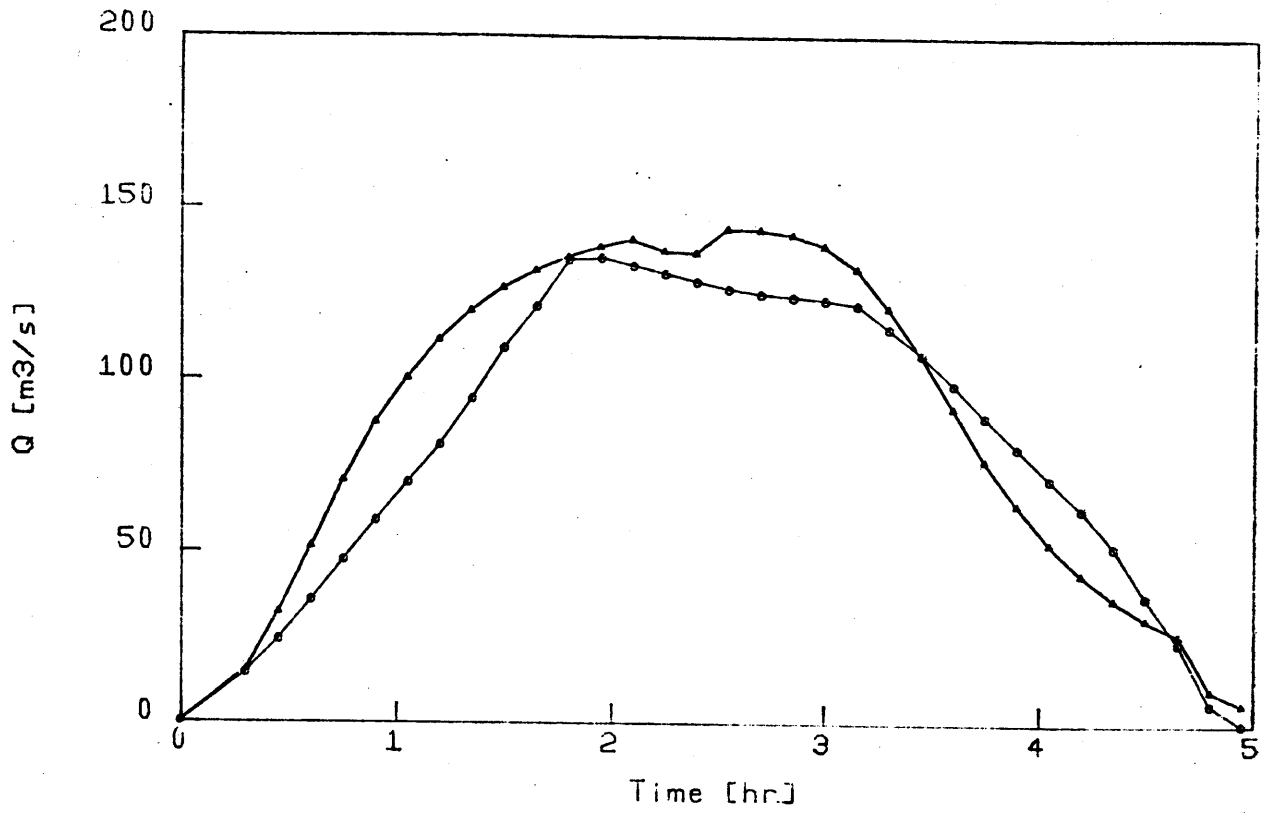

UNIBON BASIN

Discharge hydrograph - exponential vs linearized solution

(Basin representation 2)

Characteristics:

i=3.0 cm/hr t=3.0 hr A=23.0 km²

Order	I(%) 1	2	3	Order	1	2	3
	10.0	10.0	10.0	y_o (m)	0.24	0.28	0.37
⏲	Linearized solution			v_o (m/s)	1.50	1.40	1.25
△	Exponential assumption			F_o	0.98	0.85	0.66
				S_o (m/km)	82.70	46.60	23.30
R_A=5.60	R_B=4.00	R_L=2.80		L (km)	1.10	3.10	8.60

Θ1=0.51 Θ2=0.31 Θ3=0.18

pr1r2=0.29 pr1u2=0.50 pr1r3=0.21 pr2r3=0.50

pr2u3=0.50 pu2r3=0.50 pu2u3=0.50

p(s1)=0.07 p(s2)=0.13 p(s3)=0.07 p(s4)=0.11

p(s5)=0.16 p(s6)=0.16 p(s7)=0.18 p(s8)=0.13

Figure 4.29

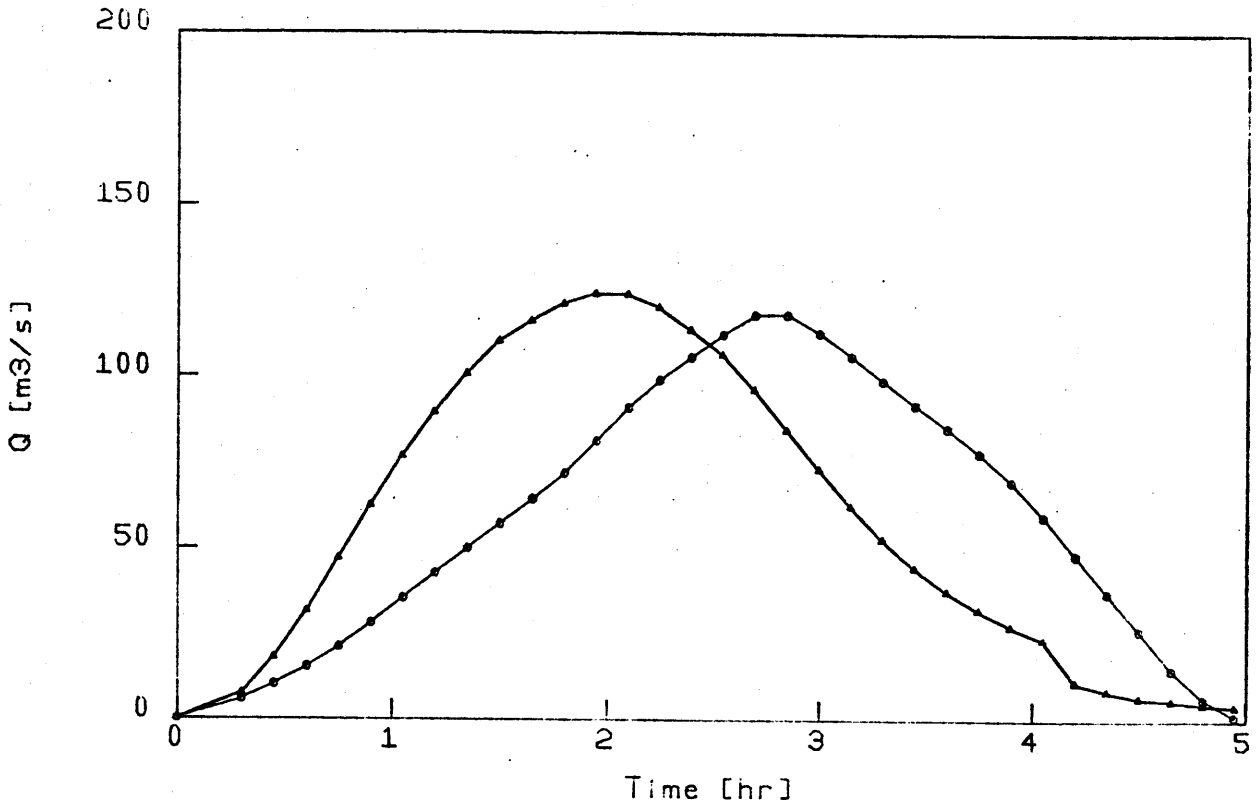

WADI UMM SALAM

Discharge hydrograph - exponential vs linearized solution

(Basin representation 2)

Characteristics:

i=1.8 cm/hr t=2.0 hr A=39.0 km²

Order	I(%) 1	2	3	Order	1	2	3
	15.0	10.0	5.0	y_o (m)	0.39	0.40	0.41
⊙	Linearized solution			v_o (m/s)	1.05	1.01	0.98
△	Exponential assumption			F_o	0.54	0.51	0.49
				S_o (m/km)	8.00	7.00	6.50
R_A=5.00	R_B=4.00	R_L=2.80		L (km)	1.30	3.60	10.00

Θ1=0.64 Θ2=0.30 Θ3=0.06

pr1r2=0.29 pr1u2=0.50 pr1r3=0.21 pr2r3=0.50

pr2u3=0.50 pu2r3=0.50 pu2u3=0.50

p(s1)=0.09 p(s2)=0.16 p(s3)=0.09 p(s4)=0.14

p(s5)=0.15 p(s6)=0.15 p(s7)=0.06 p(s8)=0.16

Figure 4.30

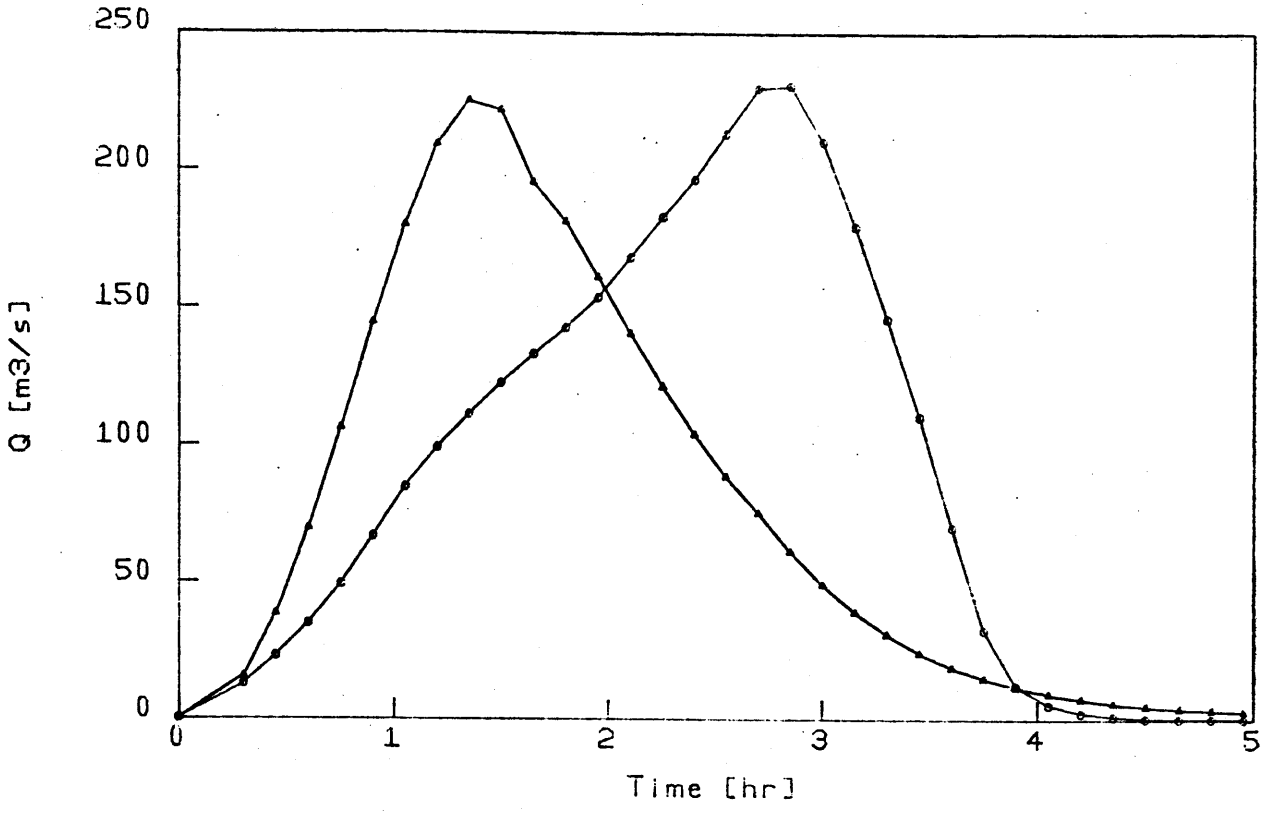

WADI UMM SALAM

Discharge hydrograph - exponential vs linearized solution

(Basin representation 2)

Characteristics:

i=3.7 cm/hr t=1.0 hr A=39.0 km²

Order	I(%) 1	2	3	Order	1	2	3
	0.0	0.0	0.0	y_o (m)	0.39	0.40	0.41
⏀	Linearized solution			v_o (m/s)	1.05	1.01	0.98
△	Exponential assumption			F_o	0.54	0.51	0.49
				S_o (m/km)	8.00	7.00	6.50
R_A=5.00	R_B=4.00	R_L=2.80		L (km)	1.30	3.60	10.00

Θ1=0.64 Θ2=0.30 Θ3=0.06

pr1r2=0.29 pr1u2=0.50 pr1r3=0.21 pr2r3=0.50

pr2u3=0.50 pu2r3=0.50 pu2u3=0.50

p(s1)=0.09 p(s2)=0.16 p(s3)=0.09 p(s4)=0.14

p(s5)=0.15 p(s6)=0.15 p(s7)=0.06 p(s8)=0.16

Figure 4.31

Chapter 5

SUMMARY AND CONCLUSIONS

5.1 Summary and Conclusions

The main topic addressed in this work has been the representation of the channel infiltration losses in the geomorphologic IUH.

The response of the channel to an instantaneous input, considering infiltration losses, was successfully obtained through the linearization of the governing equations of motion. This response, physically based, was then incorporated into the theory of the Geomorphologic Instantaneous Unit Hydrograph to obtain the characteristics response of the whole basin, which was compared with the one resulting when the response of the channel is assumed to behave like a linear reservoir, (exponential travel time) modified for infiltration channel losses. Comparisons of the discharge hydrographs indicate that the latter assumption is adequate and is a lot easier to use. That may be considered a verification of the GIUH.

The value of the obtained linear changes response lies not only on its use in the geomorphologic IUH theory but also in its potential in traditional hydraulic routing applications. For the first time explicit accounting of channel infiltration is made in an analytical physically based linear model of channel response.

REFERENCES

Benjamin, J. R. and Cornell, C. A., Probability, Statistics, and Decision for Civil Engineers, McGraw-Hill Book Company, 1970.

Burkham, D. E., "Depletion of Streamflow by Infiltration in the Main Channels of the Tucson Basin, Southeastern Arizona," U.S. Geological Survey, Water-Supply Paper 1939-B, 1970a.

Burkham, D. E., "A Method for Relating Infiltration Rates to Streamflow Rates in Perched Streams," Geological Survey Research, U.S. Geological Survey, Prof. Paper 700-D, 1970b.

Chan, S. and R. L. Bras, "Derived Distribution of Water Volume Above a Given Threshold Discharge", Technical Report No. 234, Ralph M. Parsons for Water Resources and Hydrodynamics, Massachusetts Institute of Technology, 1978.

Chan, S. and R. L. Bras, "Urban Stormwater Management: Distribution of Flood Volumes," Water Resources Research, 15(2), pp. 371-382, 1979.

Cordova, J. R., and R. L. Bras, "Stochastic Control of Irrigation Systems," Technical Report No. 239, Ralph M. Parsons Laboratory for Water Resources and Hydrodynamics, Massachusetts Institute of Technology, 1979.

Cordova, J. R., and I. Rodriguez-Iturbe, "Geomorphologic Estimation of Extreme Flow Probabilities," accepted for publication Journal of Hydrology, 1982

Dahl, N. J., Non-steady Flow in Open Channels, Series Paper 10, The Royal Veterinary and Agricultural University, Copenhagen, 1981.

Doetsch, G., Introduction to the Theory and Application of the Laplace Transformation, New York, Springer-Verlag, 1961.

Eagleson, P. S., Dynamic Hydrology, McGraw-Hill, New York, 1970.

Eagleson, P. S., Dynamic of Flood Frequency," Water Resources Research 8(4), pp. 878-898, 1972.

Eagleson, P. S., "Climate, Soil and Vegetation 1. Introduction to Water Balance Dynamics," Water Resources Research, 14(5), pp. 705-712, 1978.

Eagleson, P. S., "Climate, Soil and Vegetation 2. The Distribution of Annual Precipitation Derived from Observed Storm Sequences," Water Resources Research, 14(5), pp. 713-721, 1978.

Eagleson, P. S., "Climate, Soil and Vegetation 3. A Simplified Model of Soil Moisture Movement in the Liquid Phase," Water Resources Research, 14(5), pp. 722-730, 1978.

Eagleson, P. S., "Climate, Soil and Vegetation 4. The Expected Value of Annual Evapotranspiration," Water Resources Research, 14(5), pp. 731-739. 1978.

Eagleson, P. S., "Climate, Soil and Vegetation 5. A Derived Distribution of Storm Surface Runoff," Water Resources Research, 14(5), pp. 740-748, 1978.

Eagleson, P. S., "Climate, Soil and Vegetation 6. Dynamics of the Annual Water Balance," Water Resources Research, 14(5), pp. 749-764, 1978.

Eagleson, P. S., "Climate, Soil and Vegetation 7. A Derived Distribution of Annual Water Yield," Water Resources Research, 14(5), pp. 765-776, 1978.

Eagleson, P. S., Water Balance Dynamics-Climate, Soil and Vegetation, MIT Press, in press, 1981.

Eagleson, P. S., "Ecological Optimality in Water-Limited natural soil-vegetation systems, 1. Theory and hypothesis," Water Resources Research, 18(2), pp. 325-340, 1982.

Eagleson, P. S. and T. E. Tellers, "Ecological Optimality in water-limited natural soil-vegetation systems, 2. Tests and Applications," Water Resources Research, 18(2), pp. 341-354, 1982.

Freeman, H., Introduction to Statistical Inference, Addison-Wesley Publishing Company, Incorporated, 1963.

Grace, R. A. and P. S. Eagleson, "The Synthesis of Short-time-increment rainfall sequences," Technical Report No. 91, Ralph M. Parsons Laboratory for Water Resources and Hydrodynamics, Massachusetts Institute of Technology, 1966.

Grayman, W. M. and P.S. Eagleson, "Streamflow Record length for Modelling Catchment Dynamics," Technical Report No. 114, Ralph M. Parsons Laboratory for Water Resources and Hydrodynamics, Massachusetts Institute of Technology, 1969.

Gupta, V. K., E. Waymire and C. T. Wang, "A Representation of an Instantaneous Unit Hydrograph from Geomorphology, "Water Resources Research, 16(5), pp. 855-862, 1980.

Harley, B. M., "Linear Routing in Uniform Open Channels," M. Eng. Science Thesis, Department of Civil Engineering, National University of Ireland, 1967.

Hebson, C. and E. Wood, "A Derived Flood Frequency Distribution, Water Resources Research, (18)5, pp. 1509-1518, 1982.

Henderson, F. M., "Some Properties of the Unit Hydrodraph," Journal of Geophys. Research, 68(16), pp. 4785-4793, 1963.

Horton, R. E., "Erosional Development of Streams and Their Drainage Basin, Hydrophysical Approach to Quantitative Morphology," Bulletin of the Geological Society of America, 56, pp. 275-370, 1945.

International Mathematical and Statistical Libraries, Incorporated, "IMSL Library," Edition 8, 1980.

Kirshen, D. M. and R. L. Bras, "The Linear Channel and Its Effect on the Geomorphologic IUH," Technical Report No. 277, Ralph M. Parsons Laboratory for Water Resources and Hydrodynamics, Massachusetts Institute of Technology, 1982.

Linsley, R. K., M. A. Kohler, and J. L. Paulhus, Hydrology for Engineers, Third ed., McGraw-Hill Book Company, 1982.

O'Meara, B. E., "Linear Routing of Lateral Inflow in Uniform Open Channels," M. Eng. Science Thesis, Department of Civil Engineering, National University of Ireland, 1968.

Philip, J. R., "General Method of Exact Solution of the Concentration Dependent diffusion Equation, "Aust. J. Phys., 13(1), pp. 1-12, 1960.

Pilgrim, P. H., "Isocrones of Travel Time and Distribution of Flood storage from a Tracer Study on a small watershed," Water Resources Research, 13(3), pp. 587-595, 1977.

Restrepo-Posada, P. J. and P. S. Eagleson, "Identification of Independent Rainstorms," Journal of Hydrology, Vol. 55, pp. 303-319, 1982.

Rodriguez-Iturbe., I., and J. B. Valdes, "The Geomorphologic Structure of Hydrologic Response," Water Resources Research, 15(5), pp. 1409- 1420, 1979.

Rodriguez-Iturbe, I., G. Devoto and J. B. Valdes, "Discharge Response Analysis and Hydrologic Similarity: The Interrelation Between the Geomorphologic IUH and the Storm characteristics," Water Resources Research, 15(6), pp. 1435-1444, 1979.

Rodriguez-Iturbe, I., M. Gonzalez and R. L. Bras, "A Geomorphoclimatic Theory of the Instantaneous Unit Hydrograph," Water Resources Research, 18(4), pp. 877-886, 1982.

Schumm, S. A., "Evolution of Drainage Systems and Slopes in Badlands at Perth Amboy, New Jersey, "Geol. Soc. Amer. Bull., 67, pp. 597-646, 1956.

Strahler, A. N., "Quantitative Analysis of Watershed Geomorphology," Transactions, American Geophysical Union, 38(6), pp. 913-920, 1957.

U. S. Weather Bureau, "Rainfall Intensity-Frequency Regime," 1-5, Tech. Pap. 29, Washington, D. C., 1957-60.

Valdes, J. B., Y. Fiallo, and I. Rodriguez-Iturbe, "Rainfall-Runoff Analysis of the Geomorphologic IUH," Water Resources Research, 15(6), pp. 1421-1434, 1979.

APPENDIX A

ANALYTICAL LINEAR SOLUTION OF THE UPSTREAM CHANNEL IUH AND SOME MATHEMATICAL PROPERTIES

A.1 The Linearized Equation of Motion

The final expression of the linearized equation of motion obtained in Chapter 3 (Equation 3.9) is:

$$\left(gy_o^3 - q_o^2\right)\frac{\partial^2 \delta q}{\partial x^2} - 2q_o y_o \frac{\partial^2 \delta q}{\partial x \partial t} - y_o^2 \frac{\partial^2 \partial q}{\partial t^2} - 3gS_o \frac{\partial \delta q}{\partial x} y_o^2$$

$$-2gy_o^2 \frac{S_o}{q_o}\frac{\partial \delta q}{\partial t} = -\left(gy_o^3 - q_o^2\right) K\frac{\partial \delta q}{\partial x} + 3gS_o y_o^2 Kq_o$$

$$+ 3gS_o y_o^2 K\delta q - 2y_o Kq_o \frac{\partial \delta q}{\partial t} \qquad (A.1)$$

where δq represents the perturbation about the reference discharge q_o.

Equation A.1 may be written as:

$$A\frac{\partial^2 \delta q}{\partial x^2} + B\frac{\partial^2 \delta q}{\partial x \partial t} + C\frac{\partial^2 \delta q}{\partial t^2} + D\frac{\partial \delta q}{\partial t} + E\frac{\partial \delta q}{\partial x} + F\delta q + G = 0 \qquad (A.2)$$

where

$A = (gy_o - v_o^2)$ $\qquad$ $D = 2Kv_o - 2gS_o/v_o$

$B = -2v_o$ $\qquad$ $E = (gy_o - v_o^2)K - 3gS_o$

$C = -1$ $\qquad$ $F = -3gS_oK$

$G = -3gS_oKq_o$

Let the perturbation be related to w(x,t), a new variable, as

$$\delta q(x,t) = -\frac{G}{F} + \left[w(x,t) + \frac{G}{F}\right] e^{\alpha x} \qquad (A.3)$$

where α is a constant to be determined. Substituting Equation A.3 into Equation A.2, the latter becomes

$$A \frac{\partial^2 w}{\partial x^2} + B \frac{\partial^2 w}{\partial t \partial x} + C \frac{\partial^2 w}{\partial t^2} + (\alpha B+D) \frac{\partial w}{\partial t} + (2\alpha A+E) \frac{\partial w}{\partial x}$$

$$+ (\alpha^2 A+\alpha E+F)w + (\alpha^2 A+\alpha E+F) \frac{G}{F} = 0 \qquad (A.4)$$

α is chosen such that

$$\alpha^2 A + \alpha E + F = 0$$

i.e,

$$\alpha = \begin{cases} -K \\ -\frac{F}{AF} \end{cases}$$

From now on, it is assumed that $\alpha = -K$, and therefore Equation A.4 may be written as

$$A \frac{\partial^2 w}{\partial x^2} + B \frac{\partial^2 w}{\partial t \partial x} + C \frac{\partial^2 w}{\partial t^2} + (D-KB) \frac{\partial w}{\partial t}$$

$$+ (E-2KA) \frac{\partial w}{\partial x} = 0 \qquad (A.5)$$

which is an homogeneous partial differential equation whose solution is desired for the case of a pulsed upstream inflow.

A.2 Boundary and Initial Conditions

Before the application of the input to the channel, the flow is steady state and the governing equation is:

$$\frac{\partial q}{\partial x} = -q_I(x,t)$$

or specifically,

$$\frac{dq}{dx} = -Kq$$

where q is the discharge per unit width. Integrating from the upstream point of the channel ($x=0$, $q=q_1$) to an arbitrary point ($x=x$, $q=q$), the solution for the steady state problem is:

$$q(x,t) = q_1 e^{-Kx} \qquad t \leq 0 \qquad (A.6)$$

The reference discharge q_o, around which the linearization is done, has to be chosen according to the steady state solution (Equation A.6) and, for a channel of length L, it could be the mean value, i.e.,

$$q_o = \frac{1}{L} \int_o^L q_1 e^{-Kx} \, dx$$

However, for practical reasons, q_o is assumed equal to q_1. Therefore, before the application of the input, the perturbation is $q-q_o$. Figure A.1 shows the perturbations before and after the input is applied.

At $x=0$ and $t=0$, a delta function is introduced into the channel,

$$\delta q(0,t) = \delta(t)$$

Replacing this expression in Equation A.3 and solving for $w(0,t)$,

$$w(0,t) = \delta(t) \qquad (A.7)$$

As noted above, prior to the delta function,

$$\delta q(x,0) = q_o e^{-Kx} - q_o \qquad (A.8)$$

which implies that

$$w(x,0) = 0 \qquad (A.9)$$

$$\frac{\partial}{\partial t} [w(x,t)] \Big|_{t=0} = 0 \qquad (A.10)$$

Equations A.7, A.9 and A.10 are the boundary and initial conditions for solving Equation A.5 which will be done using Laplace transforms.

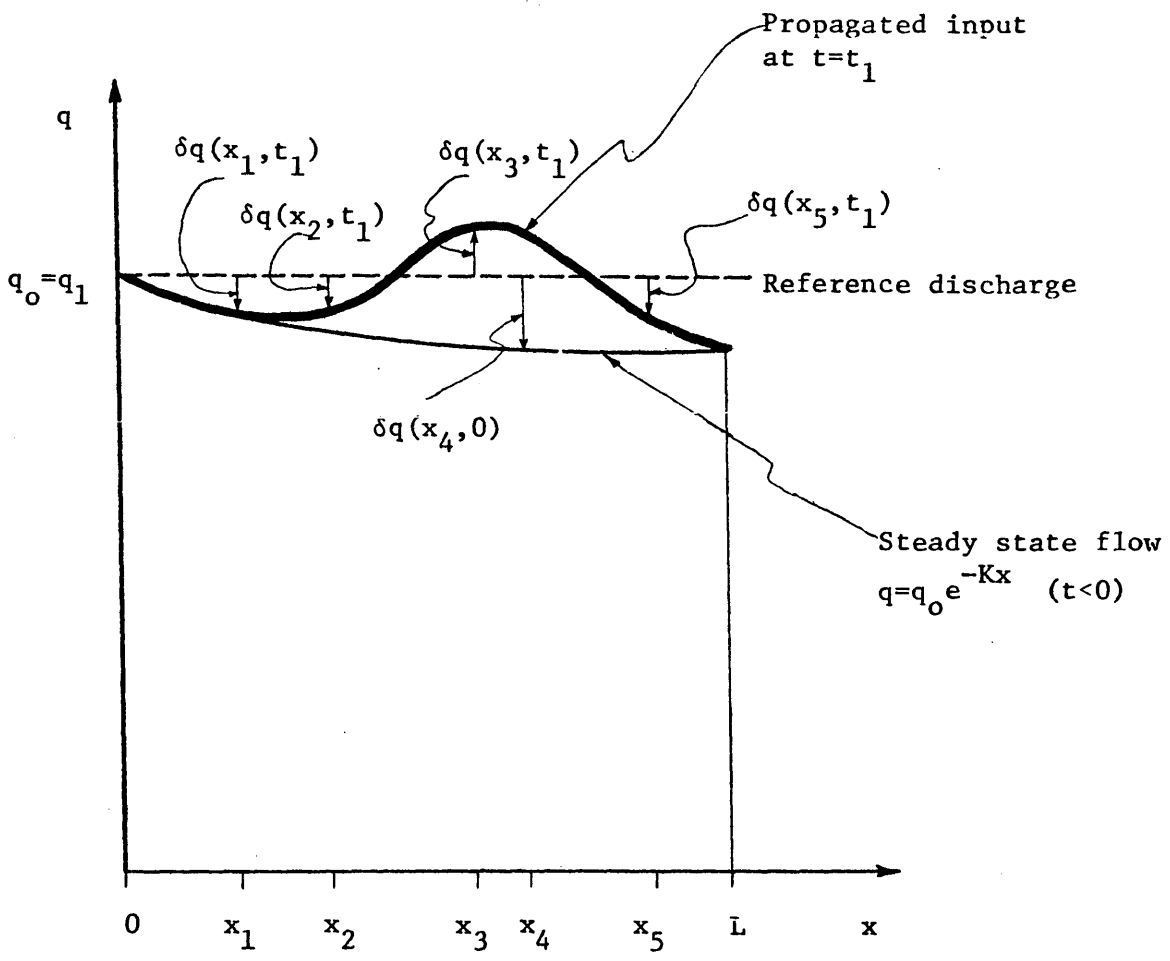

Reference discharge and propagated perturbation

Figure A.1

A.3 Linear Solution

The Laplace transform with respect to y of w(x,t) is defined as

$$\mathcal{L}_t \left\{w(x,t)\right\} = W(x,s) = \int_o^\infty e^{-st} w(x,t)dt$$

Taking the Laplace transform with respect to t on both sides of Equation A.5 and using conditions A.9 and A.10, the following second order homogeneous ordinary differential equation is obtained,

$$\Theta \frac{\partial^2 W}{\partial x^2} + \Phi \frac{\partial W}{\partial x} + \Psi W = 0 \qquad \text{(A.11)}$$

where

$\Theta = A$

$\phi = Bs + E - 2KA$

$\psi = Cs^2 + (D-KB)s$

The solution of this equation is:

$$W(x,s) = \gamma_1 \exp\left\{\frac{-(Bs+E-2KA) + [Bs+E-2KA)^2 - 4A(Cs^2+(D-KB)s)^{-\frac{1}{2}}]}{2A} x\right\}$$
$$+ \gamma_2 \exp\left\{\frac{-(Bs+E-2KA) - [(Bs+E-2KA)^2 - 4A(Cs^2+(D-KB)s)]^{\frac{1}{2}}}{2A} x\right\} \qquad \text{(A.12)}$$

where γ_1 and γ_2 are constants to be determined using the boundary condition and some properties of the Laplace transform.

For any Laplace transform.

$$\lim_{s\to\infty} W(x,s) = 0$$

Therefore, as s tends to infinity the exponential part of the first term in Equation A.12 tends also to infinity, and γ_1 has to be set equal to zero. On the other hand, the upstream boundary condition is a delta

function and, for this particular function, the Laplace transform is 1. Then,

$$W(0,s) = \mathcal{L}_t \left\{ w(0,t) \right\} = \int_0^\infty e^{-st} \delta(t) dt = 1$$

or

$$W(0,s) = \gamma_2 \exp(\theta)^{\frac{1}{2}} = \gamma_2 = 1$$

and therefore,

$$W(x,s) = \exp \left\{ \frac{-(Bs+E-2KA) - [(Bs+E-2KA)^2 - 4A(Cs^2+(D-KB)s)^{\frac{1}{2}}}{2A} x \right\}$$

or,

$$W(x,s) = \exp\{-x(as^2+bs+c)^{\frac{1}{2}} + exs+fx\} \qquad (A.13)$$

where

$$a = \frac{B^2-4AC}{4A^2} \qquad b = \frac{2BE-4AD}{4A^2}$$

$$c = \frac{(2KA-E)^2}{4A^2} \qquad e = -\frac{B}{2A}$$

$$f = \frac{2KA-E}{2A}$$

In order to obtain the solution of w(x,t) and therefore the solution of $\delta q(x,t)$, it is necessary to calculate the inverse Laplace transform of W(x,s). Following the same procedure used by Harley (1967), Equation A.13 can be rewritten as:

$$W(x,s) = \exp[-(a^{\frac{1}{2}}-e)xs-(b/2a^{\frac{1}{2}}-f)x] \qquad (A.14)$$
$$+ \exp(exs+fx)[\exp(-x(as^2+bs+c)^{\frac{1}{2}})-\exp(-bx/2a^{\frac{1}{2}}- a^{\frac{1}{2}}xs)$$

Therefore,

$$w(x,t) = \mathcal{L}_s^{-1}[W(x,s)] = \exp[-(b/2a^{\frac{1}{2}}-f)x]\mathcal{L}_s^{-1}\{\exp[-(a^{\frac{1}{2}}-e)xs]\}$$

$$+ \exp(fx)\mathcal{L}_s^{-1}\{\exp(exs)[\exp(-x(as^2+bs+c)^{\frac{1}{2}})-\exp(-bx/2a^{\frac{1}{2}}a^{\frac{1}{2}}xs)]\} \quad (A.15)$$

To evaluate the first term of the right hand side of the last equation, the the translation formula is used:

$$\mathcal{L}_s^{-1}[e^{-ms}F(s)] = u(t-m)f(t-m)$$

where

$$u(t) = \begin{cases} 0 & \text{if } t < 0 \\ 1 & \text{if } t \geq 0 \end{cases}$$

For this particular case,

$$m = (a^{\frac{1}{2}}-e)x \text{ and } F(s) = 1$$

The inverse Laplace transform of $F(s) = 1$ is $f(t) = \delta(t)$ and then,

$$\exp[-(b/2a^{\frac{1}{2}}-f)x]\mathcal{L}_s^{-1}\{\exp[-a^{\frac{1}{2}}-e)xs]\} =$$

$$\exp[-(b/2a^{\frac{1}{2}}-f)x]\ \delta[t-(a^{\frac{1}{2}}-e)x]$$

For the second term of Equation A.15, Doetsch (1961), pp. 241, gives the inverse Laplace transform of

$$\exp[-x(as^2+bs+c)^{\frac{1}{2}}]-\exp(-bx/2a^{\frac{1}{2}}-a^{\frac{1}{2}}xs)$$

as

$$\begin{cases} 0 & t \leq t \leq a^{\frac{1}{2}}x \\ (d/a)^{\frac{1}{2}}x\ \exp(-bt/2a)\ \dfrac{I_1[d^{\frac{1}{2}}(t^2-ax^2)^{\frac{1}{2}}/a]}{(t^2-ax^2)^{\frac{1}{2}}} & t \geq a^{\frac{1}{2}}x \end{cases}$$

where

$$d = (b/2)^{\frac{1}{2}}-ac$$

$I_1[\cdot]$ = first order modified Bessel function of the first kind.

Using this result and the translation formula again, the inverse Laplace transform of the second term of Equation A.15 is

$$\exp(fx)(d/a)^{\frac{1}{2}}x \exp(-b(t+ex)/2a) \frac{I_1[d^{\frac{1}{2}}((t+ex)^2-ax^2)^{\frac{1}{2}}/a]}{((t+ex)^2-ax^2)^{\frac{1}{2}}} u[t-(a^{\frac{1}{2}}-e)x]$$

Finally, w(x,t) is

$$w(x,t) = \exp[-(b/2a^{\frac{1}{2}}-f)x]\ \delta[t-(a^{\frac{1}{2}}-e)x]$$

$$+\exp(fx)(d/a)^{\frac{1}{2}}x \exp(-b(t+ex)/2a) \frac{I_1[d^{\frac{1}{2}}((t+ex)^2-ax^2)^{\frac{1}{2}}/a]}{((t+ex)^2-ax^2)^{\frac{1}{2}}} u[t-(a^{\frac{1}{2}}-e)x] \quad (A.16)$$

Recalling Equation A.3, $\delta q(x,t)$ is related to $w(x,t)$ by

$$\delta q(x,t) = q_o e^{-Kx} - q_o + w(x,t)e^{-Kx} \quad (A.17)$$

The first two terms of the above equation correspond to the value of the perturbation before the introduction of the impulse function (see Equation A.8), whose effect is represented by the last term of Equation A.17. Therefore, the channel response to an impulse function at its most upstream point (x=0) including infiltration losses is given by

$$h(x,t) = e^{-Kx} w(x,t) \quad (4.18)$$

or,

$$h(x,t) = \exp[-(b/2a^{\frac{1}{2}}-f+K)x]\ \delta[t-(a^{\frac{1}{2}}-e)x]$$

$$+ \exp[(f-K)x](d/a)^{\frac{1}{2}}x \exp(-b(t+ex)/2a) \frac{I_1[d^{\frac{1}{2}}((t+ex)^2-ax^2)^{\frac{1}{2}}/a]}{((t+ex)^2-ax^2)^{\frac{1}{2}}} u[t-(a^{\frac{1}{2}}-e)x] \quad (A.19)$$

After some manipulations, Equation A.19 can be expressed as:

$$h(x,t) = \exp(-rt+zx)(d/a)^{\frac{1}{2}}x \frac{I_1[d^{\frac{1}{2}}((t-x/c_1)(t-x/c_2))^{\frac{1}{2}}/a]}{((t-x/c_1)(t-x/c_2))^{\frac{1}{2}}} u(t-x/c_1)$$

$$+ \exp(-px)\ \delta(t-x/c_1) \qquad \text{(A.20)}$$

where,

$$a = \frac{1}{gy_o(1-F_o^2)^2}$$

$$c_1 = v_o + (gy_o)^{\frac{1}{2}}$$

$$c_2 = v_o - (gy_o)^{\frac{1}{2}}$$

$$d = \frac{b^2}{4} - ac$$

$$b = \frac{S_o}{y_o v_o} \frac{2+F^2}{(1+F_o^2)^2} + \frac{K}{v_o} \frac{F_o^2}{1-F_o^2}$$

$$c = \frac{K^2}{4} + \frac{3}{2} K \frac{S_o}{y_o} \frac{1}{1-F_o^2} + \frac{9}{4} \frac{S_o^2}{y_o^2} \frac{1}{(1-F_o^2)^2}$$

$$p = \frac{S_o}{2y_o} \frac{2-F_o}{(1+F_0)F_o} - \frac{3}{2} KF_o + \frac{K}{2}$$

$$r = g \frac{S_o}{v_o} + \frac{gS_oF_o^2}{2v_o} - \frac{3}{2} Kv_o(1-F_o^2)$$

$$z = \frac{S_o}{2y_o} - \frac{K}{2} + \frac{3}{2} KF_o^2$$

$$v_o = \frac{q_o}{y_o}$$

$$F_o = \frac{v_o}{(gy_o)^{\frac{1}{2}}}$$

A.4 Evaluation of the Area Under h(x,t)

The area under h(x,t), keeping x fixed, may be obtained using the definition of the Laplace transform. The Laplace transform of h(x,t) is

$$H(x,t) = \int_0^\infty e^{-st} h(x,t)dt \tag{A.21}$$

At s=0,

$$H(x,0) = \int_0^\infty h(x,t)dt = A_h \tag{A.22}$$

which is the desired area. Introducing Equation A.18 into A.21,

$$H(x,s) = e^{-Kx} \int_0^\infty e^{-st} w(x,t)dt$$

$$= e^{-Kx} W(x,s)$$

From Equation A.13,

$$H(x,s) = e^{-Kx} \exp\{-x(as^2+bs+c)^{\frac{1}{2}}+exs+fx\} \tag{A.23}$$

At s=0,

$$H(x,0) = e^{-Kx} \exp\{x(f-\sqrt{c})\}$$

But

$$f = -\sqrt{c}$$

Therefore, using Equation A.22

$$A_h = e^{-Kx}$$

A.5 Evaluation of the Area Under r(t)

If A_r is the area under r(t):

$$A_r = \int_0^\infty r(t)dt$$

From Equation 3.15

$$A_r = \frac{1}{L}\int_0^\infty dt \int_0^L h(x,t)dx$$

The Laplace transform of r(t) is:

$$R(s) = \mathcal{L}_t[r(t)]$$

$$= \int_0^\infty e^{-st} r(t)dt$$

$$= \frac{1}{L}\int_0^\infty dt\, e^{-st} \int_0^L h(x,t)dx$$

Introducing Equation A.18:

$$R(s) = \frac{1}{L}\int_0^\infty dt e^{-st} \int_0^L e^{-Kx} w(x,t)dx$$

$$= \frac{1}{L}\int_0^L dx e^{-Kx} \int_0^\infty e^{-st} w(x,t)dt$$

$$= \frac{1}{L}\int_0^L e^{-Kx} W(x,s)dx$$

At s=0, $A_r = R(0)$. Recalling from Section A.4 that $W(x,s) = 1$ for all x,

$$A_r = \frac{1}{L} \int_0^L e^{-Kx} \, dx$$

$$= \frac{1}{KL} (1 - e^{-KL})$$